

Figure 1.1: Map of reservoirs identified as mercury-impaired on the 2010 303(d) List

## 2010 303(d)-listed reservoirs as labeled on Figure 1.1

<b>Reservoir*</b>	<b>Map # on Figure 1.1</b>	<b>Reservoir*</b>	<b>Map # on Figure 1.1</b>
Almanor, Lake	6	Nacimiento, Lake	62
Anderson Lake	41	Natoma, Lake	30
Beach Lake**	70	New Bullards Bar Reservoir	19
Berryessa, Lake	15	New Hogan Lake	48
Big Bear Lake	68	New Melones Lake	51
Black Butte Lake	7	Nicasio Reservoir	31
Bon Tempe Lake	32	O'Neill Forebay	45
Britton, Lake	5	Oroville, Lake	18
Calaveras Reservoir	39	Oxbow Reservoir	26
Camanche Reservoir	46	Pardee Reservoir	47
Camp Far West Reservoir	24	Pillsbury, Lake	9
Casitas, Lake	63	Pine Flat Lake	59
Castaic Lake	65	Puddingstone Reservoir	67
Chabot, Lake (Alameda Co.)	37	Pyramid Lake	64
Chesbro Reservoir	42	Robinson's Pond	74
Combie, Lake	25	Rollins Reservoir	23
Davis Creek Reservoir	13	San Antonio Reservoir	61
Del Valle Reservoir	38	San Luis Reservoir	44
Don Pedro Lake	54	San Pablo Reservoir	34
East Park Reservoir	11	Scotts Flat Reservoir	22
El Dorado Park Lakes	71	Shadow Cliffs Reservoir	72
Englebright Lake	20	Shasta Lake	4
Folsom Lake	29	Shastina, Lake	1
Hell Hole Reservoir	27	Sherwood, Lake	66
Hensley Lake	57	Slab Creek Reservoir	28
Herman, Lake	33	Solano, Lake	16
Hetch Hetchy Reservoir	52	Sonoma, Lake	14
Hodges, Lake	69	Stevens Creek Reservoir	40
Indian Valley Reservoir	12	Stony Gorge Reservoir	8
Kaweah, Lake	60	Thermalito Afterbay	17
Lafayette Reservoir	35	Trinity Lake	2
Marsh Creek Reservoir	36	Tulloch Reservoir	50
McClure, Lake	53	Turlock Lake	55
Mendocino, Lake	10	Uvas Reservoir	43
Mile Long Pond	73	Whiskeytown Lake	3
Millerton Lake	58	Wildwood, Lake	21
Modesto Reservoir	56	Woodward Reservoir	49

\* In this report, we use a standardized name format in which reservoir or lake goes last. Some of the reservoir names on this list have a comma included because their proper or common name begins with either reservoir or lake. For example, Lake Casitas is listed as "Casitas, Lake."

\*\* Note that "Beach Lake" will be changed on upcoming 303(d) List to "Black Crown Lake." For consistency with the 2010 303(d) List, this reservoir is referred to throughout staff report as "Beach Lake."

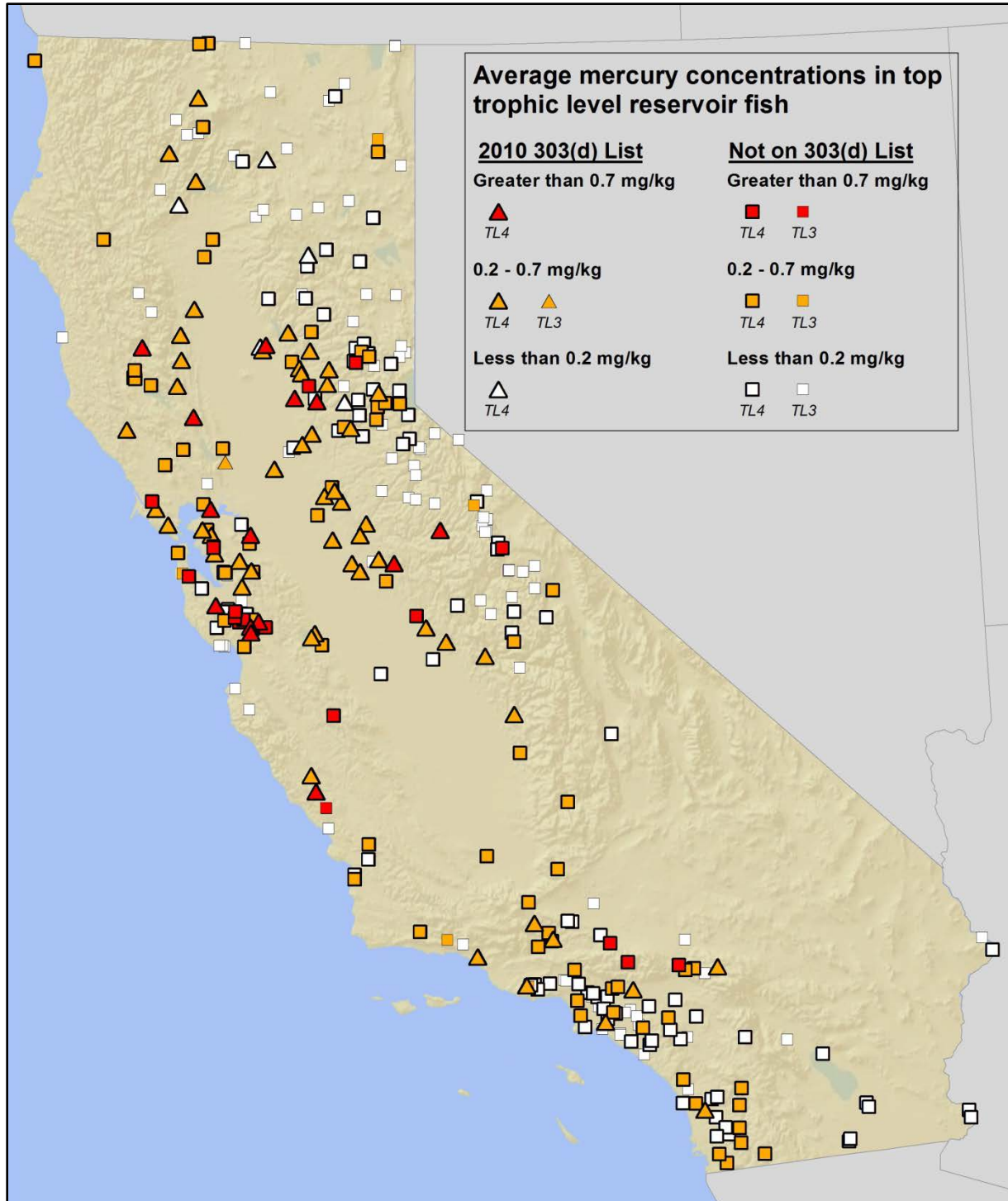


Figure 3.1: Map of average methylmercury concentrations in top trophic level reservoir fish

This map summarizes average methylmercury concentrations in trophic level (TL) 4 fish (150 mm to 500 mm) in reservoirs and indicates which reservoirs are on the 2010 303(d) List. If TL4 species were not sampled at a particular reservoir, staff calculated the average methylmercury concentration in TL3 species. TL4 species include predator species such as largemouth, smallmouth, and spotted bass, Sacramento pikeminnow, and brown trout. TL3 species include rainbow trout, carp, and bluegill, among others.

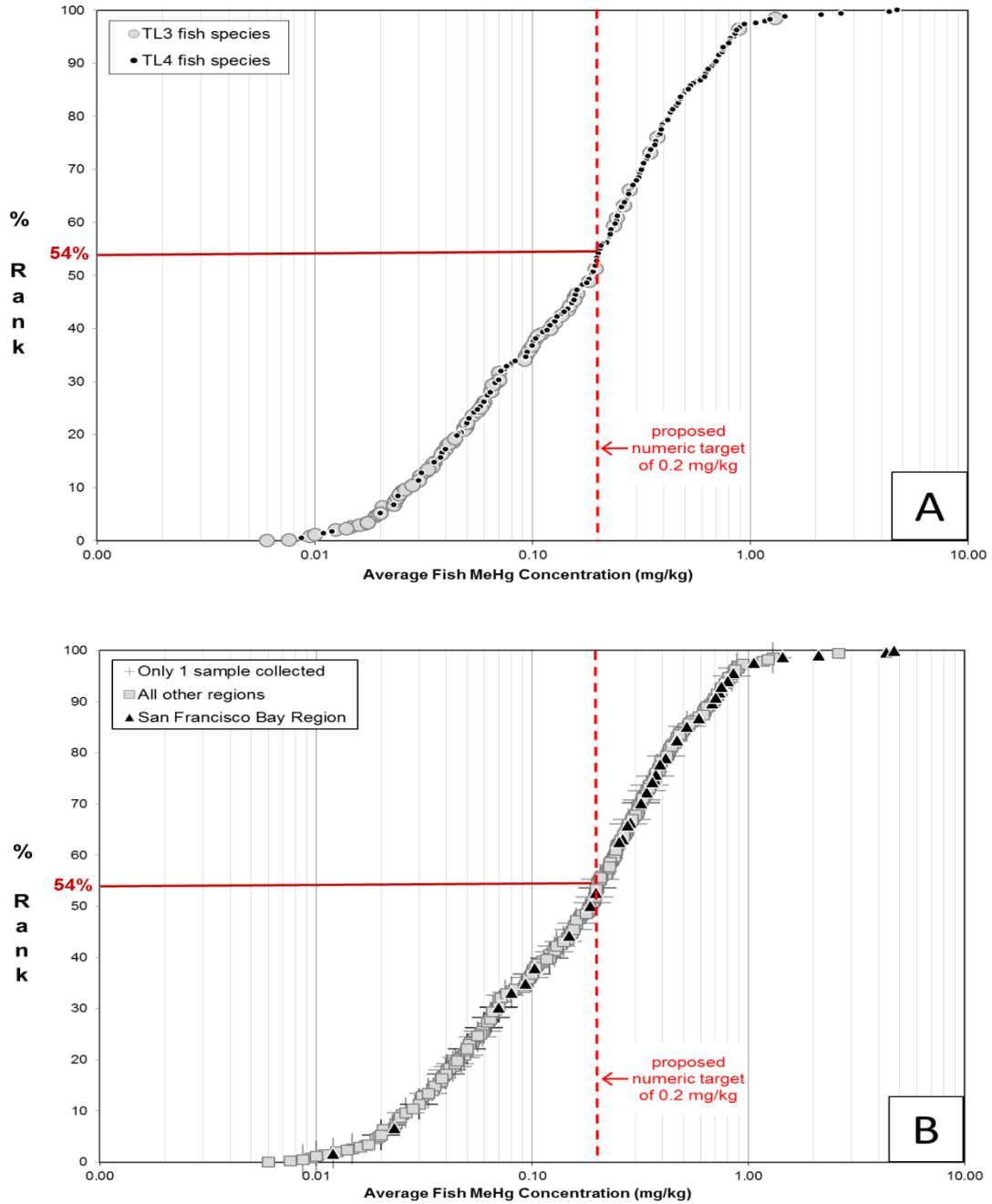


Figure 3.2: Plots of average fish methylmercury concentrations in top trophic level reservoir fish

Nearly half of the 348 reservoirs sampled have average fish methylmercury concentrations above the proposed sport fish target. [A] The grey symbols are reservoirs where only TL3 fish were sampled, largely because TL4 species are not resident in many high elevation Sierra Nevada reservoirs. [B] The black triangles are reservoirs in the Coast Range in the San Francisco Bay Region. The grey plus symbols indicate reservoirs that have only one fish sample.

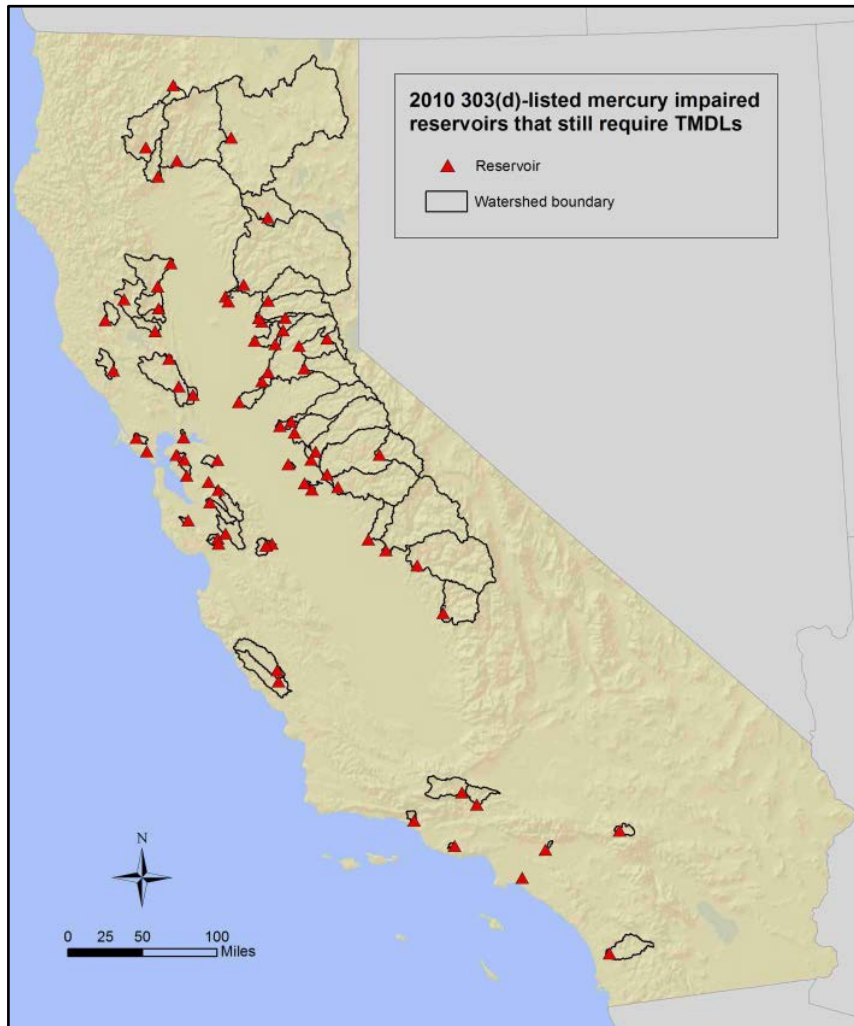


Figure 3.3: Map of watershed boundaries for 303(d)-listed reservoirs

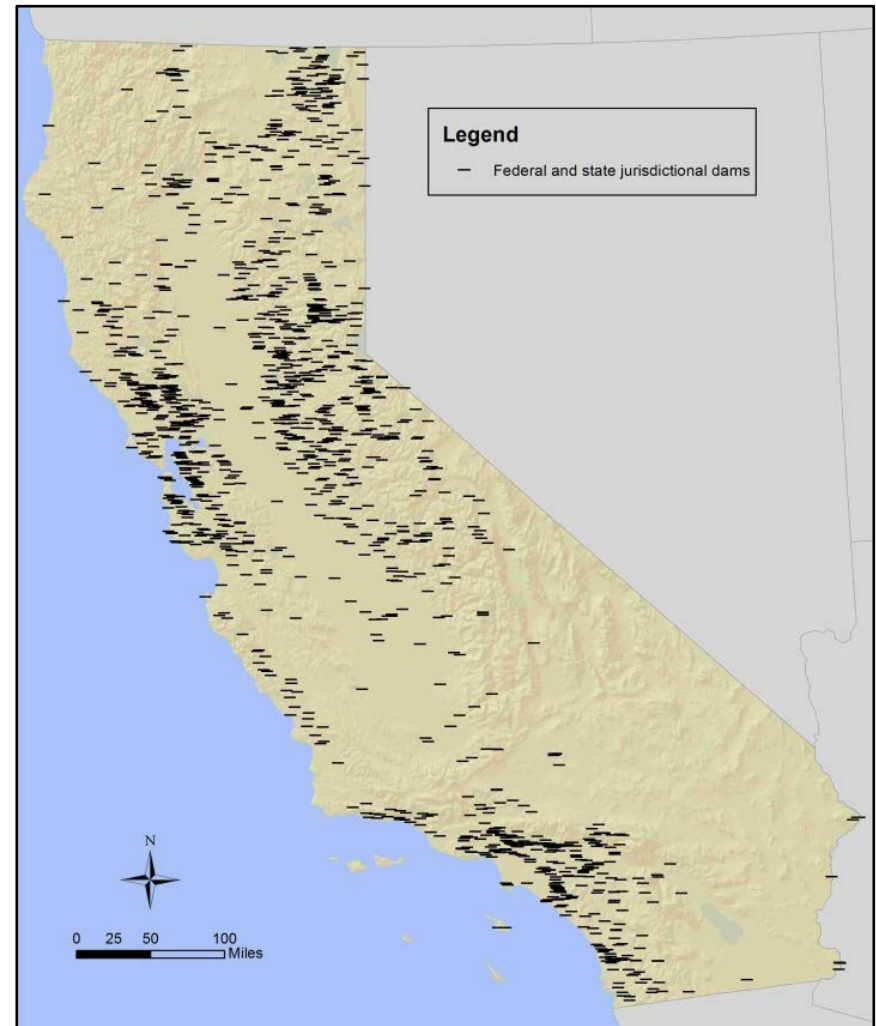


Figure 3.4: Map of state and federal jurisdictional dams  
[Source: DWR 2010a and 2010b]

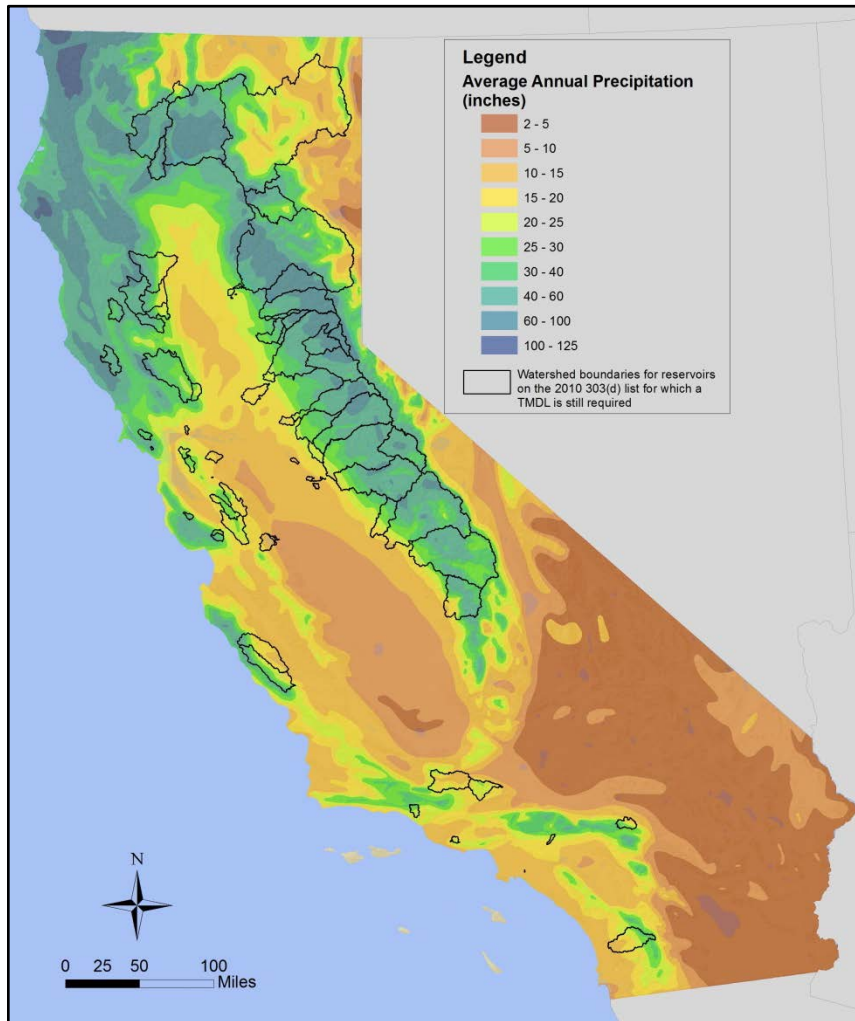


Figure 3.5: Map of average annual precipitation  
[Source: DWR et al. 1994]

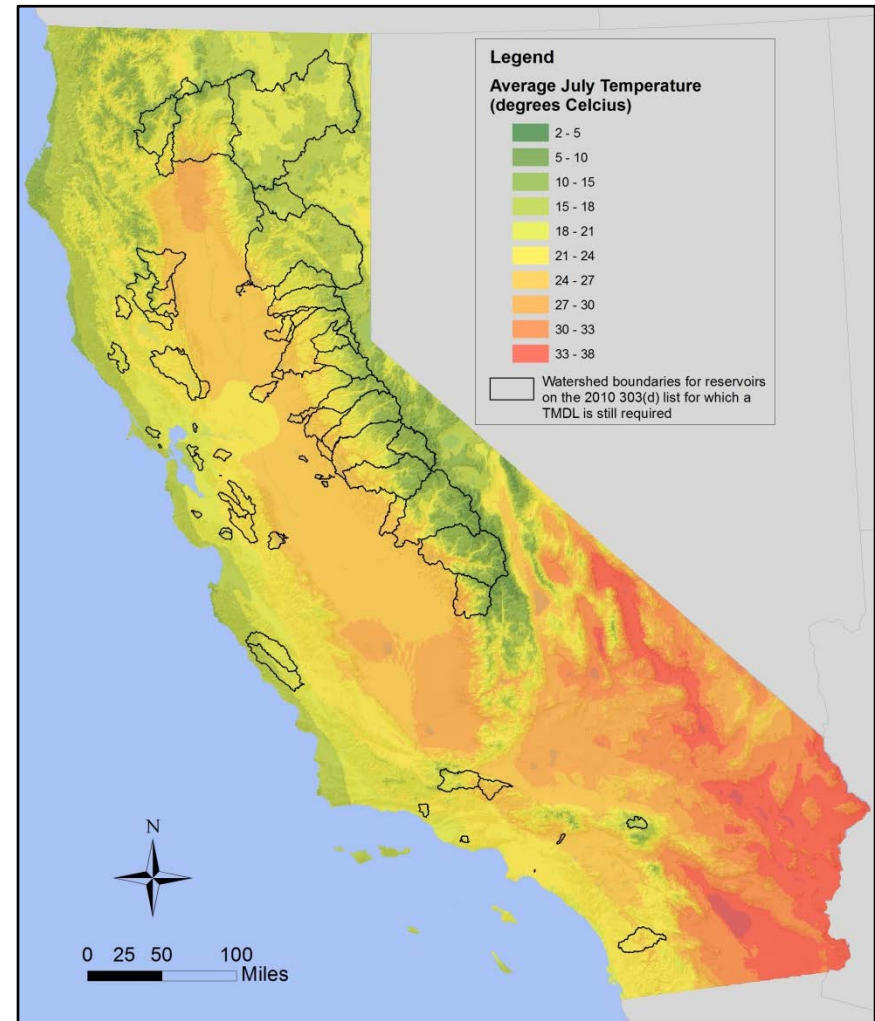


Figure 3.6: Map of average July temperature  
[Source: Hijmans et al. 2005]

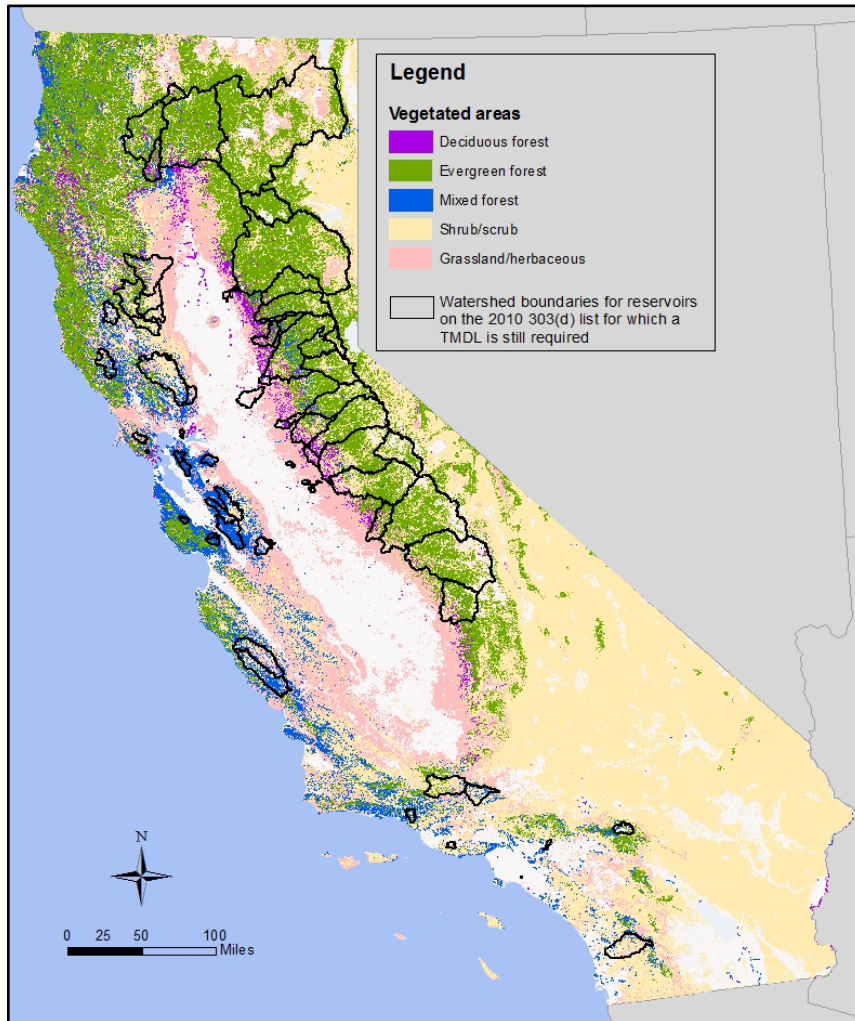


Figure 3.7: Map of vegetated areas

[Sources: USCB 2012a and 2012b; MRLC 2011; Fry et al. 2011]

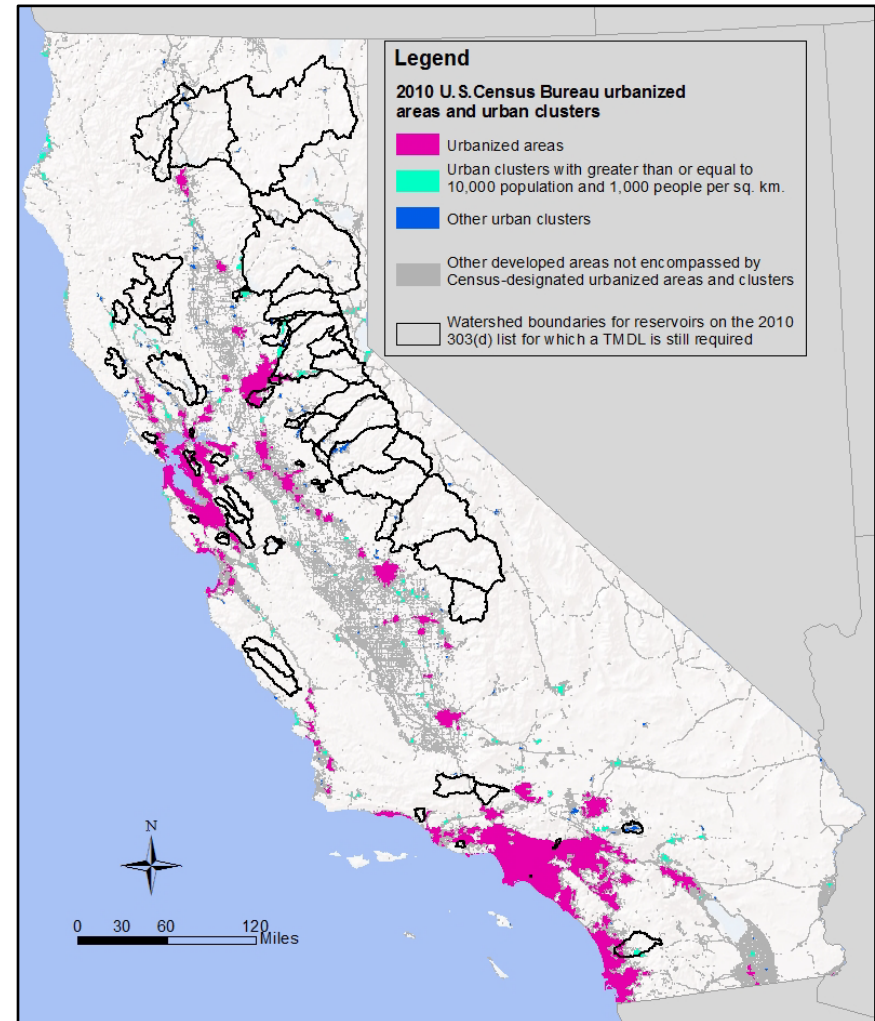


Figure 3.8: Map of urbanized and other developed areas

The bright pink and blue areas are high population regions. The grey indicates other developed areas such as major and minor roads throughout cultivated areas and other rural areas of the state.

[Sources: USCB 2012a and 2012b; MRLC 2011; Fry et al. 2011]

## Chapter 4 Conceptual Model: The Mercury Cycle and Bioaccumulation

### Section 4. 1 The Mercury Cycle

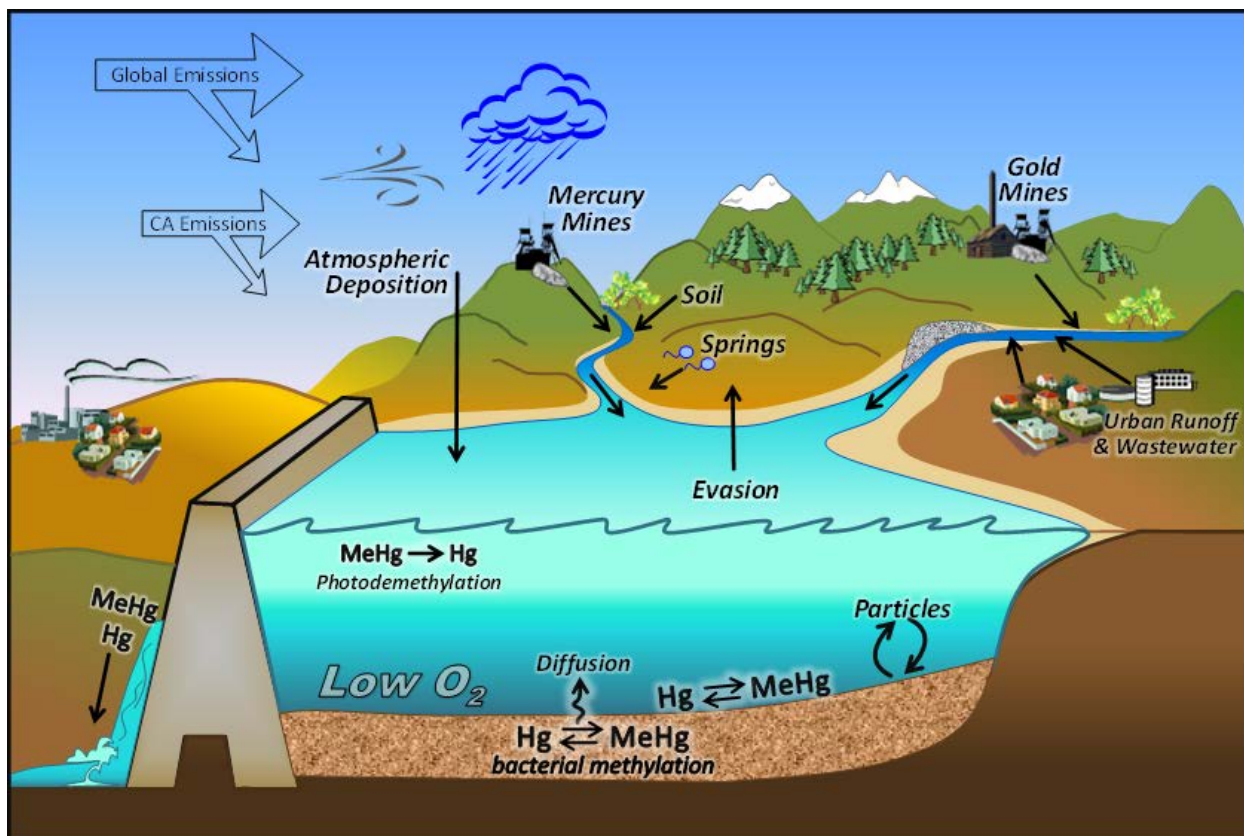


Figure 4.1: Mercury cycling in reservoirs

The top of the graphic depicts sources of mercury (both natural and anthropogenic) to reservoirs, which are primarily inorganic mercury. Once the mercury is transported to the reservoir some of the mercury is lost back to the atmosphere through evasion and some is transported downstream; however, the majority of the mercury settles in the bottom sediment of the reservoir. The inorganic mercury that remains in the reservoir can be converted to methylmercury by anaerobic sulfate-reducing bacteria in anoxic sediment or in the anoxic hypolimnion (dark blue) during thermal stratification. Some methylmercury is converted back to inorganic mercury through both abiotic and biotic processes, and some of the methylmercury is bioaccumulated up the reservoir's food web.



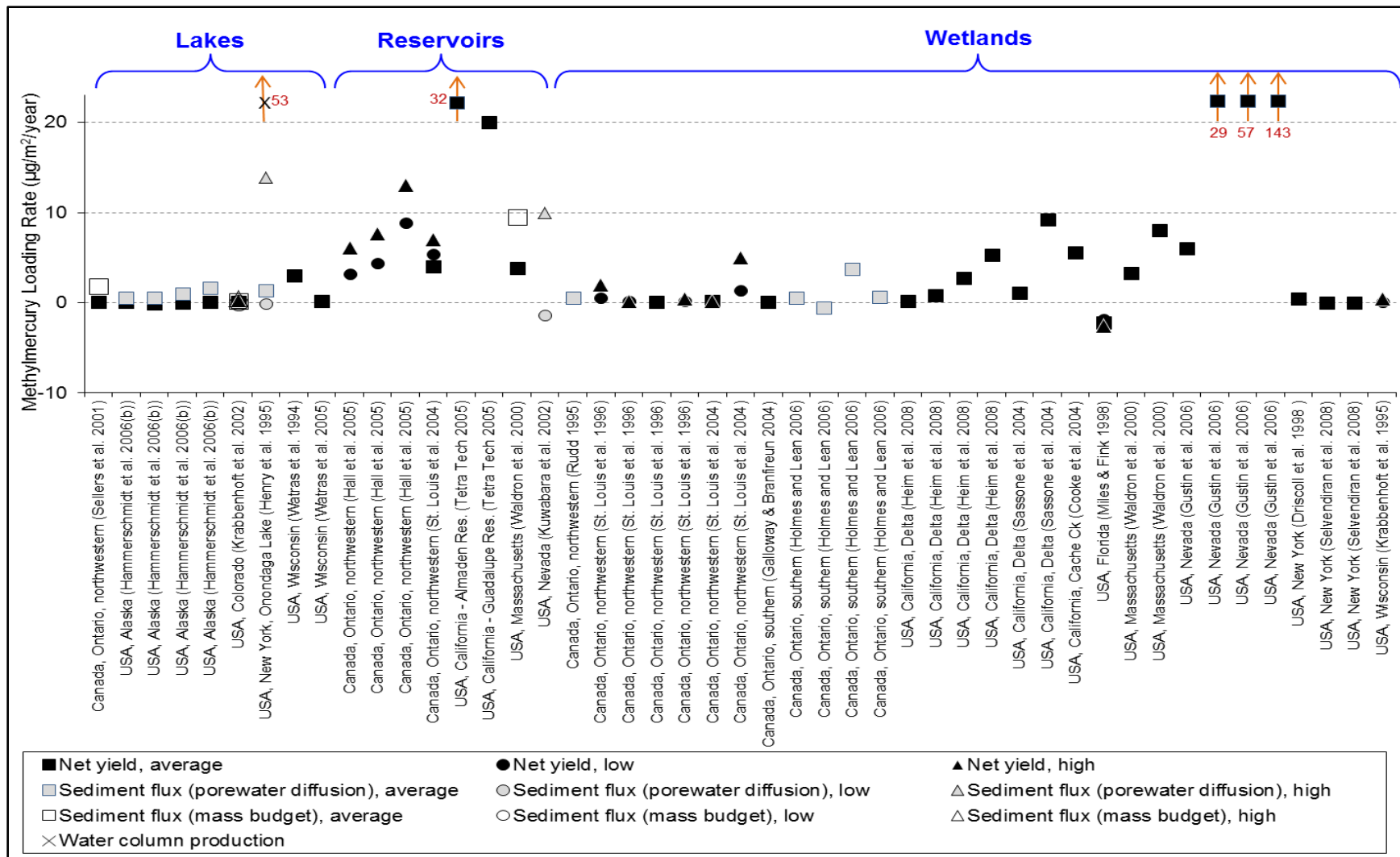


Figure 4.2: Methylmercury loading rates for lakes, reservoirs, wetlands, forests, agriculture, and urban land uses (A) Lakes, reservoirs, and wetlands

Methylmercury loading rates from reservoir and wetland land uses are substantially greater than the rates from agriculture, forests and urban.

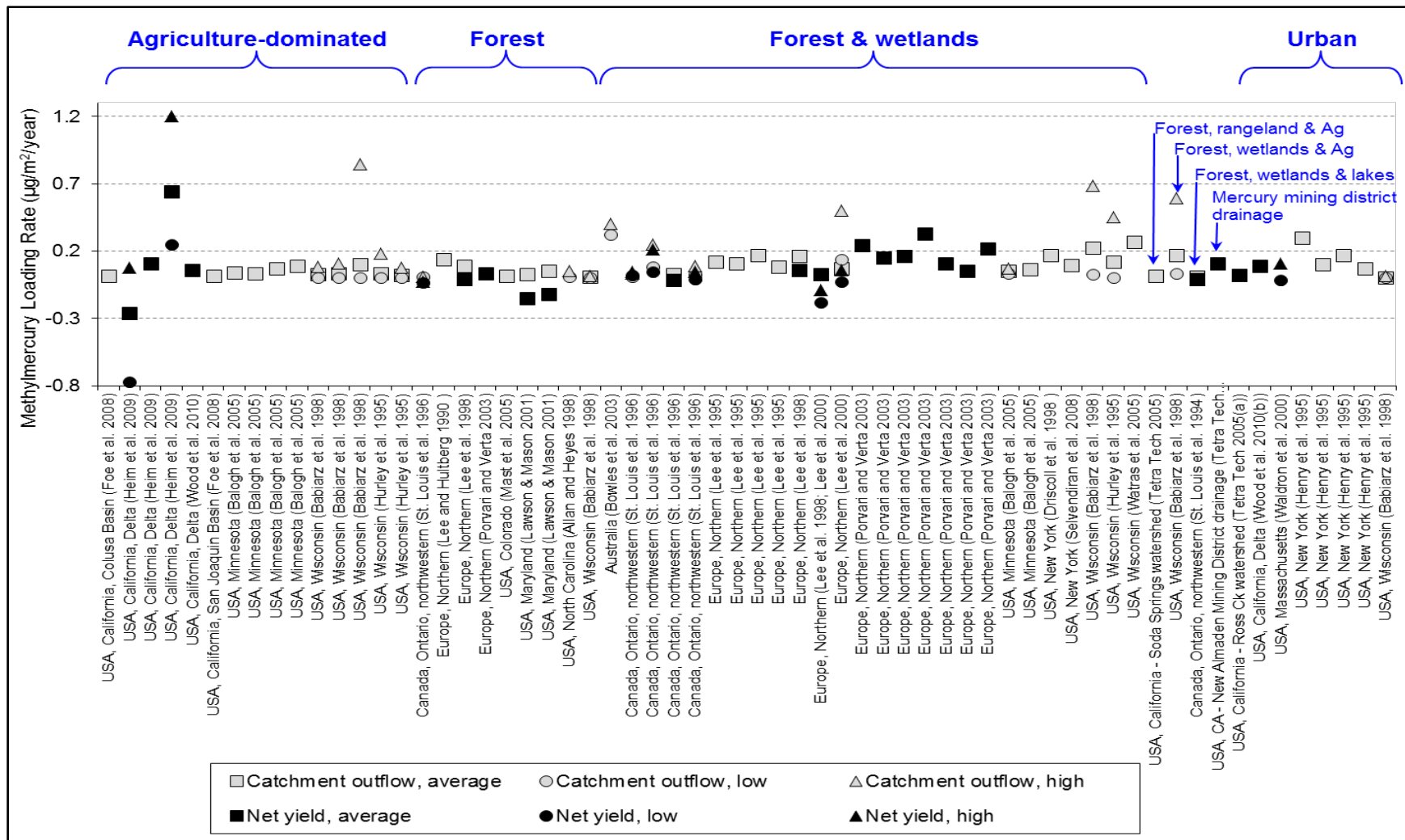


Figure 4.2: Methylmercury loading rates for lakes, reservoirs, wetlands, forests, agriculture, and urban land uses  
(B) Upland areas

Methylmercury loading rates for reservoir and wetland land uses are substantially greater than the rates for agriculture, forests and urban land uses.

## Section 4.2 Bioaccumulation

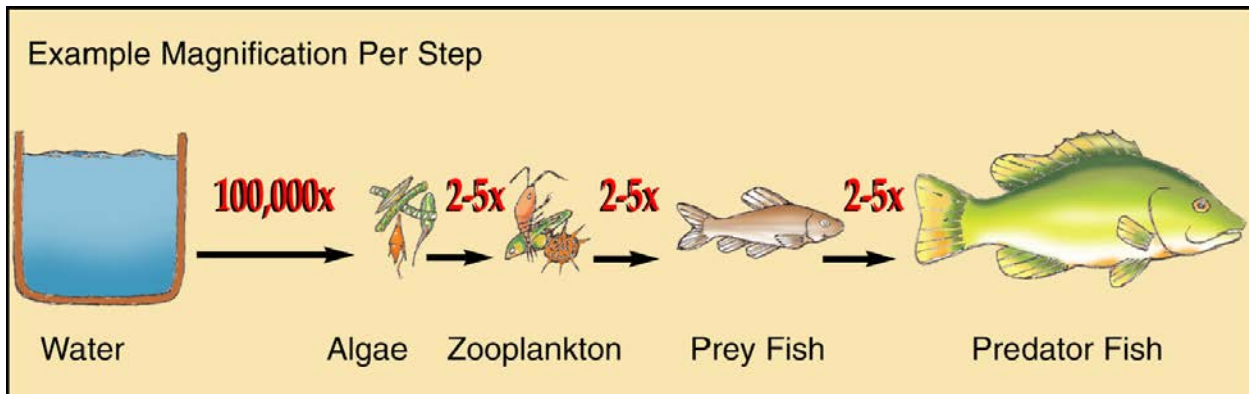


Figure 4.3: Food chain biomagnification of methylmercury

The single largest increase in methylmercury concentration in the aquatic environment is from water to algae at the base of the food web. The highest concentrations of methylmercury occur in the top trophic level fish, and these pose the greatest risk to human and wildlife fish consumers. One can deduce that adding additional levels to the food web could greatly magnify methylmercury concentrations in the upper trophic levels. Thus, food web dynamics greatly affects methylmercury accumulation in reservoirs.

[Source: Figure 5-7 in Tetra Tech 2005a]

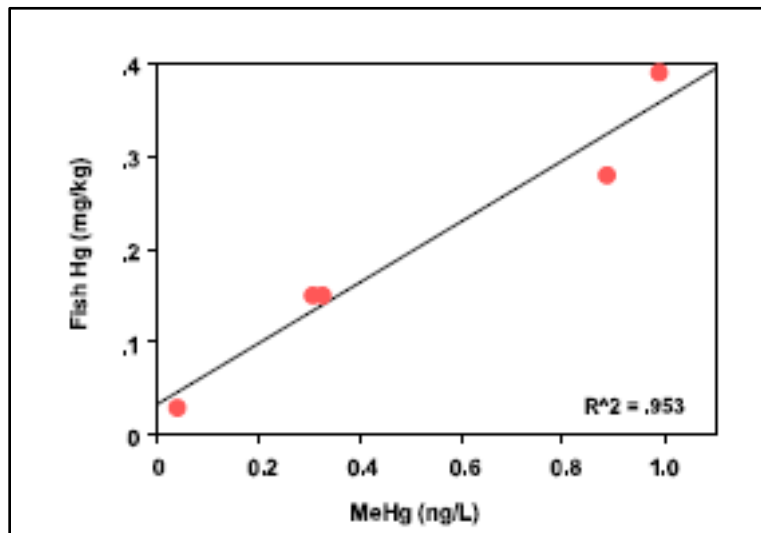


Figure 4.4: Relationship between mercury concentrations in California roach and unfiltered methylmercury concentrations in water samples in the Guadalupe River Watershed

A strong positive correlation was found between stream aqueous methylmercury concentrations and resident roach methylmercury concentrations in the Guadalupe River Watershed.

[Source: Figure 3-28 in Tetra Tech 2005a]

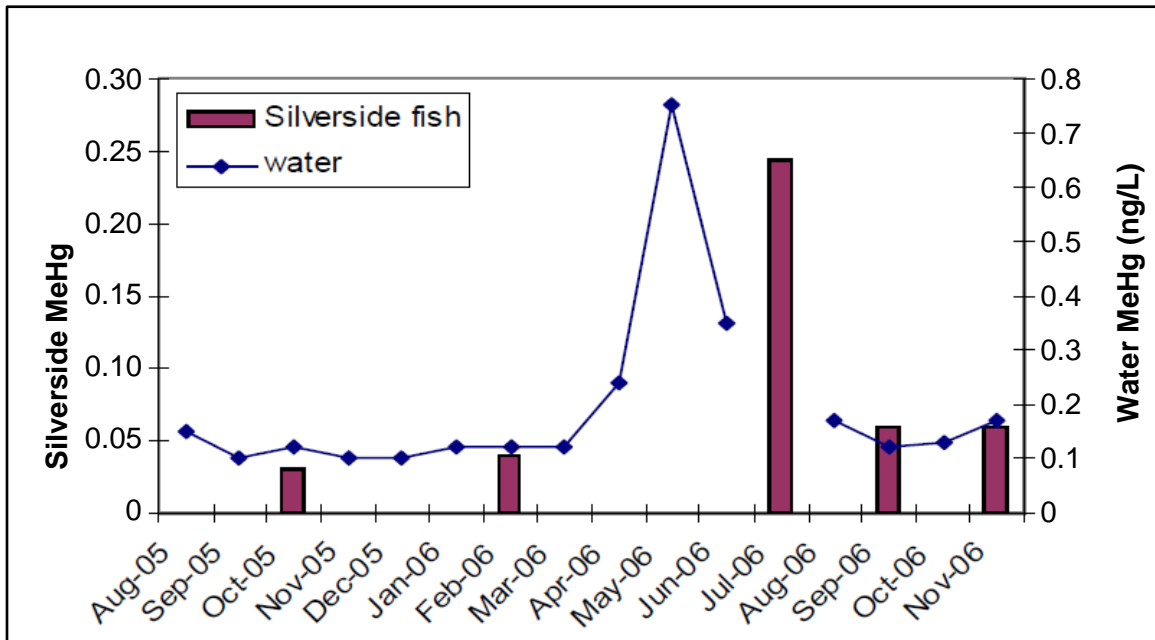


Figure 4.5: Plot of San Joaquin River small fish mercury concentrations and aqueous methylmercury concentrations

This graph illustrates increases in small fish methylmercury (MeHg) concentrations following increases in aqueous MeHg concentrations. This compares average MeHg concentrations in juvenile, small (45 – 75 mm) Mississippi silverside fish to monthly aqueous MeHg concentrations collected from the San Joaquin River at Vernalis. An extreme increase in small fish MeHg concentrations was seen in July 2006 following a May 2006 spike in aqueous MeHg. MeHg concentrations in juvenile silverside averaged 0.24 mg/kg at Vernalis (Slotton et al. 2007, page 59). (MeHg concentrations in other species of small fish also spiked; spikes in aqueous and small fish methylmercury also occurred in the Cosumnes River.) Both fish and aqueous MeHg levels decreased to nearly pre-flood levels by September.

[Sources: Foe et al. 2008, Figure 13; water data from Foe et al. 2008; small fish data from Slotton et al. 2007]

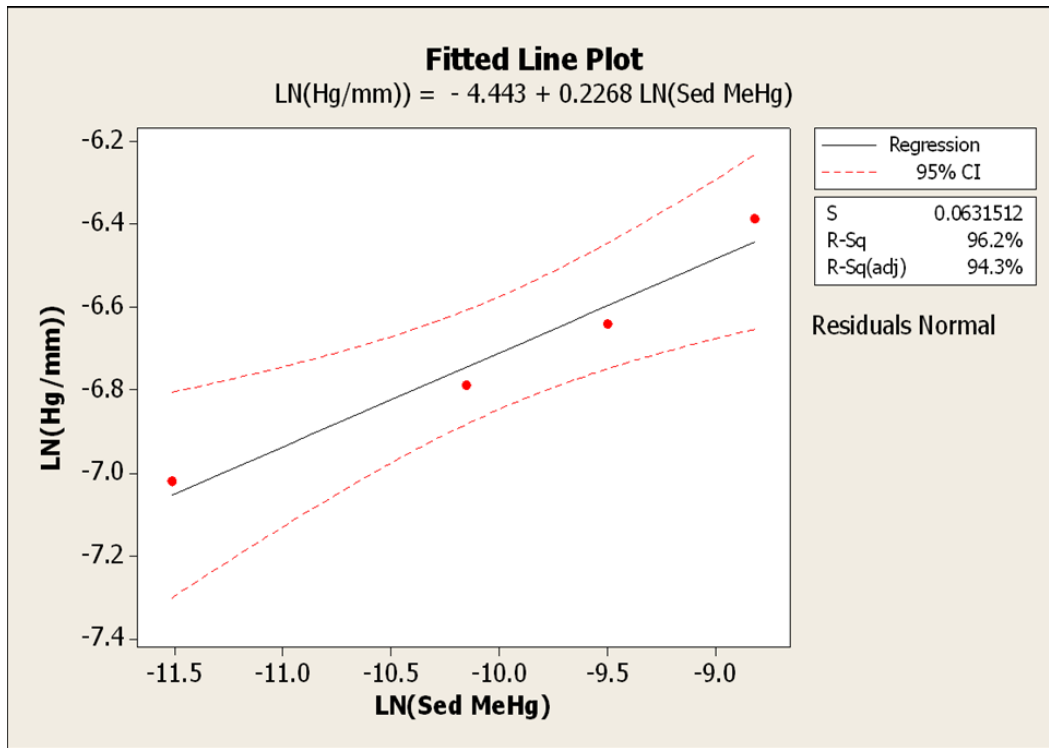


Figure 4.6: Fitted line plot for Lake Oroville length-normalized spotted bass methylmercury concentrations versus sediment methylmercury concentrations

A strong positive correlation was found between natural logarithm transformed sediment methylmercury concentrations and length normalized (MeHg mg/kg/mm) spotted bass methylmercury concentrations collected from the same arms of Lake Oroville in a California Department of Water Resources fish and sediment contaminant study (DWR 2006). The correlation suggests that Lake Oroville food web methylmercury bioaccumulation is highly influenced by in-lake production of methylmercury.

### Section 4.3 The Mercury Cycle Particular to Reservoirs

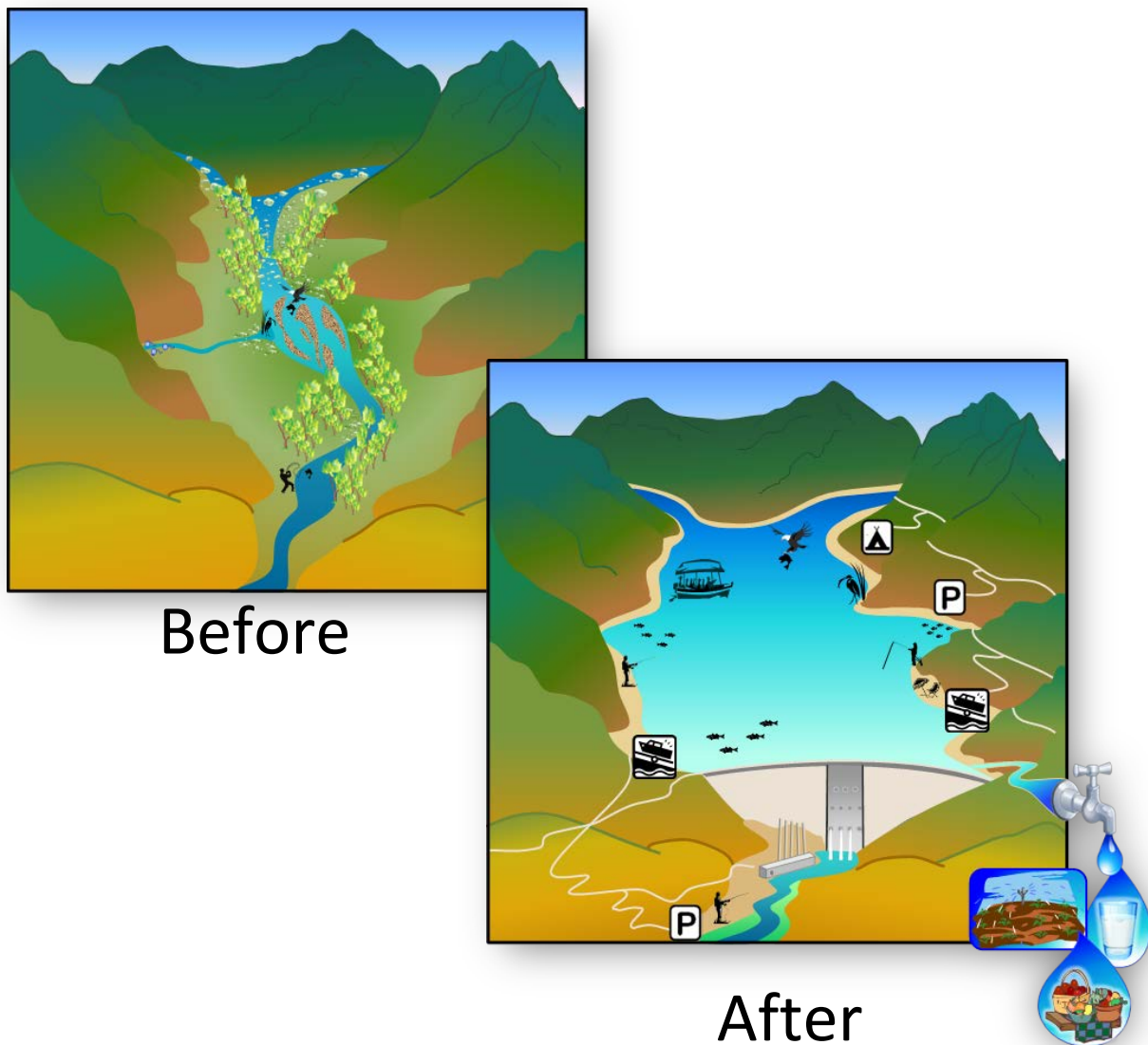


Figure 4.7: A cartoon illustrating the effect of reservoir flooding on terrestrial ecosystems. The “Before” graphic depicts an environment with a high gradient, fast flowing river that is shaded, cold, turbulent, and well oxygenated. The “After” graphic displays how the reservoir environment has slowed, warmed, and changed water chemistry. The flooding of terrestrial soils creates conditions that enhance mercury methylation. The warmed water of the reservoir allows non-native warm water fisheries to exist. These warm water predatory fish tend to bioaccumulate higher levels of methylmercury than native cold water fish species.

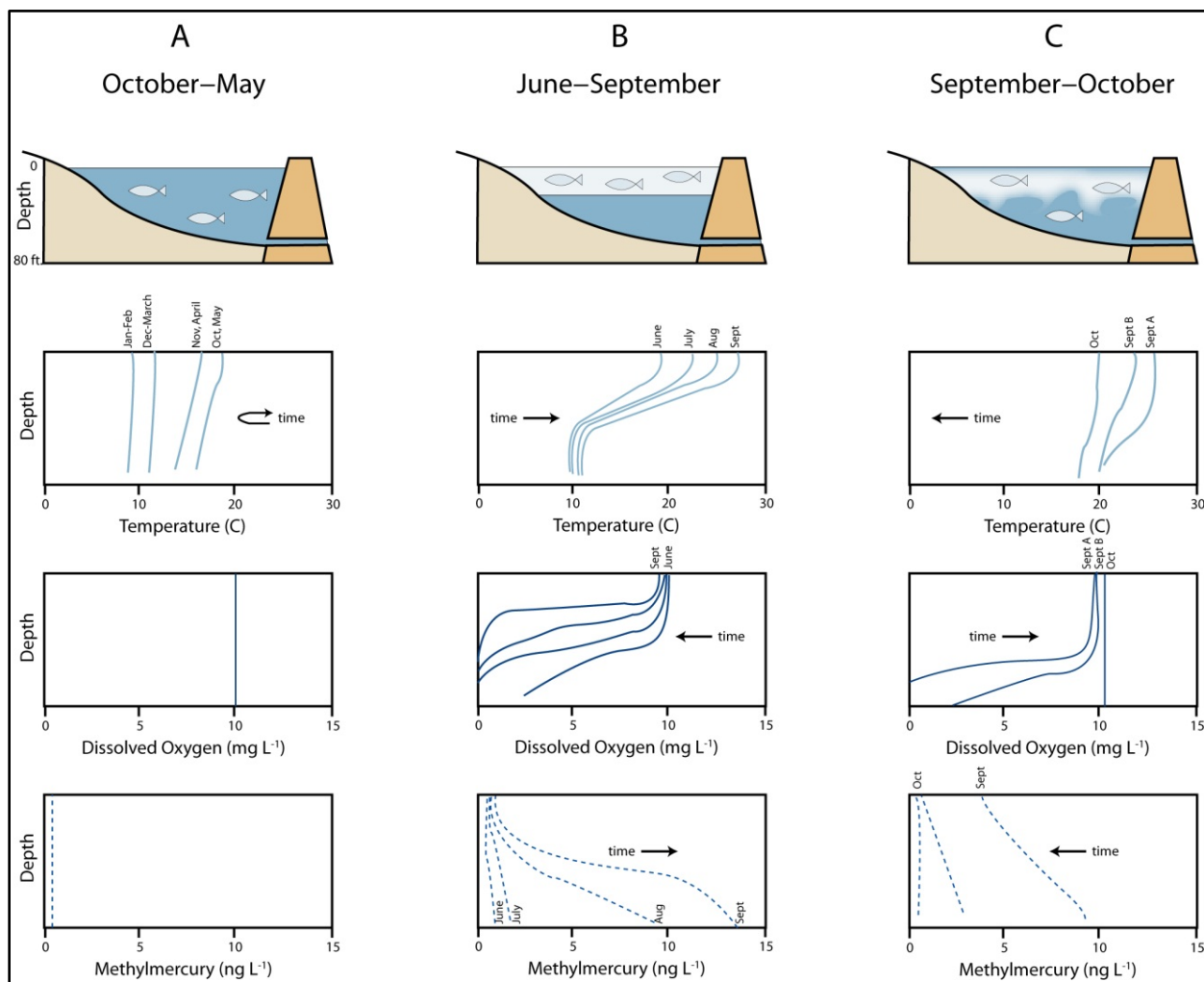


Figure 4.8: Annual hydrologic cycle in reservoirs: temperature, dissolved oxygen, and methylmercury

(A) From early fall through early spring, the reservoir water temperature is fairly uniform throughout the water column, and water mixes.

(B) Warm summer air temperatures create a temperature gradient within the reservoir. The difference between the temperature of the surface and bottom reservoir water creates density gradients that resist vertical mixing. Oxygen is depleted in the deep waters from respiration and organic carbon decomposition. These anoxic conditions stimulate mercury methylation, and methylmercury builds up in the unmixed deep waters.

(C) During late summer, cooling air temperatures cool reservoir surface waters. The decreasing temperature gradient between the surface and bottom waters allows the waters to mix. The accumulated methylmercury in the bottom water becomes distributed throughout the water column, where it is available to enter the food web.

[Source: Figure 5-13 in Tetra Tech 2005a]

ORP (mV)	Electron Acceptor	Redox Condition
+700 to +400	Oxygen (O <sub>2</sub> )	Oxidized
+400 to +300	Nitrate (NO <sub>3</sub> <sup>-</sup> )	Moderately reduced
+200 to +100	Manganese (Mn <sup>4+</sup> )	Moderately reduced
+100 to -100	Iron (Fe <sup>3+</sup> )	Reduced
-100 to -200	Sulfate (SO <sub>4</sub> <sup>2-</sup> )	Reduced
-200 to -300	Methane production (CO <sub>2</sub> )	Highly reduced

Figure 4.9: Oxidation reduction potential (ORP) scale and ranges where reduction becomes thermodynamically preferred for some common chemicals

This matrix illustrates the ecological oxidation-reduction (redox) sequence from oxygen to nitrate, manganese, iron, sulfate, and finally to methanogenesis. These electron receptors are listed in the second column and redox potential (ORP) is listed in the first column. Before stratification, reservoir conditions start at the first row in aerobic conditions, i.e., when oxygen is present and the redox potential is above 400 millivolts (mV). As oxygen, then nitrate, manganese, and iron are depleted, the redox potential drops, as indicated by reading from top to bottom. Significantly, methylmercury is primarily produced by anaerobic sulfate-reducing bacteria.

[Source: Delaune and Reddy 2005]



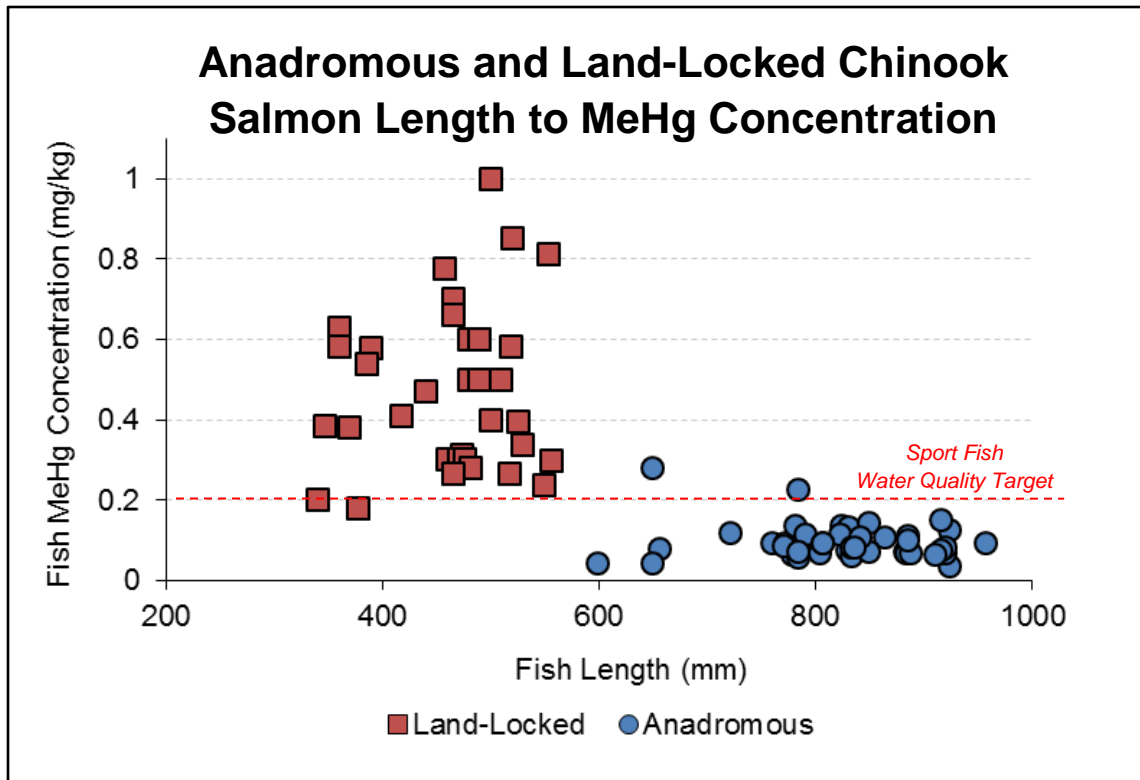


Figure 4.10: Plot of methylmercury concentrations in anadromous and land-locked Chinook

This plot shows methylmercury concentrations in land-locked Chinook salmon in California reservoirs (red squares on the left) and in anadromous Chinook salmon in California rivers (blue circles on the right). Land-locked Chinook are smaller and have much higher mercury levels than anadromous Chinook. Anadromous fisheries are being restored for many reasons, and a positive outcome of that effort is lower fish methylmercury levels.

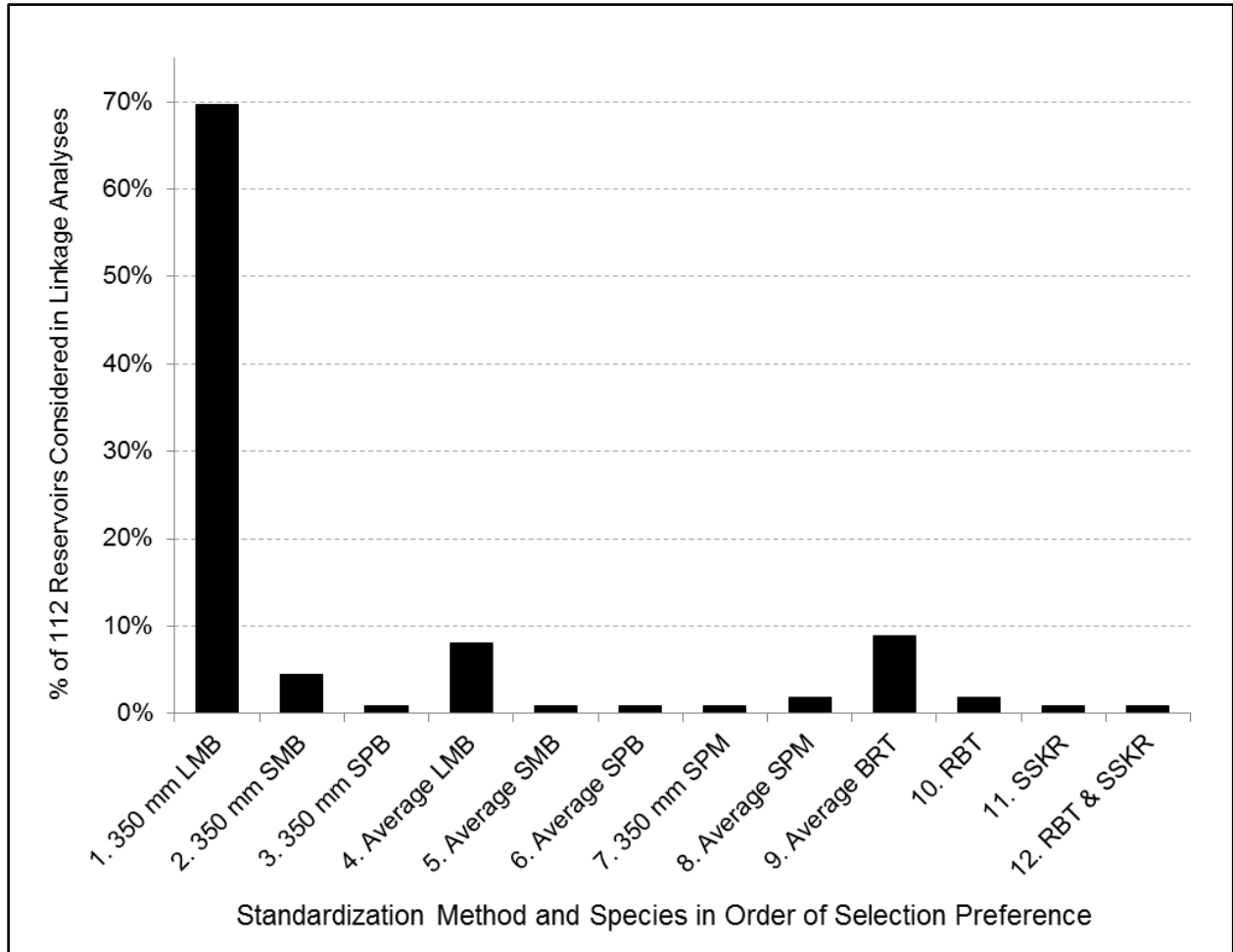


Figure 5.1: Bar chart summarizing fish species and fish methylmercury and length standardization methods employed for linkage analysis

Methods similar to Tremblay and others (1998) and Davis and others (2010) were used to determine length-standardized fish methylmercury concentrations. The standardized fish for most reservoirs was 350 mm length largemouth bass (LMB). If no LMB were available for a given reservoir, then other predatory fish data were used to calculate standardized fish methylmercury concentrations. Preference was given to other black bass species, smallmouth bass (SMB) and spotted bass (SPB).

Preference was given to black bass species with enough data to length standardize their methylmercury concentrations. If not enough data were available to standardize for length for any black bass species at a given reservoir, the average concentration for the highest trophic level black bass species was used.

If no black bass data were available, Sacramento pikeminnow (SPM) and brown trout (BRT) were used. If no predatory fish data were available, lower trophic level fish—rainbow trout (RBT) and Sacramento sucker (SSKR)—were used.

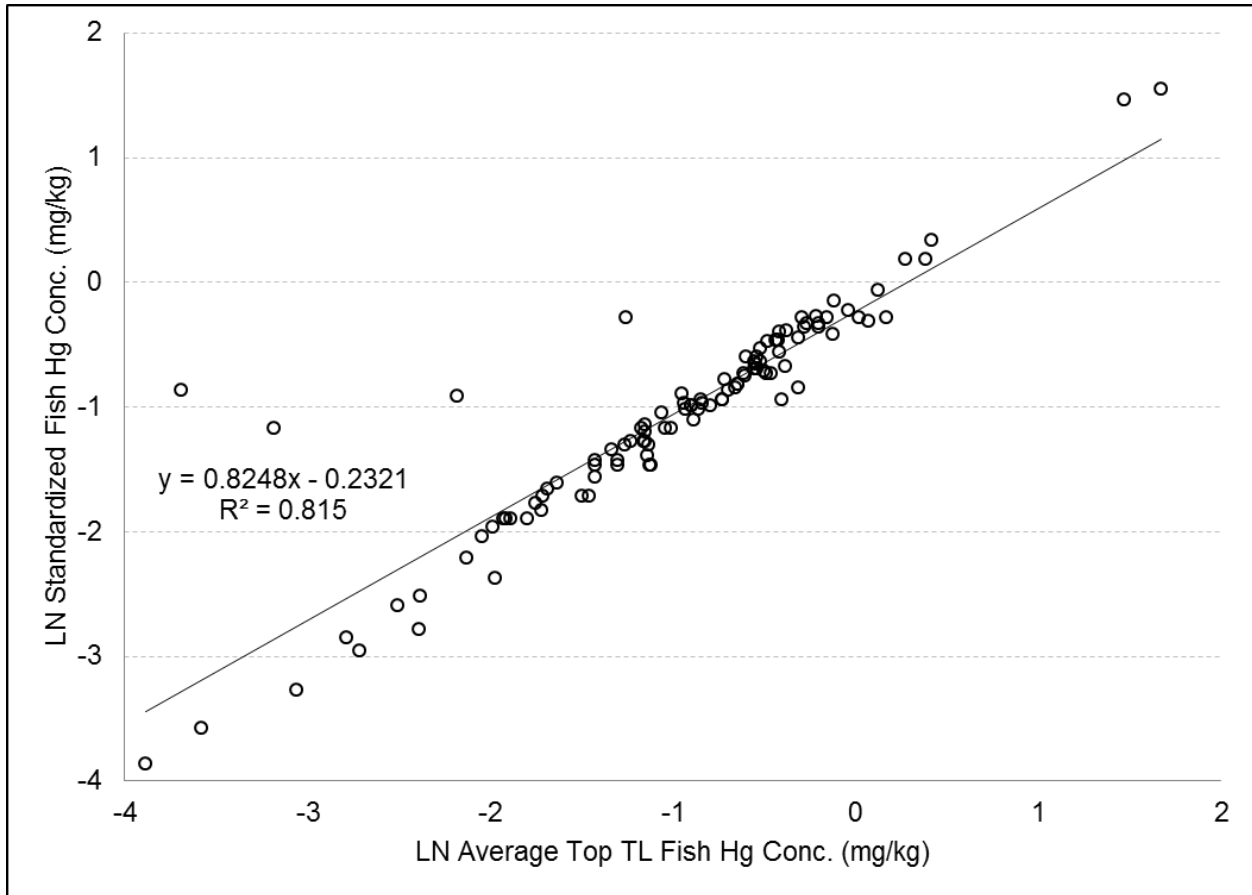


Figure 5.2: Plot of correlation between standardized fish mercury concentrations and the average fish mercury concentrations in legal-sized top trophic level fish (length 200 – 500 mm TL4 or 150 – 500 mm TL3) for reservoirs in the Linkage Analysis

The correlation between standardized fish methylmercury (MeHg) concentrations and average MeHg concentrations in legal-sized TL4 fish is statistically significant ( $n = 107$  reservoirs,  $R^2 = 0.82$ ). Note that the size of TL4 standardized fish (150 – 500 mm) differs slightly from size used for Statewide Water Quality Objective and sport fish target (200 – 500 mm).

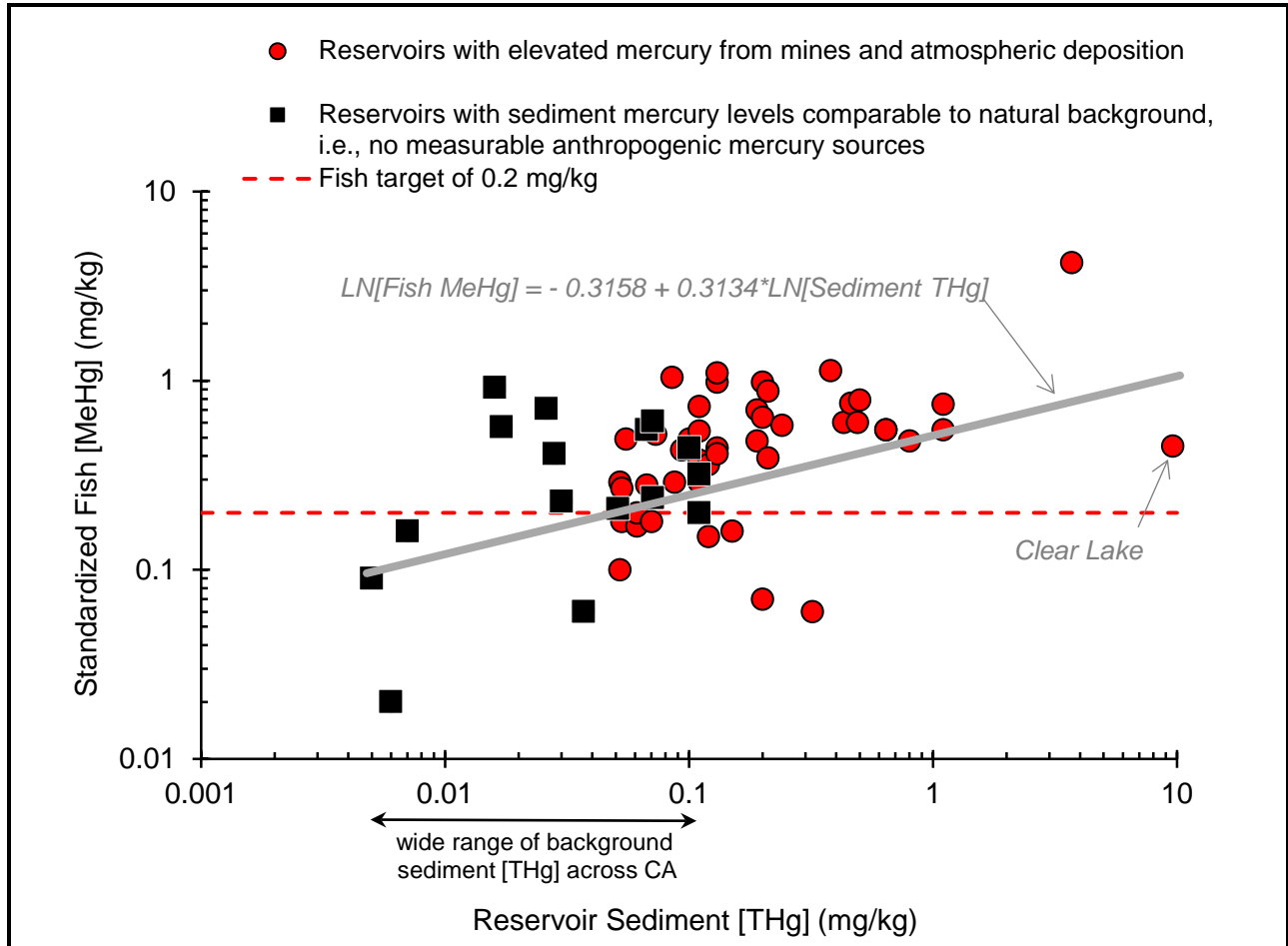


Figure 5.3: Plot of correlation between standardized fish methylmercury concentrations and geomean sediment mercury concentrations in California reservoirs

This graph plots geomean sediment total mercury (THg) concentrations against standardized fish methylmercury (MeHg) concentrations in California reservoirs, both with log scales. The black boxes are reservoirs where their sediment THg concentrations are comparable to natural background. The red circles are reservoirs with elevated mercury from mines and atmospheric deposition. Reservoirs in different parts of the state have different natural background levels of mercury. See Chapter 6 (section 6.2) for a review of natural (pre-industrial) and modern background mercury concentrations in soils and sediments throughout California.

There is a statistically significant correlation between standardized fish MeHg and sediment THg ( $n = 62$  reservoirs, adjusted  $R^2 = 0.227$ ,  $p < 0.001$ ). However, there is substantial fish MeHg variability not explained by sediment THg concentrations. There can be high fish MeHg in reservoirs where there is low sediment THg, low fish MeHg where there is high sediment THg, and reservoirs where there is extensive mercury contamination but the fish MeHg are not as high as we would expect from the high sediment THg concentrations. Further, there are many reservoirs with sediment THg concentrations comparable to natural background that have fish MeHg levels that exceed the sport fish water quality target (0.2 mg/kg). In summary, this plot illustrates how multiple factors are at play, more than just mercury pollution sources and associated sediment mercury concentrations.

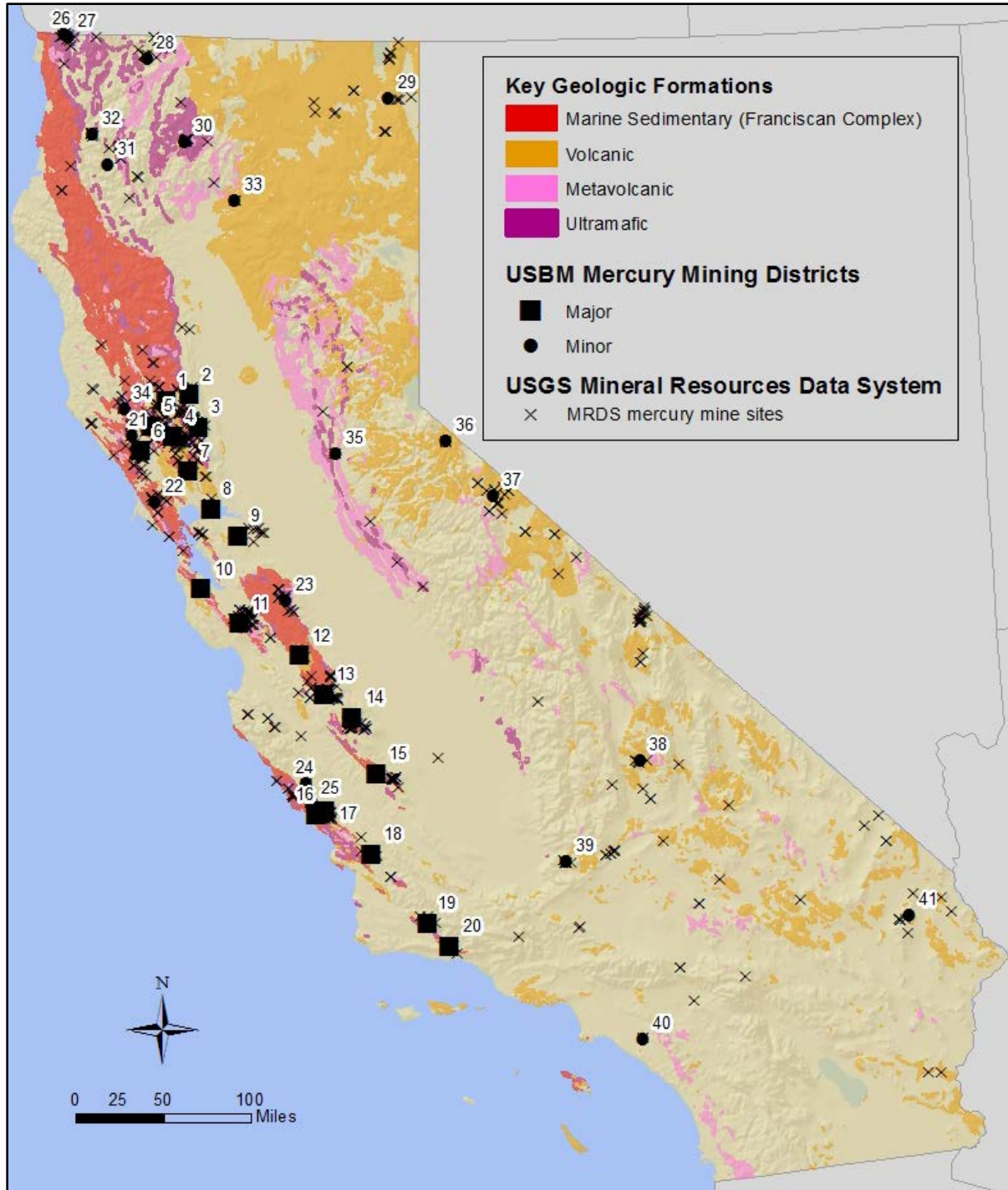


Figure 6.1: Statewide map of historic mercury mining districts, mercury mine sites, and geologic formations where naturally mercury-enriched soils may occur

The names of the numbered major and minor mercury mining districts are listed on the following page.

[Sources: CDOC-DMG 2000; USBM 1965, Figure 7; USGS 2008]

## Mercury Mining Districts in California as Labeled on Figure 6.1

<b>Map Code</b>	<b>Name</b>	<b>Type</b>	<b>Map Code</b>	<b>Name</b>	<b>Type</b>
1	Clear Lake	Major	21	Skaggs Springs	Minor
2	Wilbur Springs	Major	22	Petaluma	Minor
3	Knoxville	Major	23	Del Puerto – Orestimba	Minor
4	East Mayacmas	Major	24	Bryson & San Capoforo	Minor
5	West Mayacmas	Major	25	Pine Mt	Minor
6	Guerneville	Major	26	Diamond Creek	Minor
7	Oakville	Major	27	Patrick Creek	Minor
8	Sulphur Springs Mt	Major	28	Klamath River	Minor
9	Mount Diablo	Major	29	Alturas	Minor
10	Emerald Lake	Major	30	Altoona	Minor
11	New Almaden	Major	31	New River	Minor
12	Stayton	Major	32	Mill Creek	Minor
13	Central San Benito	Major	33	Clover Creek	Minor
14	New Idria	Major	34	Occident	Minor
15	Parkfield	Major	35	Nashville	Minor
16	Cambria – Oceanic	Major	36	Mogul	Minor
17	Adelaide	Major	37	Bridgeport	Minor
18	Rinconada	Major	38	Coso	Minor
19	Cachuma	Major	39	Tehachapi	Minor
20	Los Prietos	Major	40	Tustin	Minor
			41	San Bernardino County	Minor

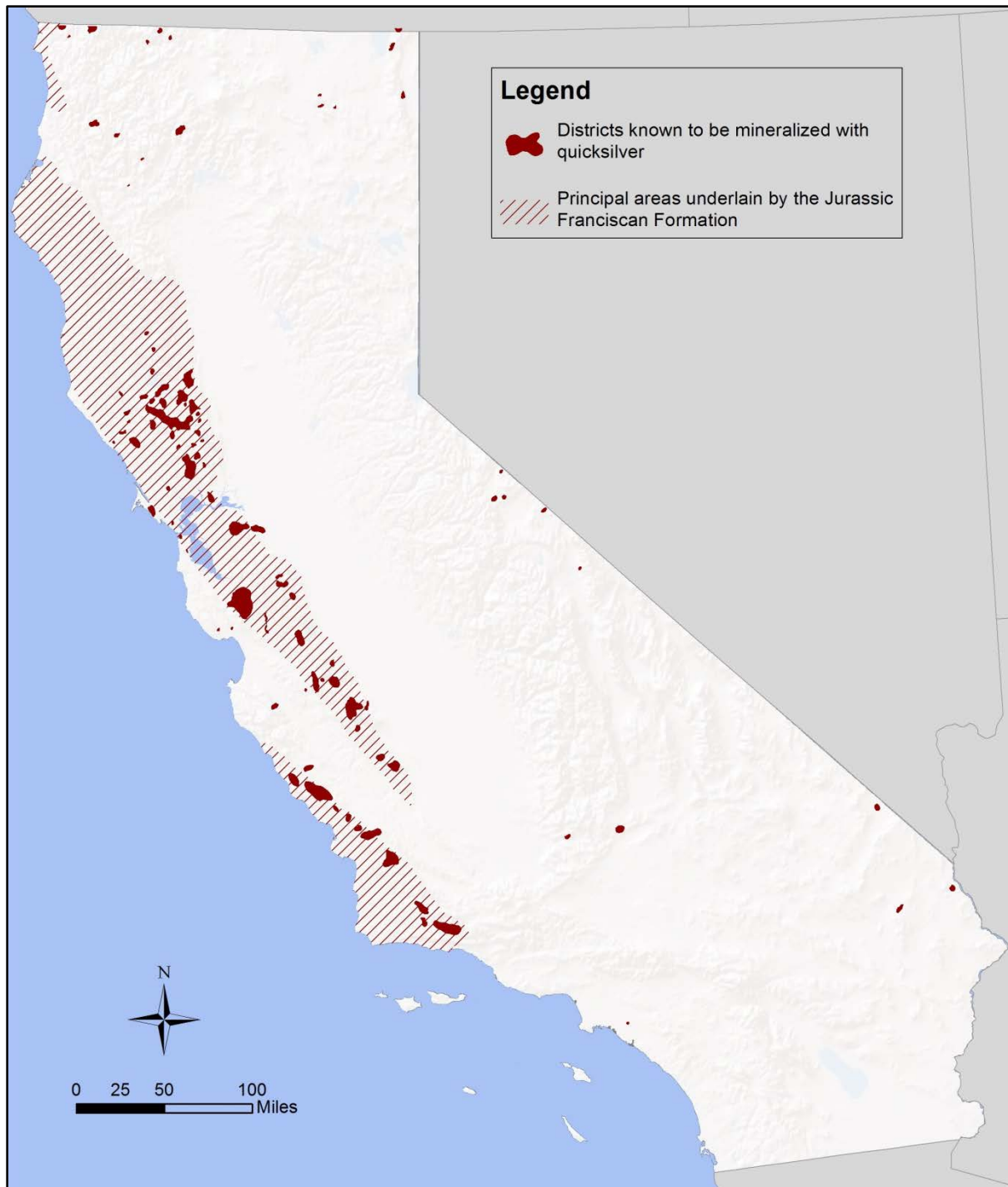


Figure 6.2: Statewide map of quicksilver (mercury) mineralized provinces in California identified in 1939 “Economic Mineral Map of California No. 1–Quicksilver”

The “districts known to be mineralized with quicksilver” (solid red) and “principal areas underlain by the Jurassic Franciscan Formation” (red hatching) mapped on the California Division of Mines’ “Economic Mineral Map of California No. 1 – Quicksilver” indicate the areas in California where naturally mercury-enriched soils may occur.

[Source: Jenkins 1939]

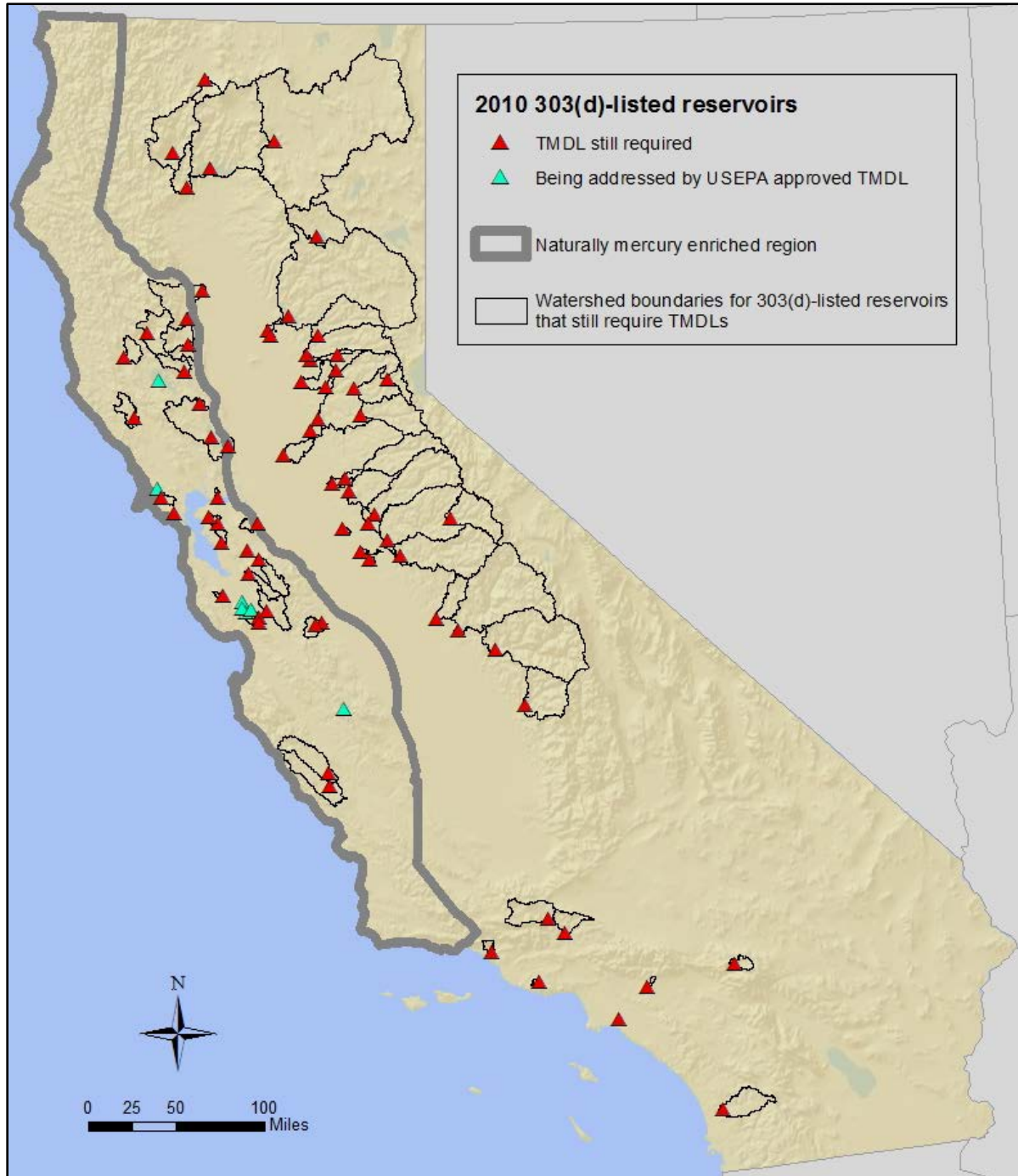


Figure 6.3: Statewide map showing the delineation of the naturally mercury-enriched region compared to 2010 303(d)-listed mercury-impaired reservoir watershed boundaries

Water Board staff based the delineation of the naturally mercury-enriched region primarily on the “Quicksilver Mineral Provinces” mapped on the California Division of Mines’ “Economic Mineral Map of California No. 1 – Quicksilver” (Jenkins 1939). The location of historic mercury mining districts (USBM 1965), historic mercury mine sites (USGS 2005), surface geology (CDOC-DMG), and background soil mercury concentrations (USGS 2008) also guided the delineation.



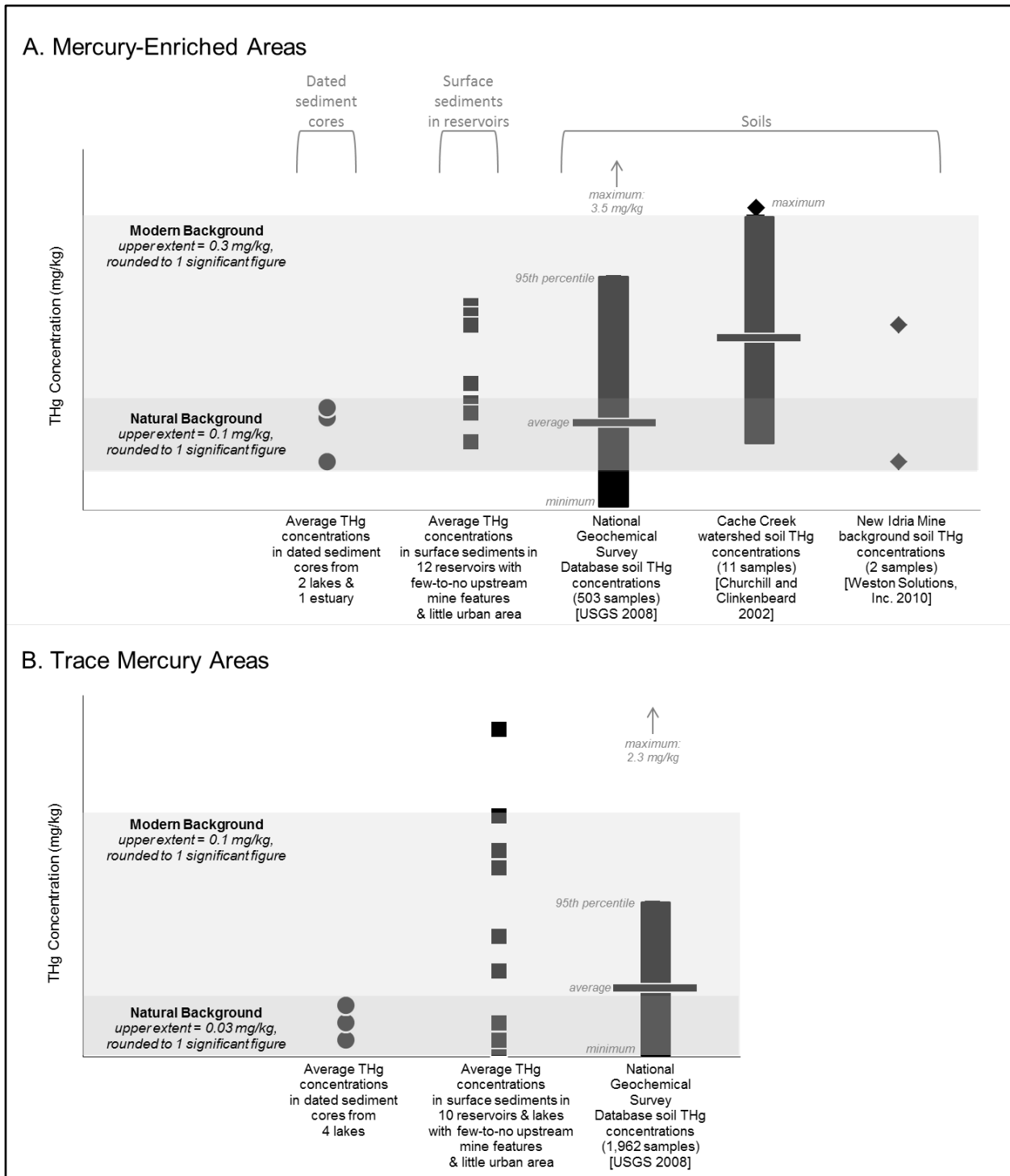


Figure 6.4: Chart illustrating natural (pre-industrial) and background soil mercury levels based on dated sediment core and soil mercury concentrations

Natural background levels are based on average mercury concentrations observed in dated lake and estuary sediment cores. Modern background levels are based on average surface sediment mercury concentrations observed in lakes and reservoirs and the 95<sup>th</sup> percentile mercury concentrations observed in soils.

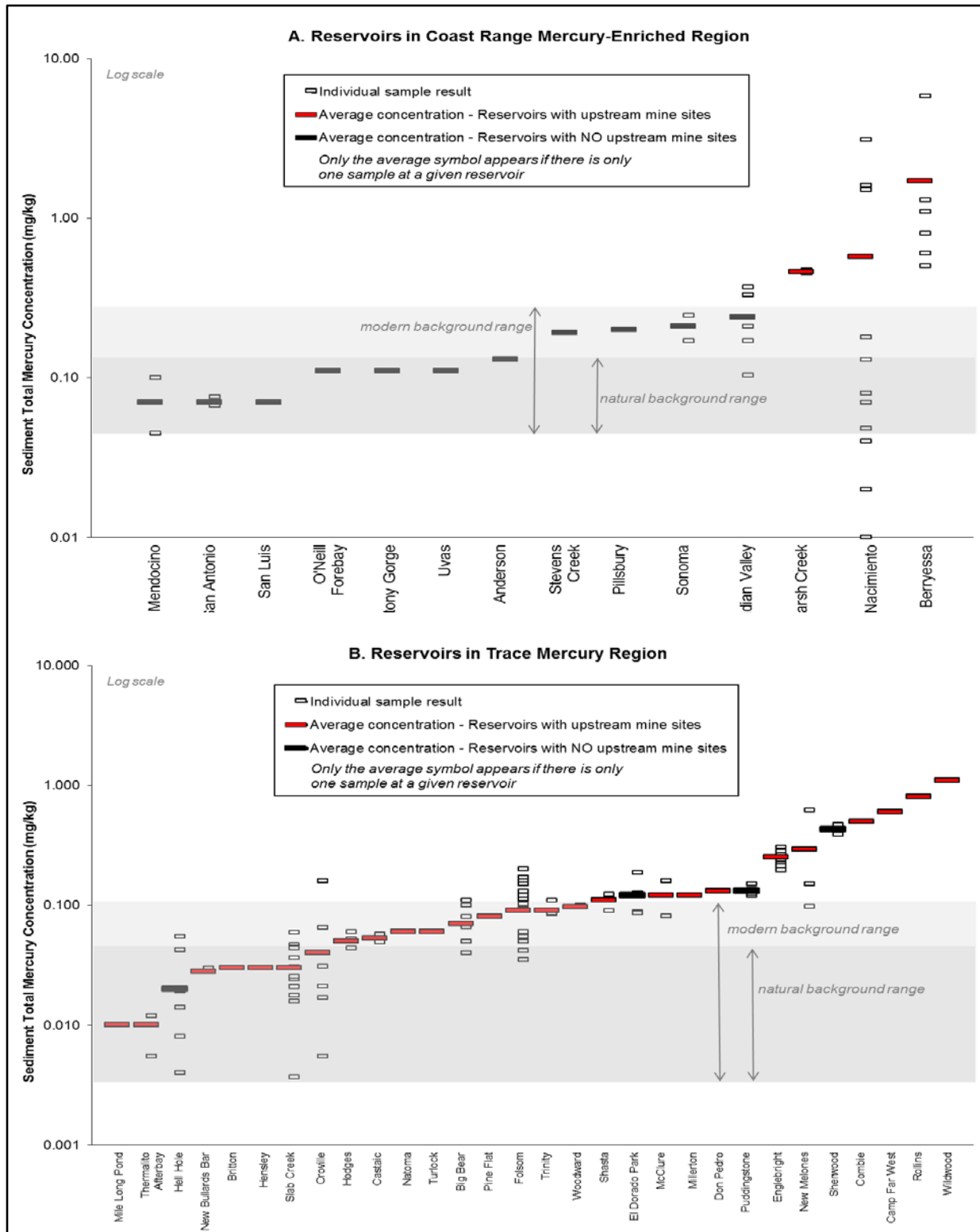


Figure 6.5: Chart comparing 2010 303(d)-listed reservoir sediment average and individual sample mercury concentrations compared to background levels

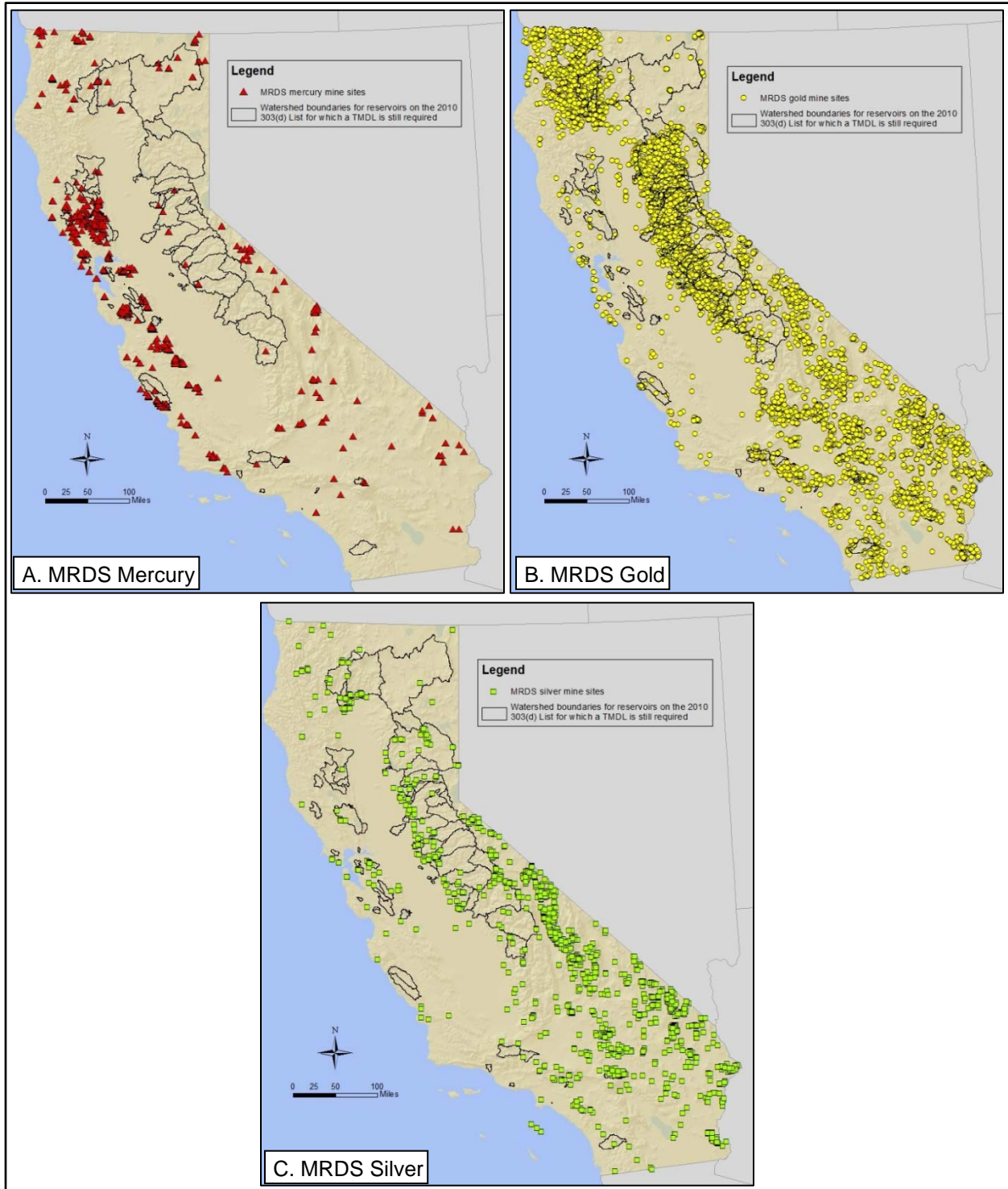


Figure 6.6: Statewide maps showing the locations of historic mercury, gold, and silver mines identified in the MRDS with the watershed boundaries of the 2010 303(d)-listed reservoirs

[Source: Mineral Resources Data System (MRDS), USGS 2005]

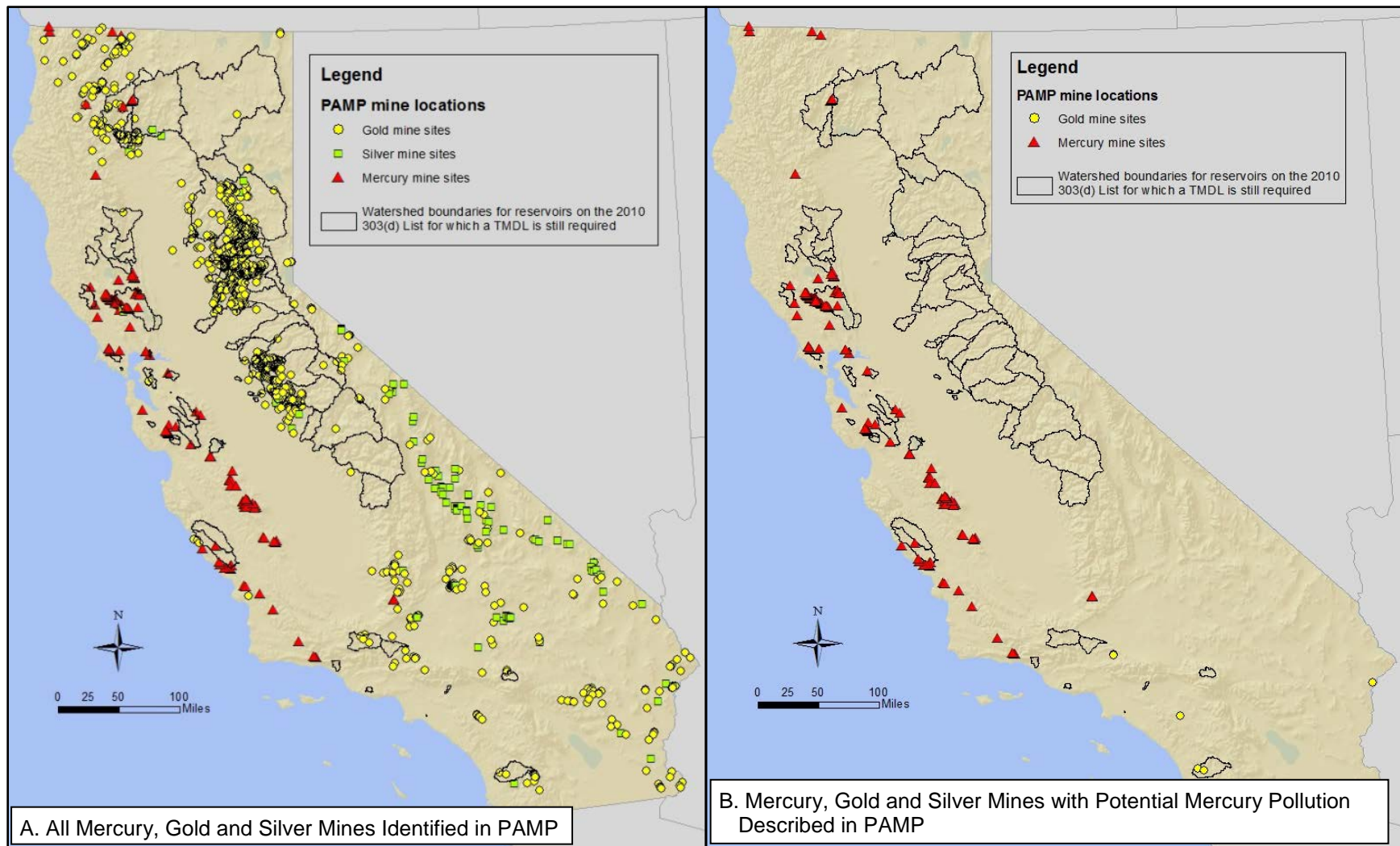


Figure 6.7: Statewide maps showing the locations of historic mercury, gold, and silver mines identified in the Principal Areas of Mine Pollution (PAMP) database with the watershed boundaries of the 2010 303(d)-listed reservoirs

[Source: Principal Areas of Mine Pollution database, OMR 2000]

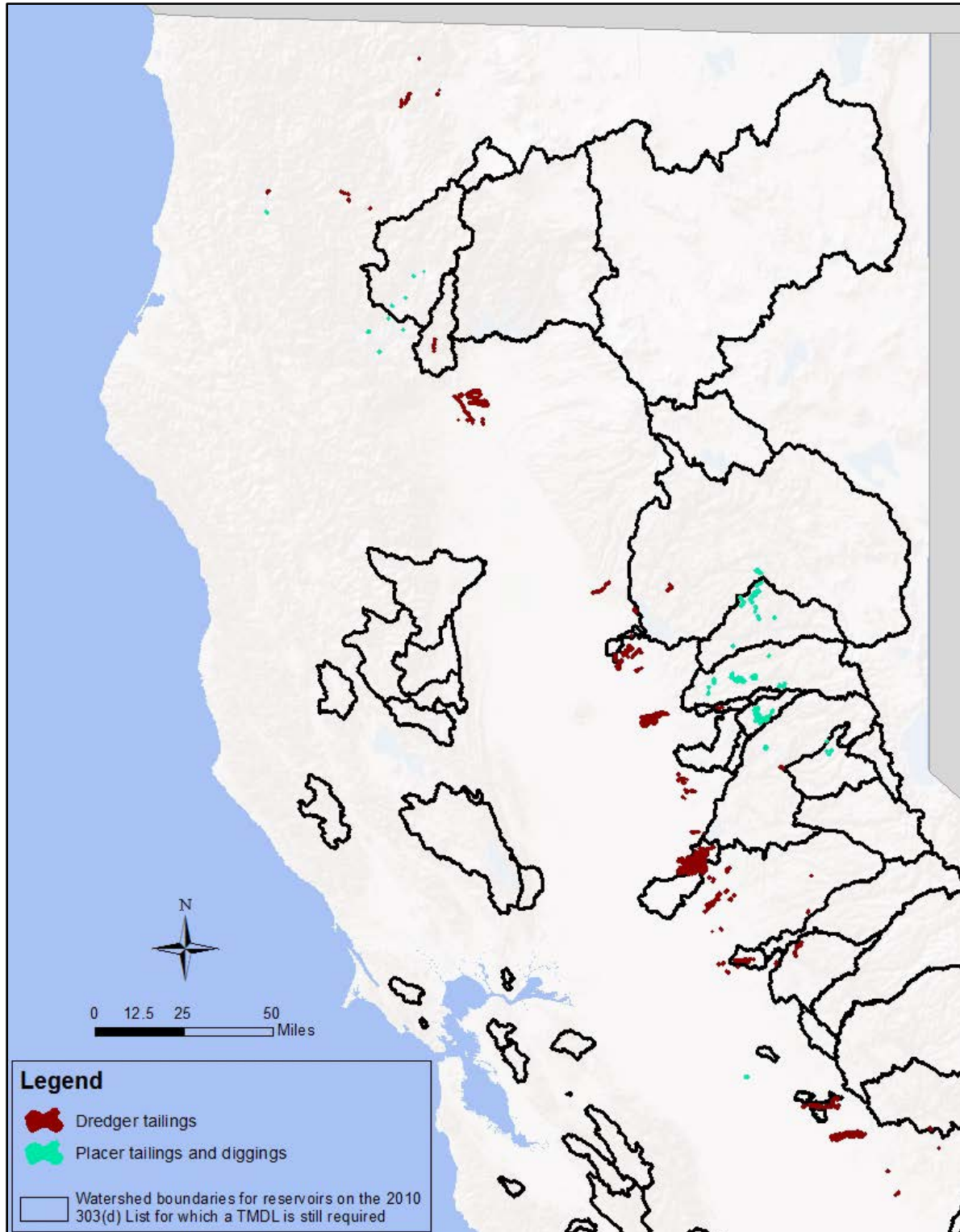


Figure 6.8: Statewide map of dredge and placer tailings and diggings identified in the California Department of Conservation's Topographically Occurring Mine Symbols (TOMS) Data Set

The boundaries of dredge and placer tailings are thickened to better show their locations.  
[Source: OMR 2001]

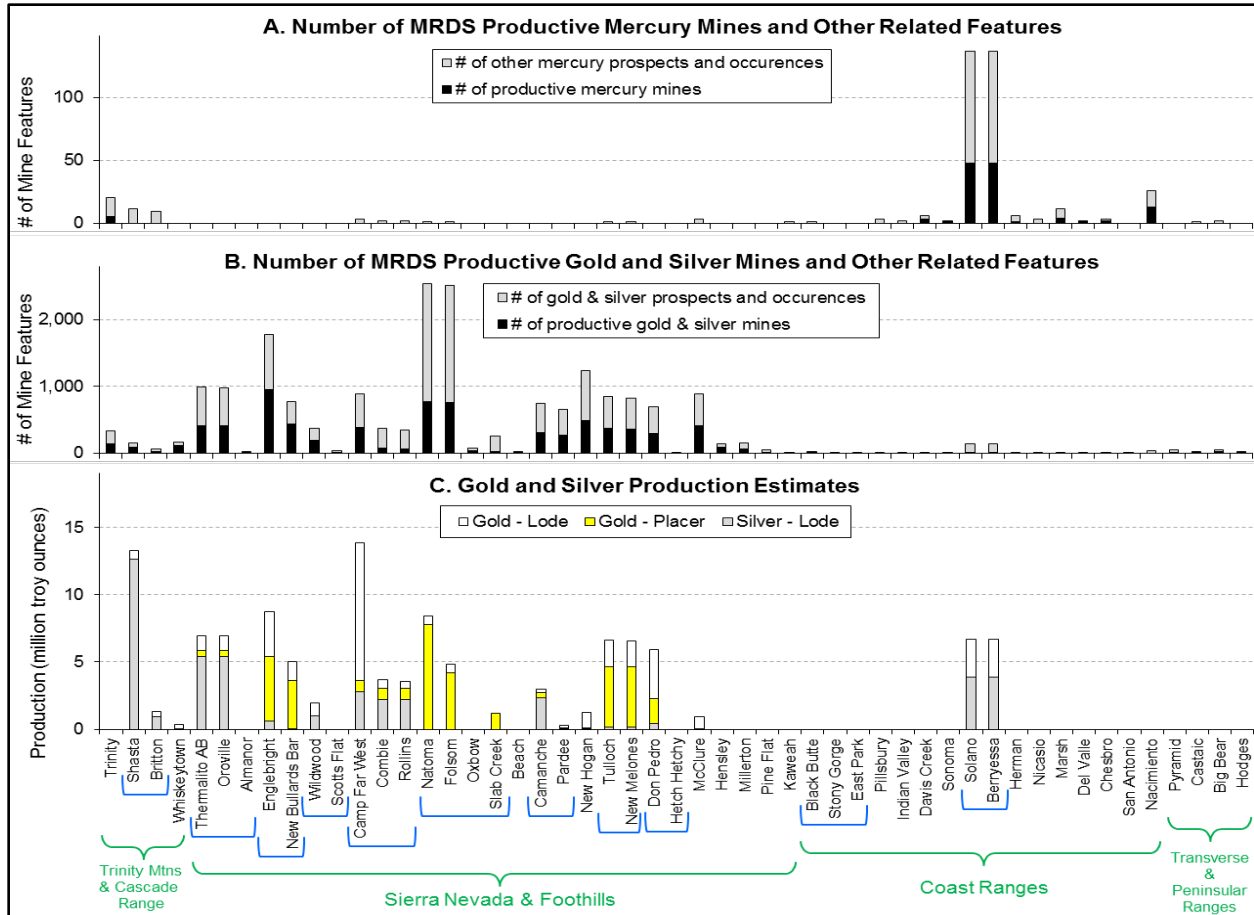


Figure 6.9: Charts illustrating watershed mercury, gold, and silver mine site density, and estimates of historic gold and silver production and associated mercury loss in 2010 303(d)-listed reservoir watersheds

Charts A and B illustrate the number of historic mercury, gold, and silver mines and other mine features (prospects and occurrences) identified by the USGS’s Mineral Resources Data System (MRDS, USGS 2005) in each 303(d)-listed reservoir watershed. Chart C illustrates estimates of gold and silver production compiled by the USGS’s Database of Significant Deposits of Gold, Silver, Copper, Lead, and Zinc in the United States (Long et al. 1998; note, this database does not include mercury production information). The 303(d)-listed reservoir watersheds are charted from north to south within each geographic region noted with green brackets. The blue brackets indicate 303(d)-listed reservoirs that are in the same watershed; the reservoirs are charted from downstream to upstream within a given watershed.

Lake Berryessa and Lake Solano in the Putah Creek watershed had by far the most upstream historic mercury mining features of any of the 303(d)-listed reservoirs, with over 100 MRDS mercury mining features. In contrast, many 303(d)-listed reservoirs in the Sierra Nevada region have hundreds to thousands of MRDS gold and silver mining features. In some watersheds, the most production is associated with placer gold mining (e.g., Lake Natoma and Folsom Lake in the American River watershed). In other watersheds, the most production is associated with lode mining of gold (e.g., Camp Far West) and silver (e.g., Shasta Lake). A comparison of Charts B and C indicates the MRDS database sometimes identifies mine features in watersheds where the USGS’s Database of Significant Deposits does not identify any significant production, but the number of MRDS features is usually low in such watersheds. However, relatively high production occurred in watersheds where there were relatively few MRDS mine features. This indicates that the number of MRDS mine features may not be a good surrogate for the amount of production in a given watershed.

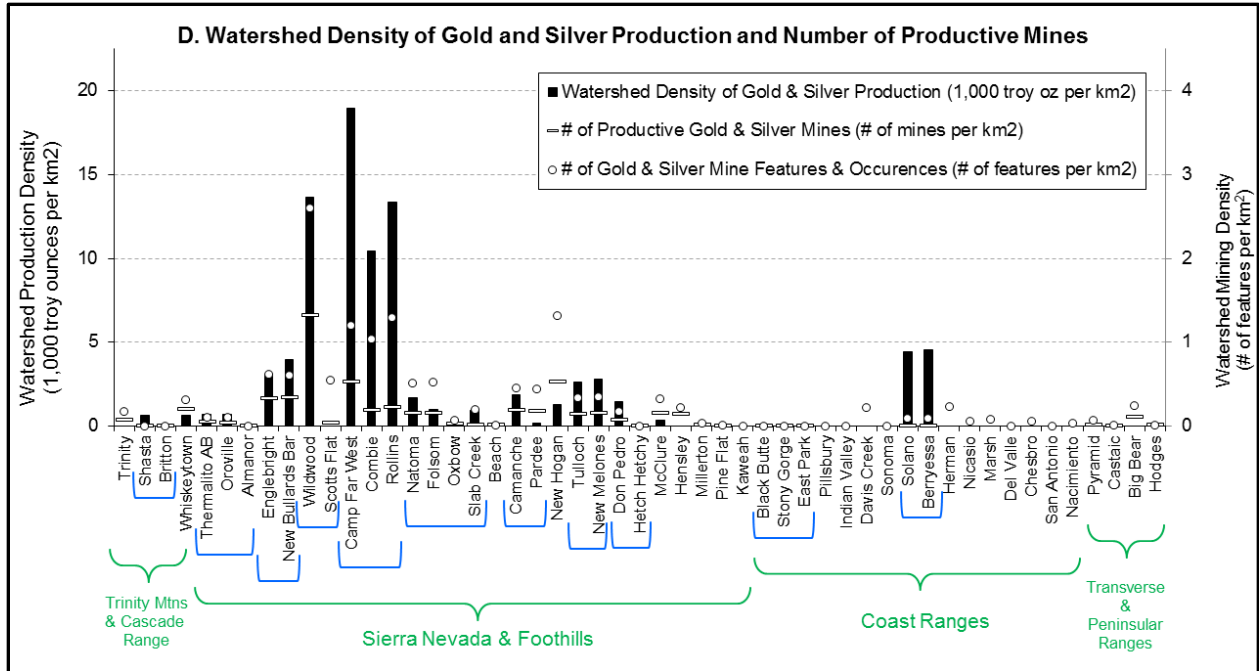


Figure 6.9, continued

Chart D illustrates the watershed density of gold and silver production (production amount per unit watershed area, shown by vertical bars) compared to the watershed mine site density (number of MRDS productive mines, shown by dashes, and other MRDS features, shown by circles). Reservoirs with watersheds with high production density and mine site density are likely to be more contaminated. Camp Far West, Combie, Rollins, and Wildwood have high upstream production densities and watershed mine site densities. In contrast, Shasta, which had a high production amount in its watershed (Chart C), has a low production density and mine site density because of the immensity of its watershed area. This indicates the potential for more watershed supply of native soils and sediments that could mix with and dilute or bury contamination associated with historic mining. Also, the mine site density and production density generally track together. However there are some exceptions. For example, New Hogan Reservoir has comparatively low production given its high mine site density, and Lake Berryessa has comparatively high production given its low mine site density.

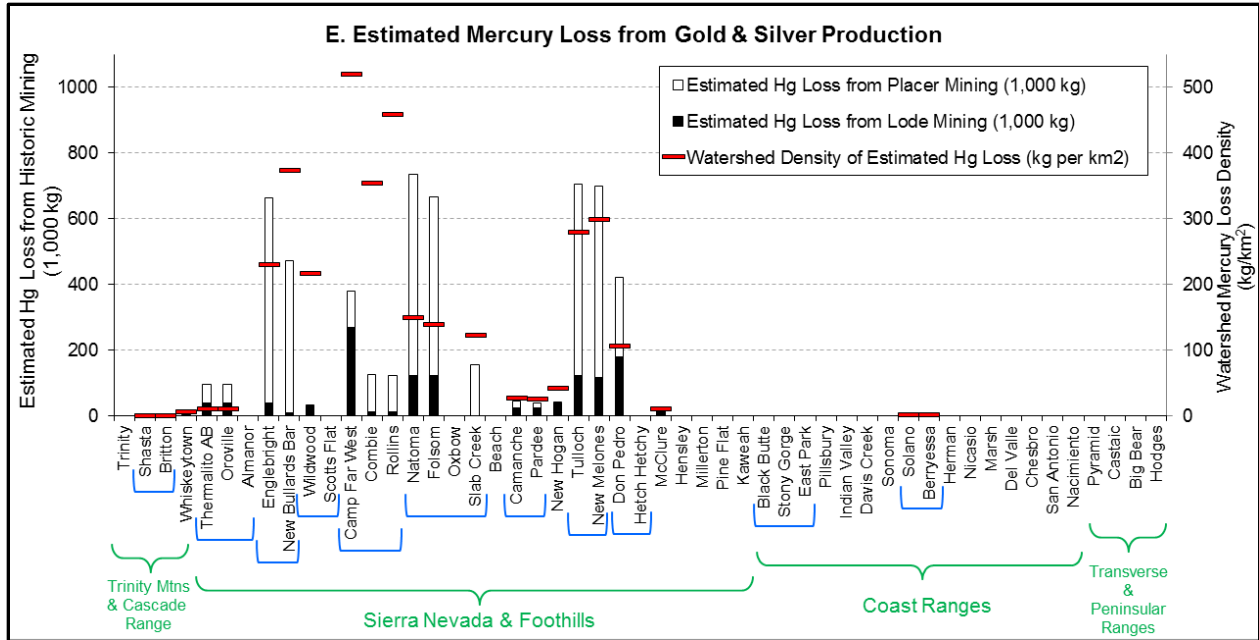


Figure 6.9, continued

Chart E provides estimates of historic mercury loss from gold and silver mining (bars) along with watershed densities of mercury loss (dashes) for each 303(d)-listed reservoir. For some reservoir watersheds, mercury loss estimates are greater than expected from gold and silver production amounts in Chart C (e.g., Tulloch and Don Pedro), while for others the mercury loss estimates are less than expected (e.g., Lake Berryessa). This is because the loss estimates consider another key factor for evaluating the level of contamination in a watershed: the type and time period of mining activities. Mercury losses were greater with placer mining than lode mining, and loss rates for both decreased with time as new mining methods were developed (Churchill 2000). Water Board staff used estimated mercury loss amounts provided by Alpers and others (2014) and Churchill (2000) for placer and lode mining districts identified in the USGS Database of Significant Deposits (Long et al. 1998) to estimate mercury loss upstream of 303(d)-listed reservoirs. High watershed mercury loss densities indicate the potential for particularly elevated contamination in reservoir sediments. The chart shows how some watersheds had both high mercury loss and high watershed densities of mercury loss (e.g., Englebright, New Bullards Bar, Camp Far West, Tulloch, and New Melones), and others had low mercury loss but high watershed loss density (e.g., Wildwood, Combie, and Rollins). The chart also shows how some reservoirs may not have had a high watershed production density, but could have elevated watershed mercury loss densities because of extensive historic placer mining (e.g., Englebright, New Bullards Bar, Natoma, Folsom, Tulloch, New Melones, and Don Pedro).



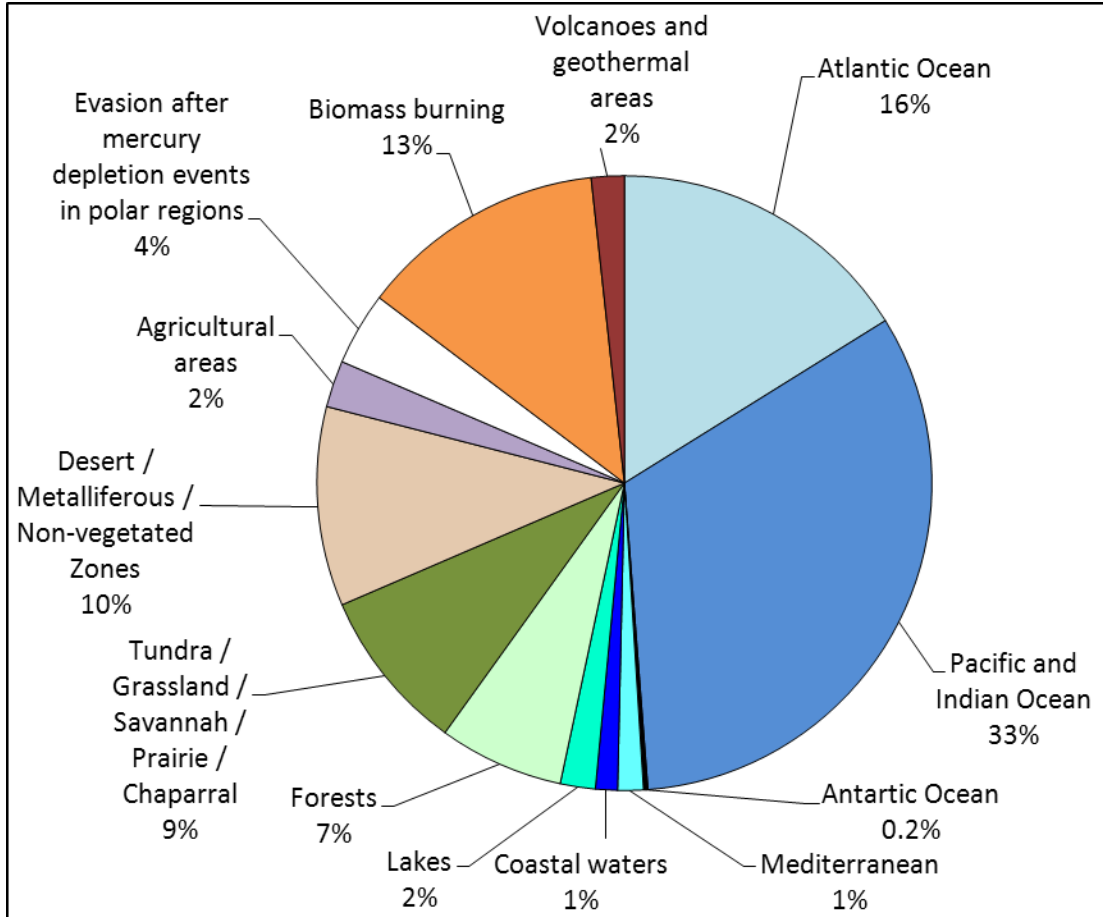


Figure 6.10: Pie chart illustrating estimates of mercury emissions for 2008 from natural processes

Emissions from natural processes include primary natural mercury emissions plus re-emissions of historic deposition originating from natural and anthropogenic sources.

[Source: Pirrone et al. 2010]

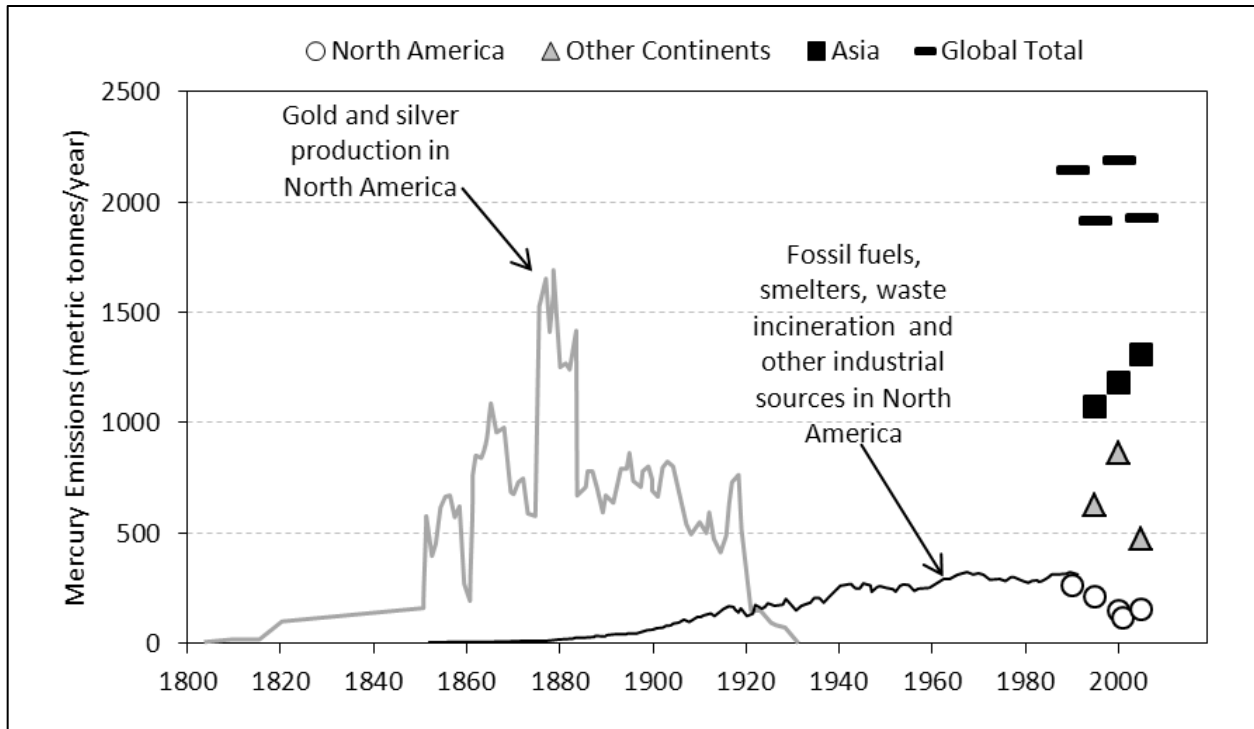


Figure 6.11: Time series of estimated historic anthropogenic mercury emissions from North America and modern anthropogenic mercury emissions from North America and other continents

This figure shows estimated historic and modern anthropogenic mercury emissions into the atmosphere from North America beginning in 1800, and for the rest of the world beginning in 1990. The grey line shows that North American mercury emissions into the atmosphere peaked before 1890 as a result of gold and silver production. The black line shows the steady increase in industrial emissions from North America. The open circles show that since 1990, North American regulations including the U.S. Clean Air Act have measurably reduced emissions. However, the black squares show that emissions from Asia have increased in recent years and are far greater than mercury emissions from North America.

[Sources: Pirrone et al. 1998; USEPA 2008b; Pacyna et al. 2002, 2006, and 2010]

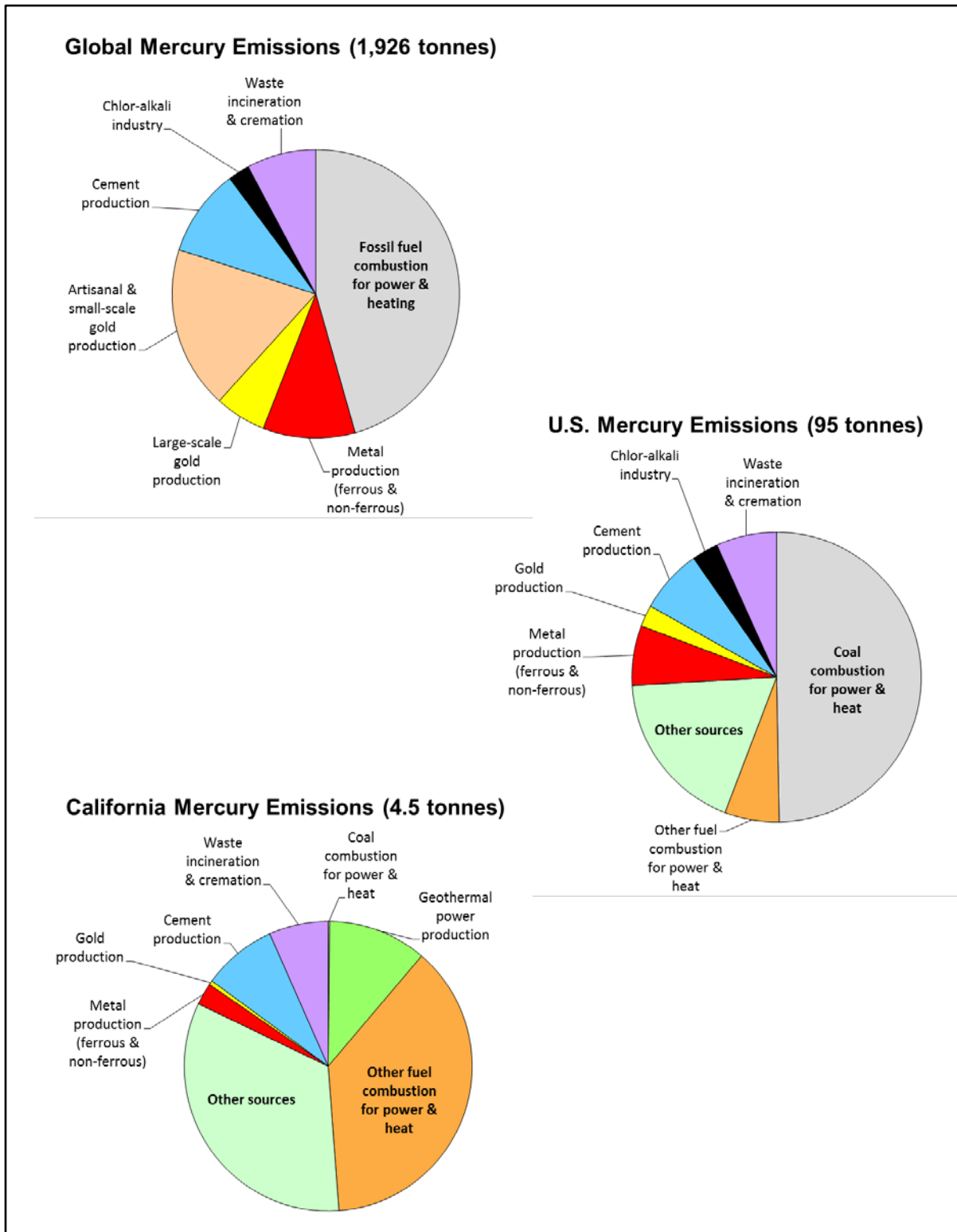


Figure 6.12: Pie charts illustrating estimates of anthropogenic mercury emissions in 2005 from global, United States, and California sources

[Sources: AMAP/UNEP 2008; Pacyna et al. 2010; USEPA 2012a; USEPA 2012b, Table 7; USEPA 2008a, Table 4-3; ICF 2011]

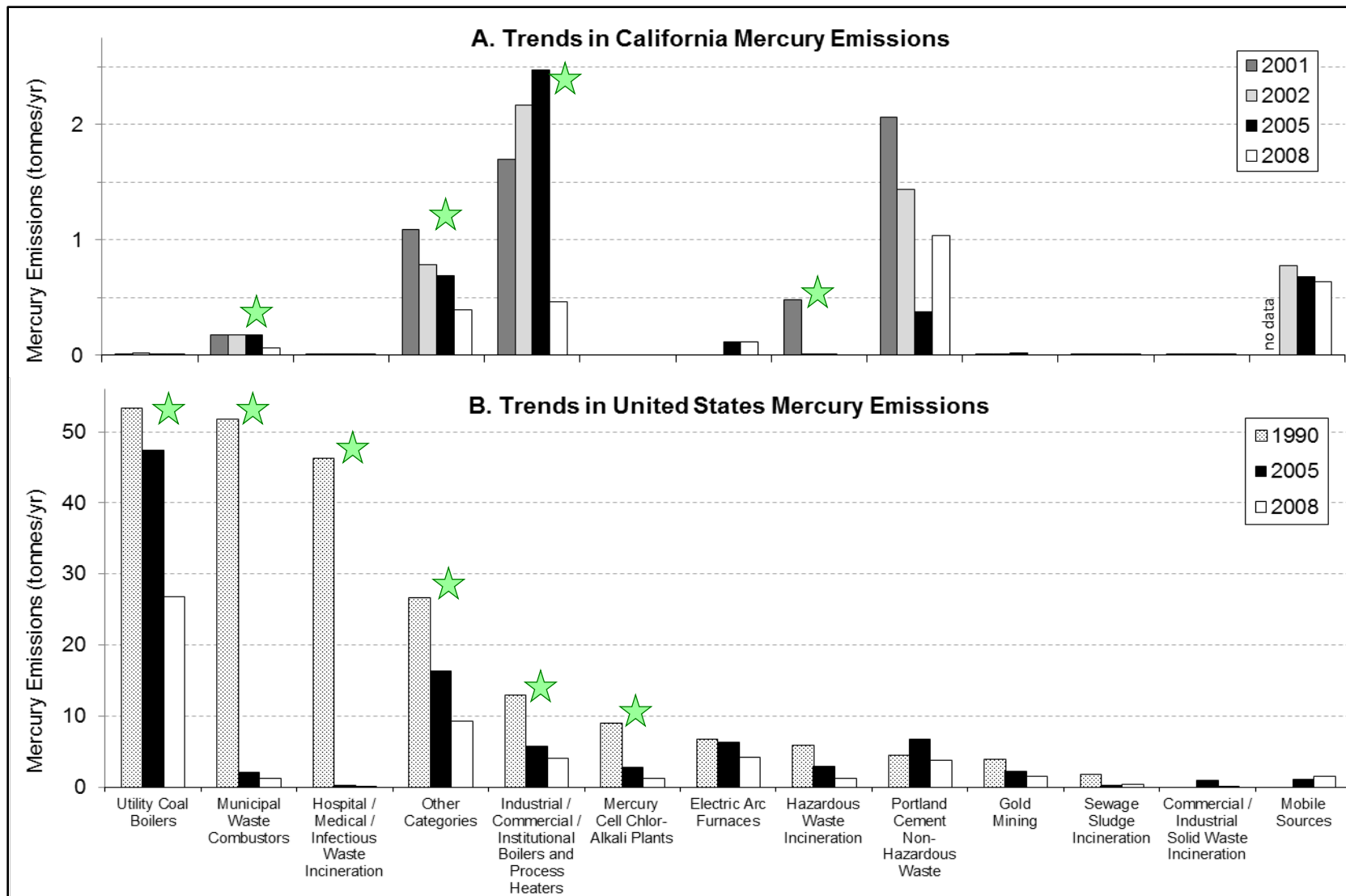


Figure 6.13: Bar chart showing trends in California and United States anthropogenic mercury emissions by sector

Green stars highlight emission sectors that have experienced substantial reductions.

[Sources: USEPA 2012a; USEPA 2012b, Table 7; USEPA 2008a, Table 4-3; ICF 2011]

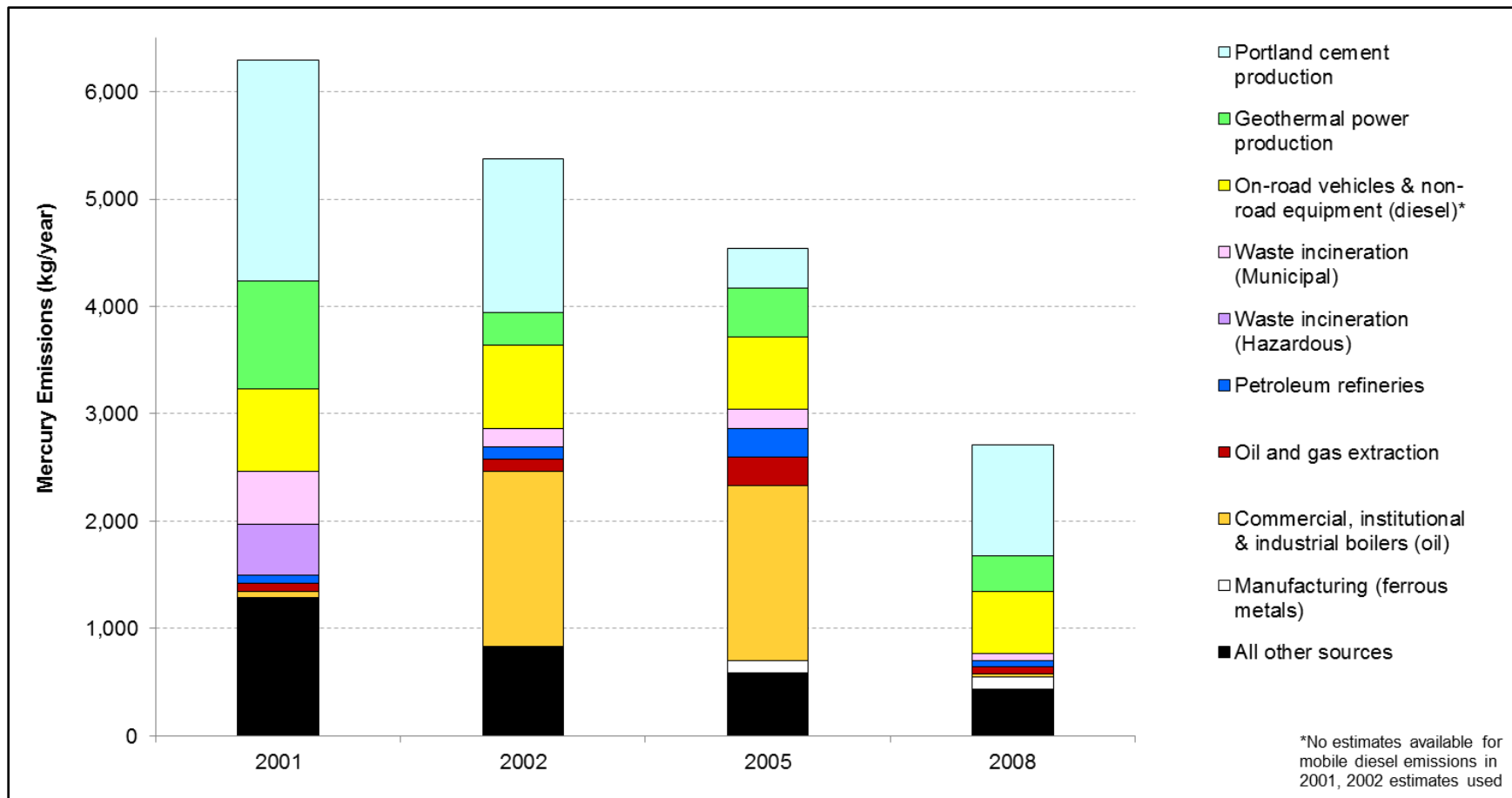


Figure 6.14: Bar chart showing trends in California anthropogenic mercury emissions by major emission type

California mercury emissions decreased by more than 50% between 2001 and 2008. Some emissions types, such as Portland cement production, vary from year to year as a result of changes in economic demand. Others, such as municipal waste incineration, have had substantial reductions due to implementing emission controls.

[Sources: USEPA 2012a; ICF 2011]

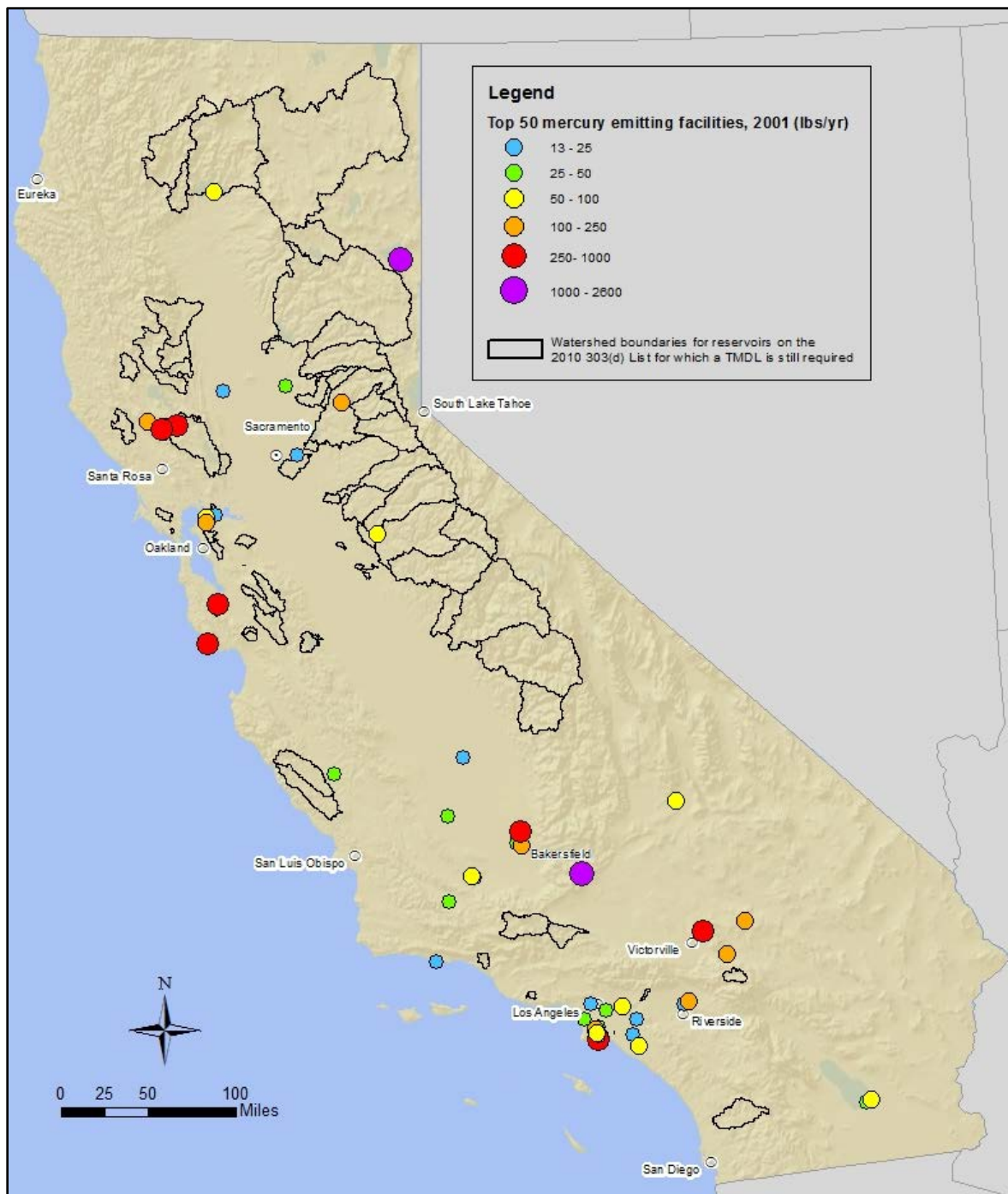


Figure 6.15: Statewide map of top 50 mercury emitting facilities in the 2001 facility emissions inventory

The 50 facilities with the highest mercury emissions accounted for about 90% or more of all facility emissions in 2001, 2002, 2005, and 2008. Emissions from cement manufacturing, geothermal power production, and petroleum industry facilities within the top 50 reporting facilities account for about 60–80% of all annual statewide facility emissions. As this map of the top 50 emitting facilities in 2001 shows, many are clustered in the northern Coast Range northeast of Santa Rosa, San Francisco Bay area, Bakersfield area, and Los Angeles area. [Sources: USEPA 2008a; ICF 2011]

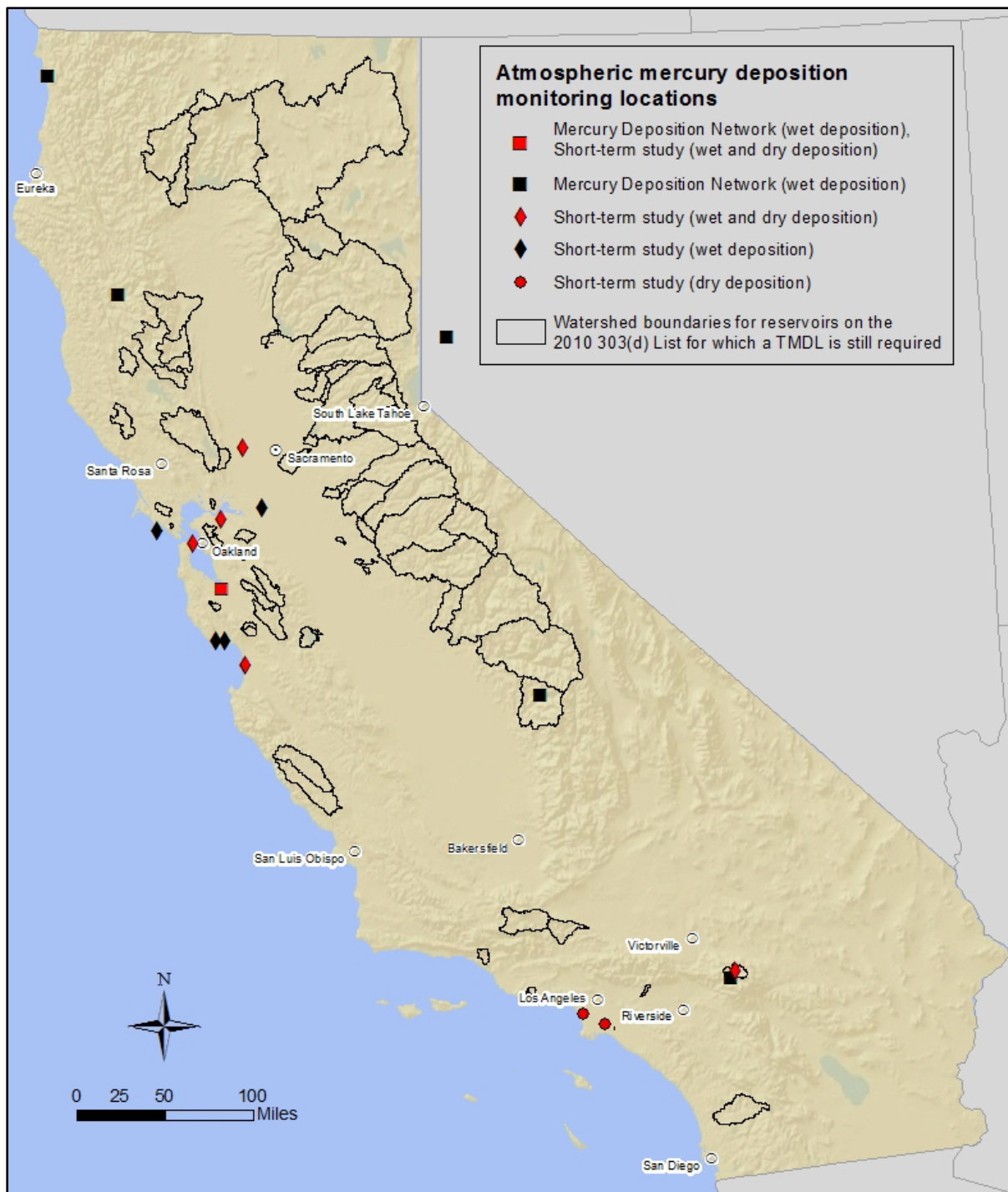


Figure 6.16: Statewide map of atmospheric mercury deposition monitoring sites in California and western Nevada

Several short-term monitoring studies and one long-term monitoring program have evaluated atmospheric mercury in wet deposition at 13 sites in California and dry deposition at 7 sites in California. No monitoring data are available for northern inland California, northern and central Sierra Nevada, and southeastern California.

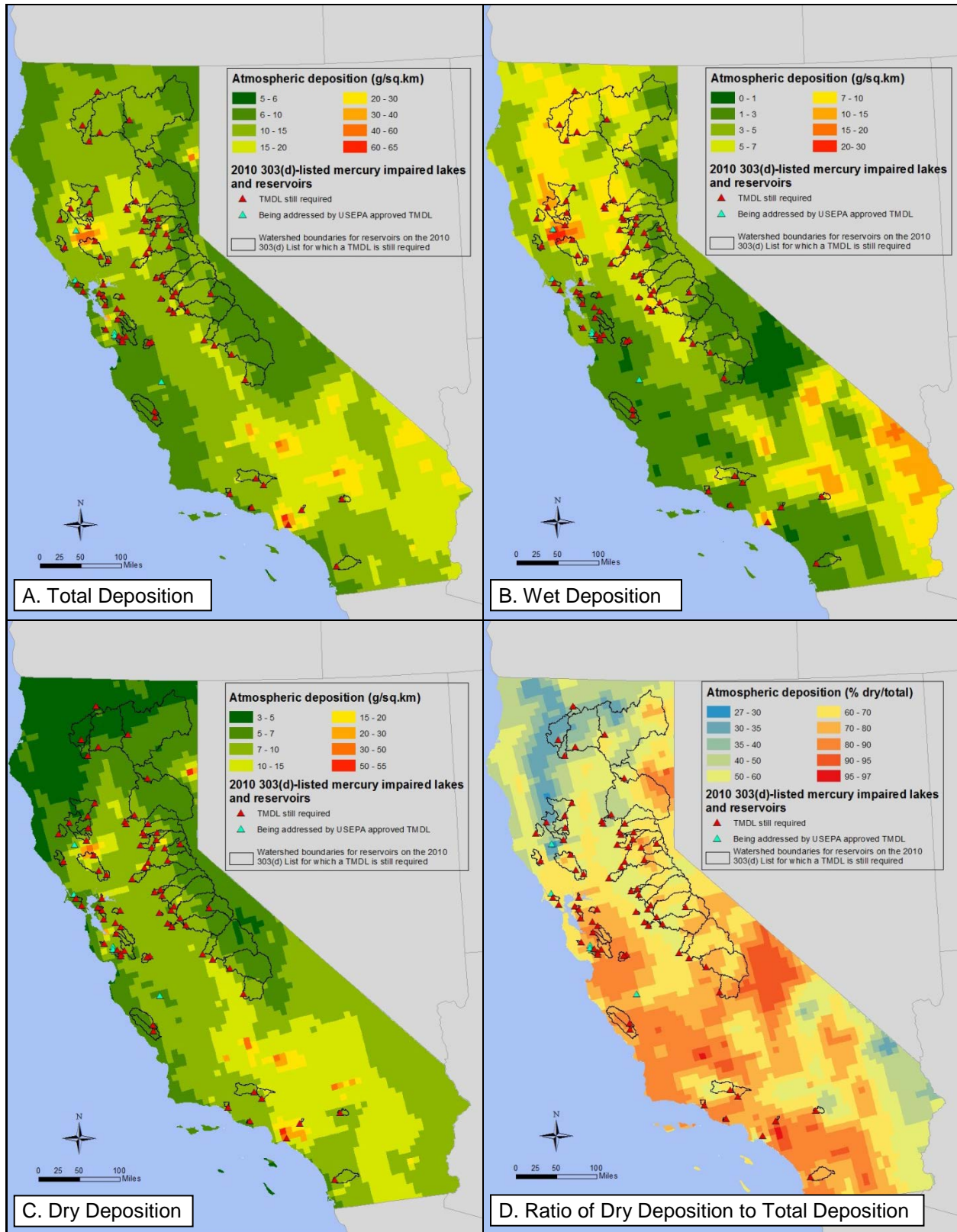


Figure 6.17: Statewide maps of REMSAD 2001 model output for total, wet and dry atmospheric deposition of mercury in California



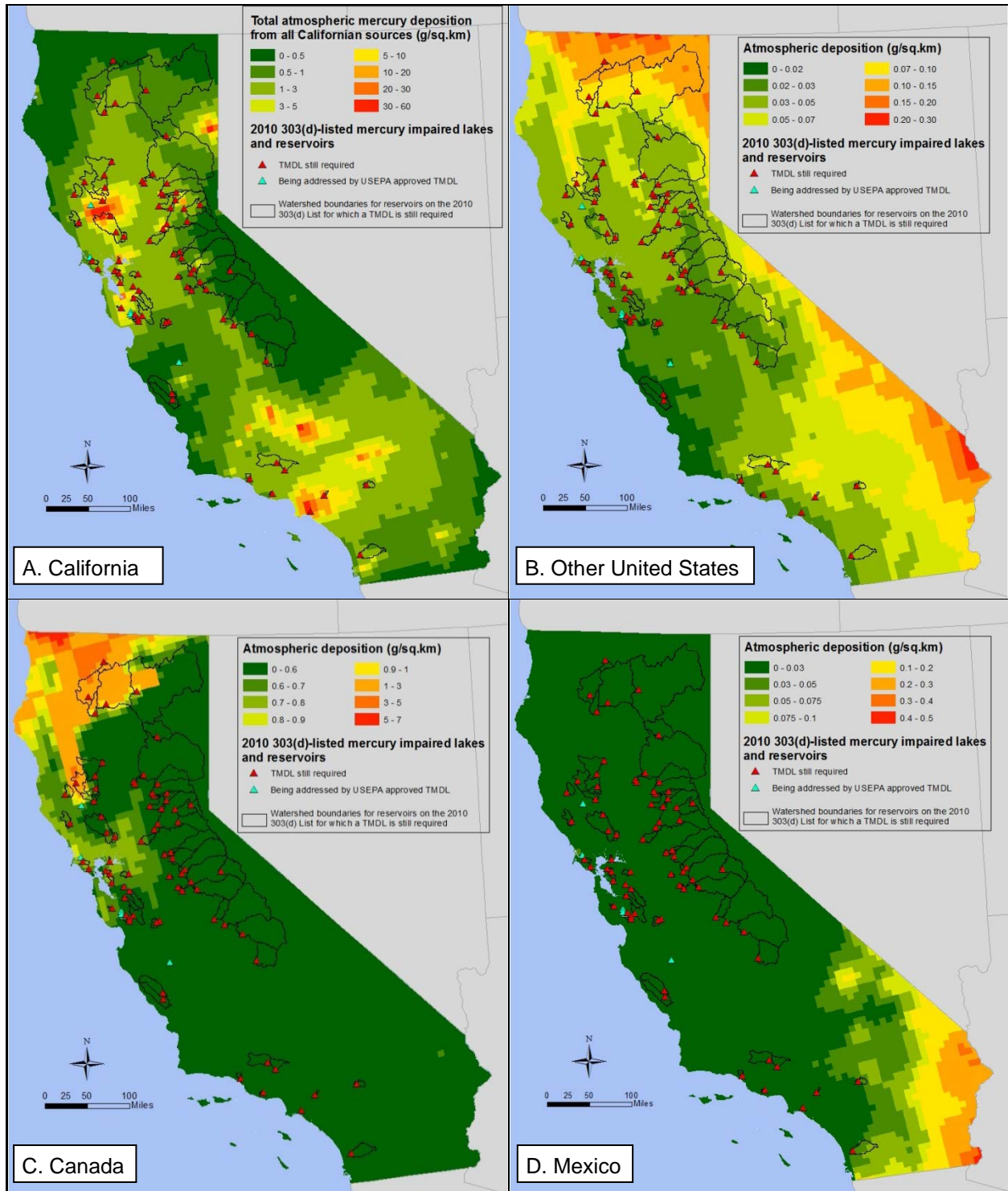


Figure 6.18: Statewide maps of REMSAD 2001 model output for atmospheric deposition of mercury in California attributed to anthropogenic emissions from California, United States, Canada, and Mexico

Note changes in color scale for each of maps A–D. The magnitude of deposition is different for the different source regions. For example, deposition attributed to anthropogenic emissions from other states (map B) peaks (red) at less than 0.3 g/km<sup>2</sup>/year. In contrast, deposition attributed to anthropogenic emissions within California (map A) peaks (red) at 100 times greater, at 30 g/km<sup>2</sup>/year.

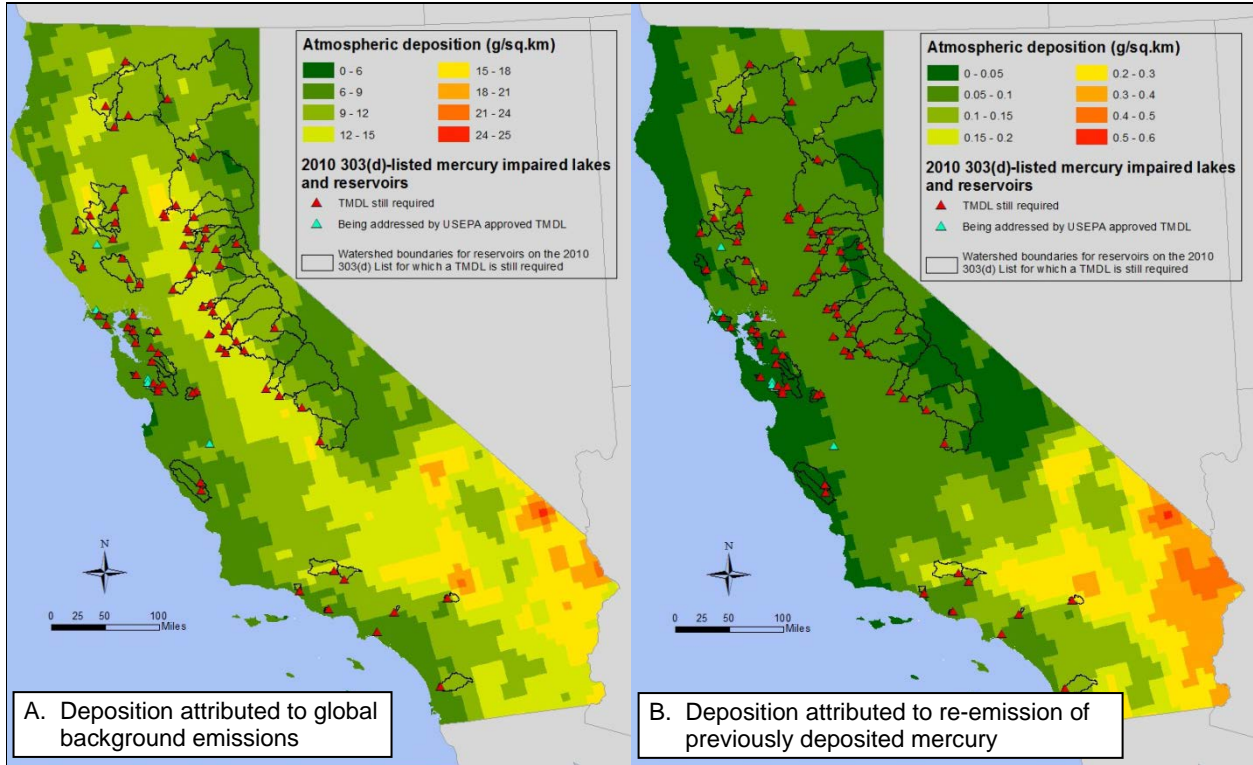


Figure 6.19: Statewide maps of REMSAD 2001 model output for atmospheric deposition of mercury in California attributed to 2000 emissions from global background sources and re-emission of previously deposited mercury (from a combination of natural and anthropogenic sources)

Global background sources do not include anthropogenic emissions from the United States, Canada, and Mexico in 2001, but may include mercury emitted from anthropogenic sources in these countries in 2000. Re-emission of previously deposited mercury includes mercury from natural and anthropogenic sources.

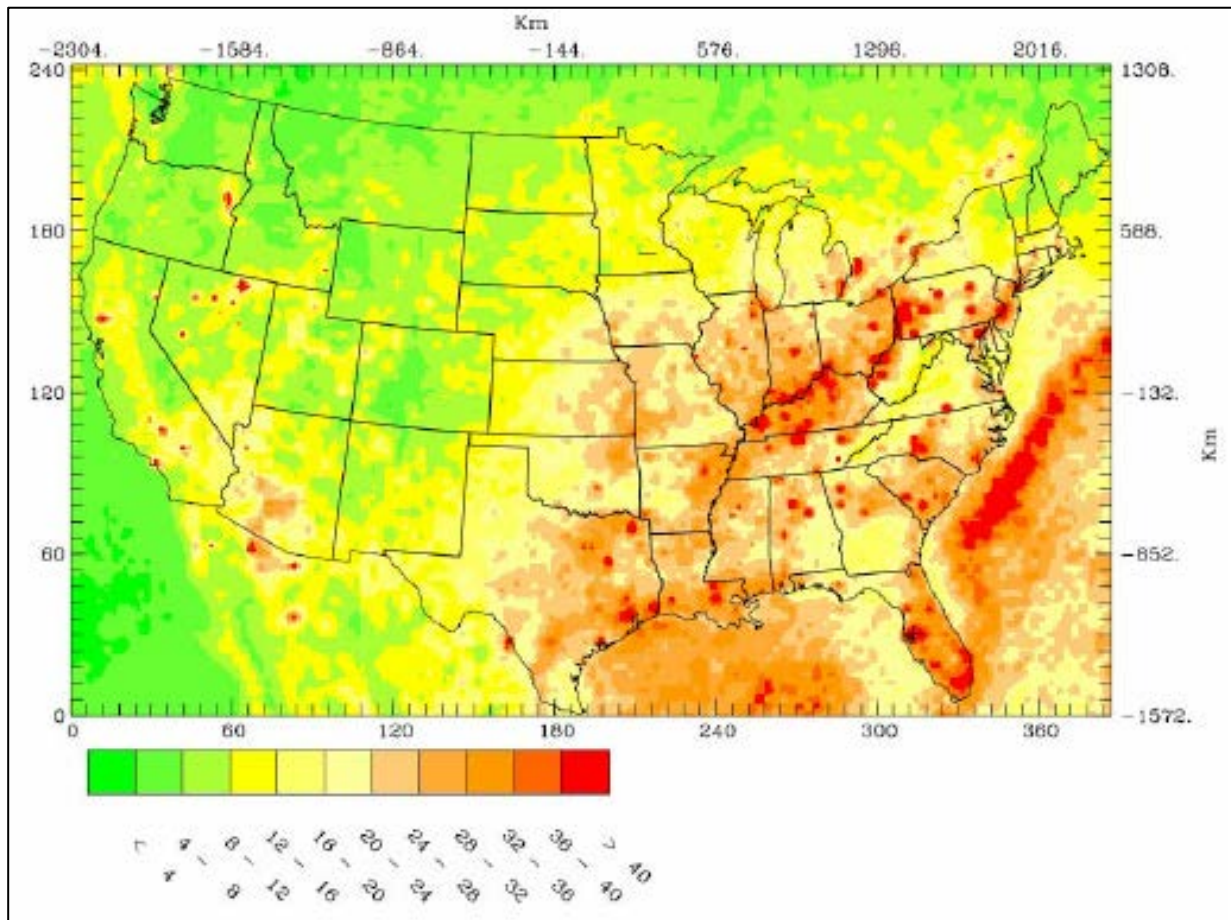


Figure 6.20: Map of REMSAD 2001 model output for total atmospheric deposition of mercury throughout the United States

[Source: USEPA 2008a, Figure 6-3c]

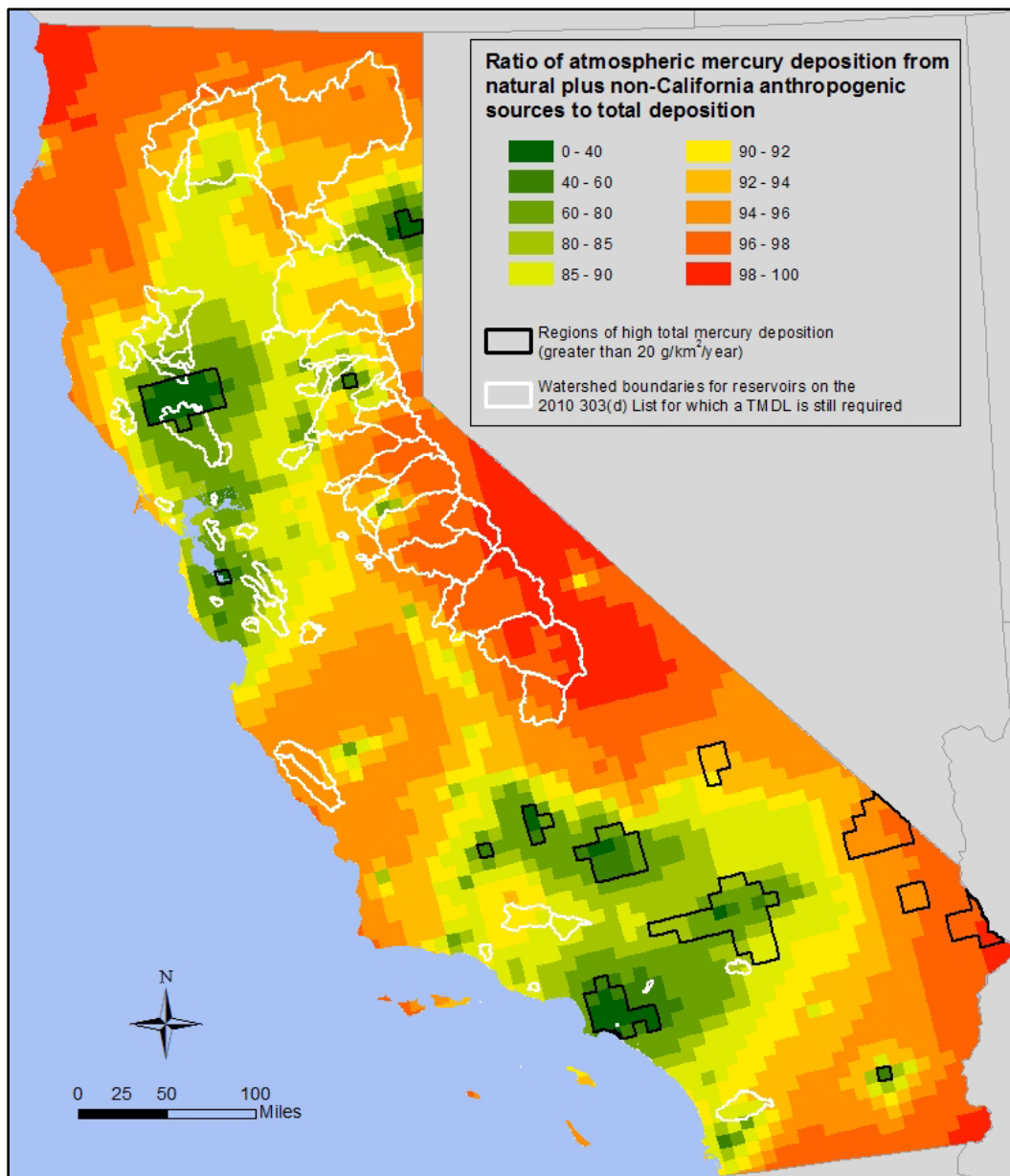


Figure 6.21: Statewide map showing the ratio of atmospheric mercury deposition attributed by REMSAD to all sources except 2001 California anthropogenic sources to total deposition

The dark green areas illustrate where the REMSAD model attributes almost all the mercury deposition to California anthropogenic emissions, while the light green, yellow, orange, and red areas illustrate where the model attributes most of the deposition to natural and global sources. The model indicates that most of the mercury deposited in the state does not come from anthropogenic emissions in the state.

The black lines outline areas where REMSAD modeled atmospheric deposition exceeds 20 g/km<sup>2</sup>/year. The model attributes the elevated mercury deposition in the southeastern portion of the state primarily to global and natural sources. REMSAD attributes the elevated mercury deposition in other areas of the state to anthropogenic emissions from within the state.

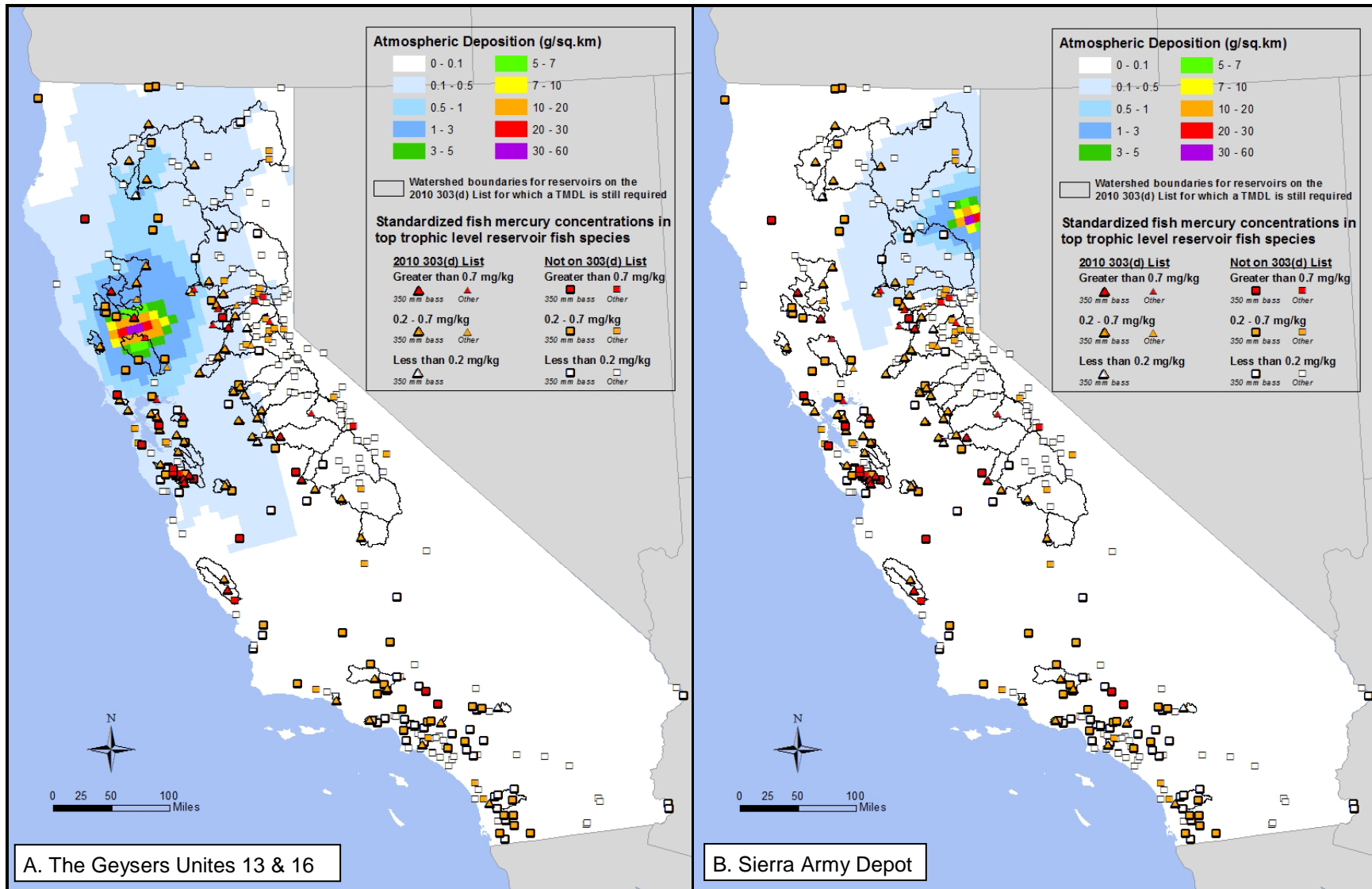


Figure 6.22: Statewide maps of REMSAD 2001 model output for atmospheric mercury deposition tagged to particular California emissions

These maps illustrate where the REMSAD model attributes mercury deposition to specific California anthropogenic emissions, and where such deposition coincides with the location of 2010 303(d)-listed reservoirs and their watershed boundaries, and other reservoirs with elevated fish methylmercury concentrations.

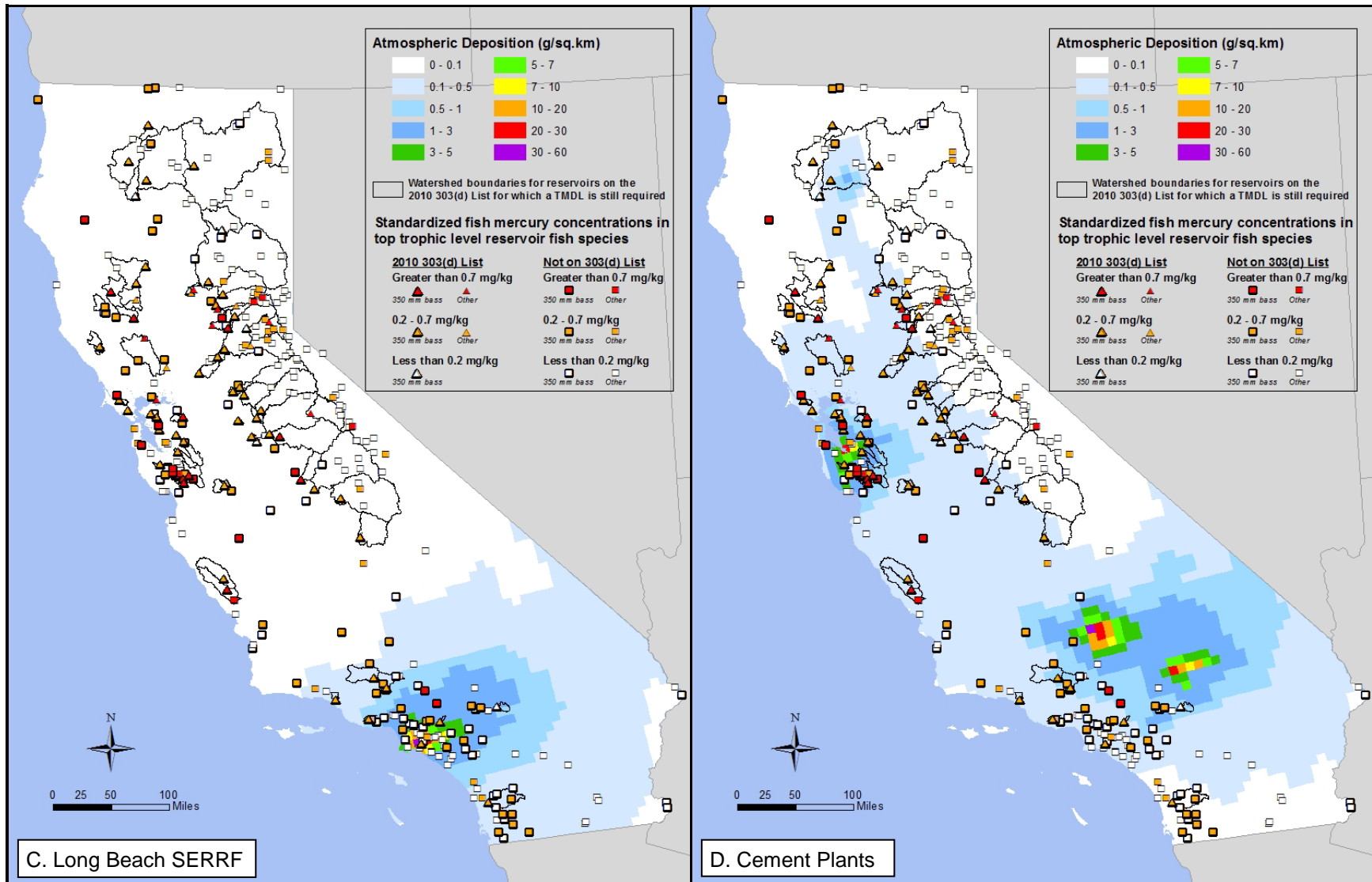


Figure 6.22: Statewide maps of REMSAD 2001 model output for atmospheric mercury deposition tagged to particular California emissions, *continued*

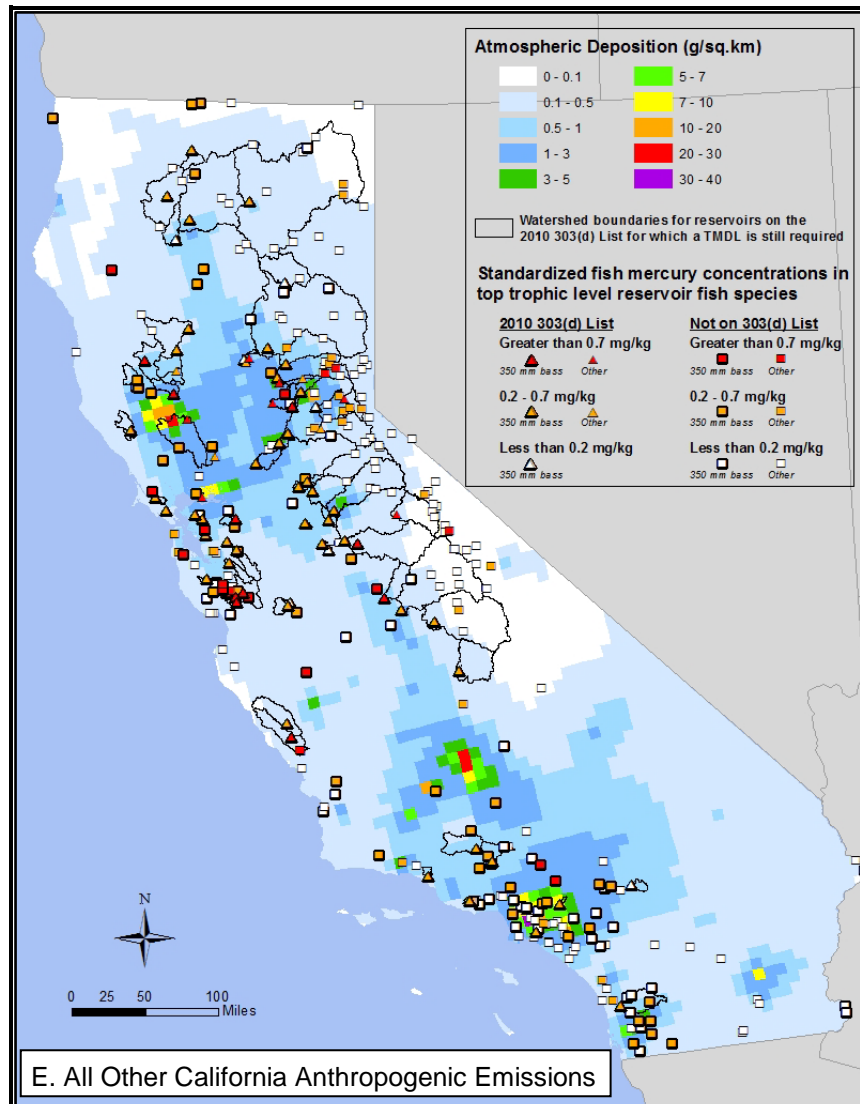


Figure 6.22: Statewide maps REMSAD 2001 model output for atmospheric mercury deposition tagged to particular California emissions, *continued*

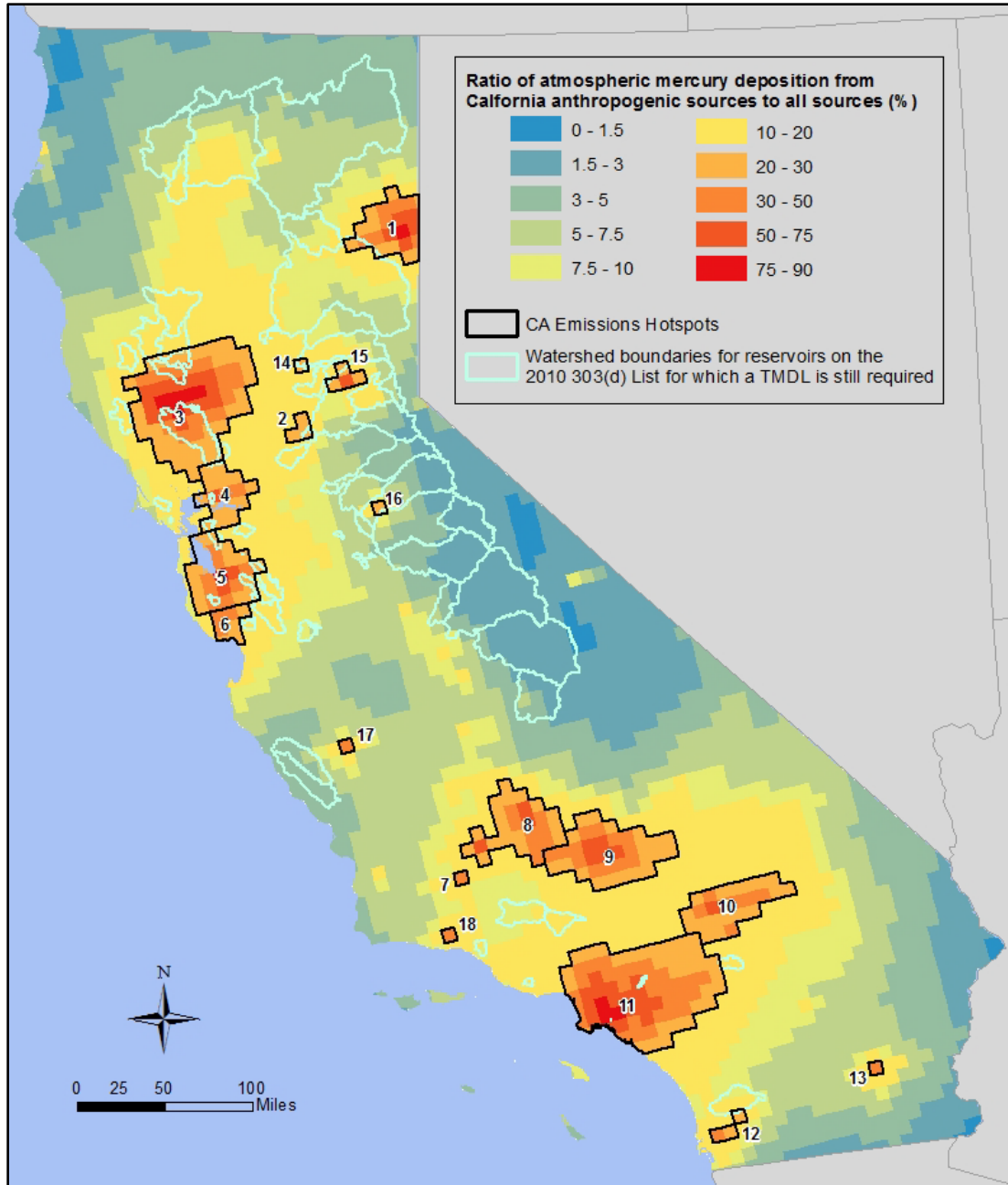


Figure 6.23: Statewide map showing the ratio of atmospheric deposition attributed by REMSAD to 2001 California anthropogenic emissions to total deposition

The black lines outline “California emissions hotspots” where the REMSAD model attributes more than 20% of all deposition to California anthropogenic emissions. Reducing California emissions could make a substantial, measurable reduction in atmospheric deposition to these areas. Almost a third of the 2010 303(d)-listed reservoirs or their watersheds intersect a California emissions hotspot. There are five reservoirs where REMSAD attributes more than 50% of atmospheric deposition to California anthropogenic emissions: Davis Creek Reservoir, Indian Valley Reservoir (hotspot #3), Lake Herman (hotspot #4), El Dorado Park Lakes, and Puddingstone Reservoir (hotspot #11)



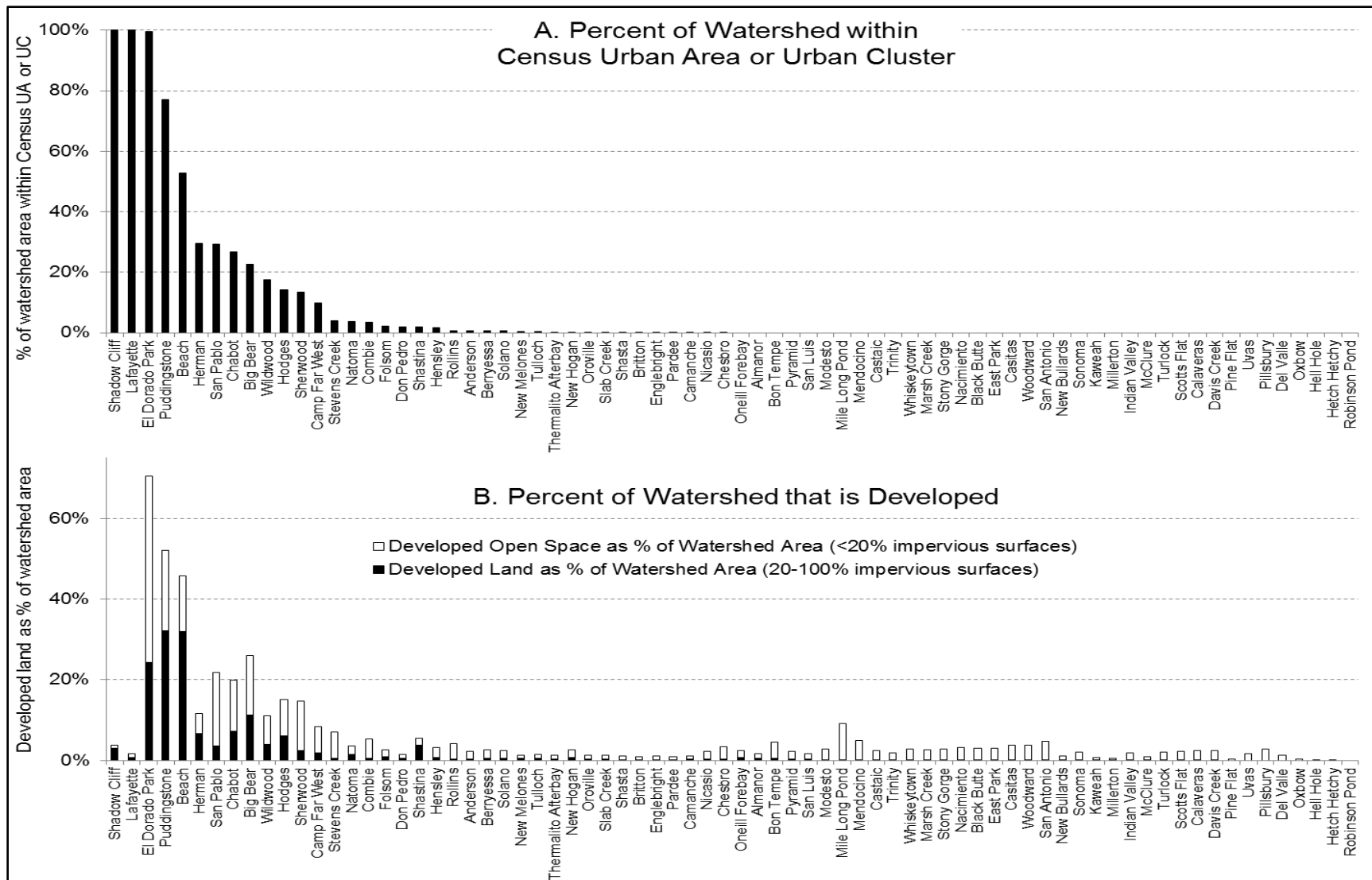


Figure 6.24: Bar charts of the percent of 2010 303(d)-listed reservoir watersheds [A] within 2010 Census-designated Urbanized Areas and Urban Clusters and [B] classified as developed by the 2006 National Land Cover Database

[Sources: MRLC 2011; Fry et al. 2011; USCB 2012a and 2012b]

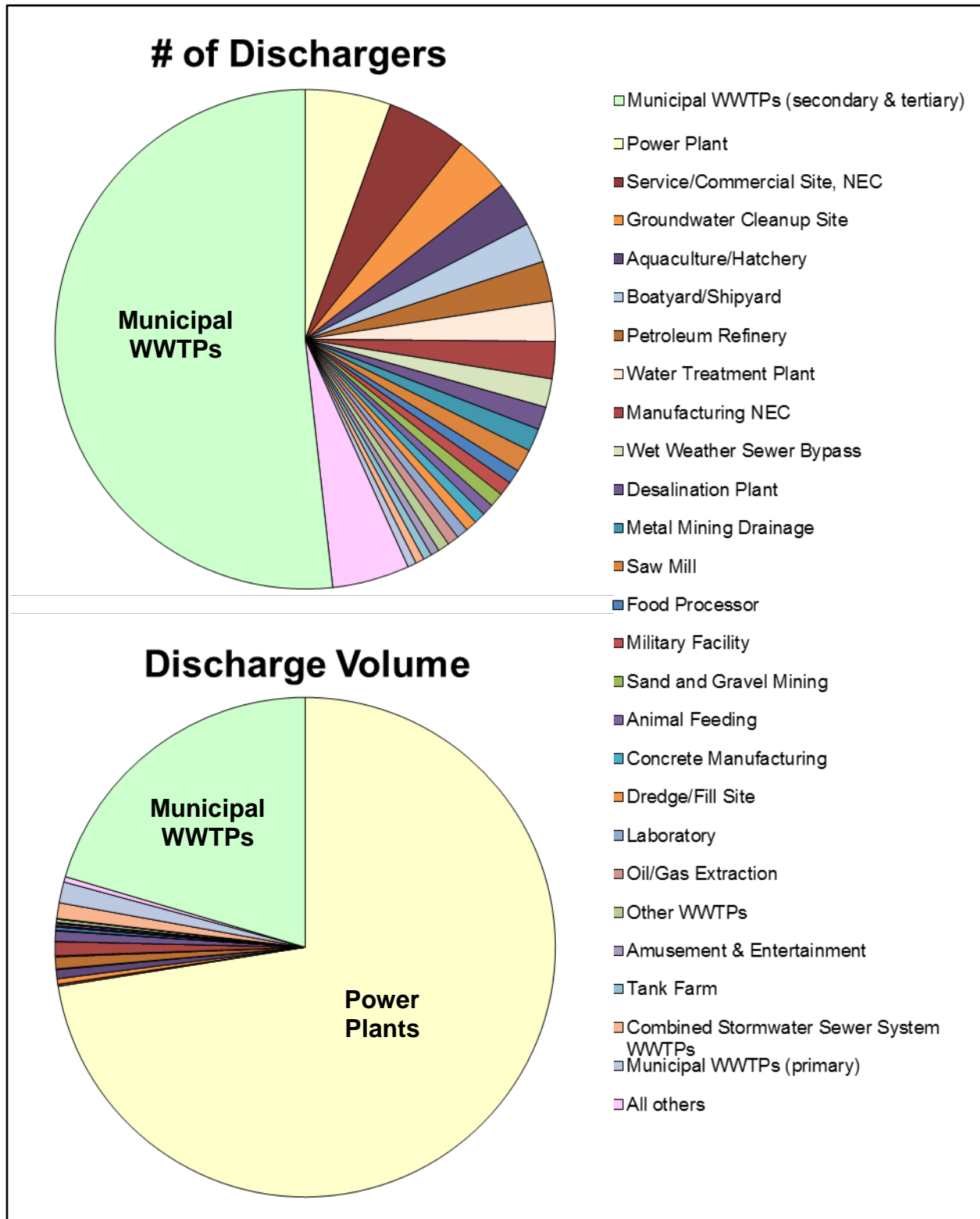


Figure 6.25: Pie charts illustrating the number of NPDES-permitted facility dischargers and sum of design flows by facility type throughout California

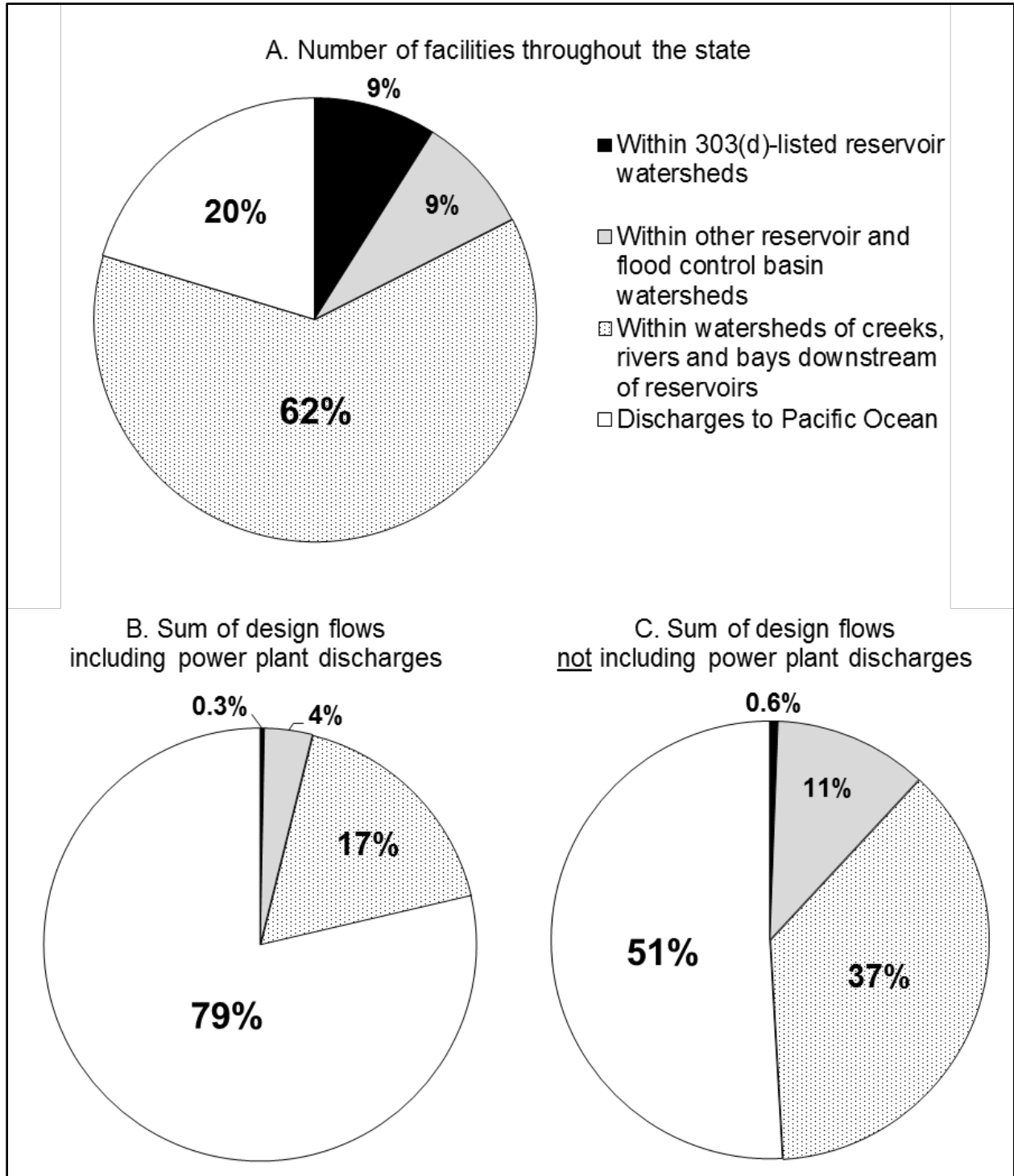


Figure 6.26: Pie charts illustrating the number of NPDES-permitted facilities and sum of permitted facility discharge volumes (design flows) by receiving water location, with and without power plant noncontact cooling water releases

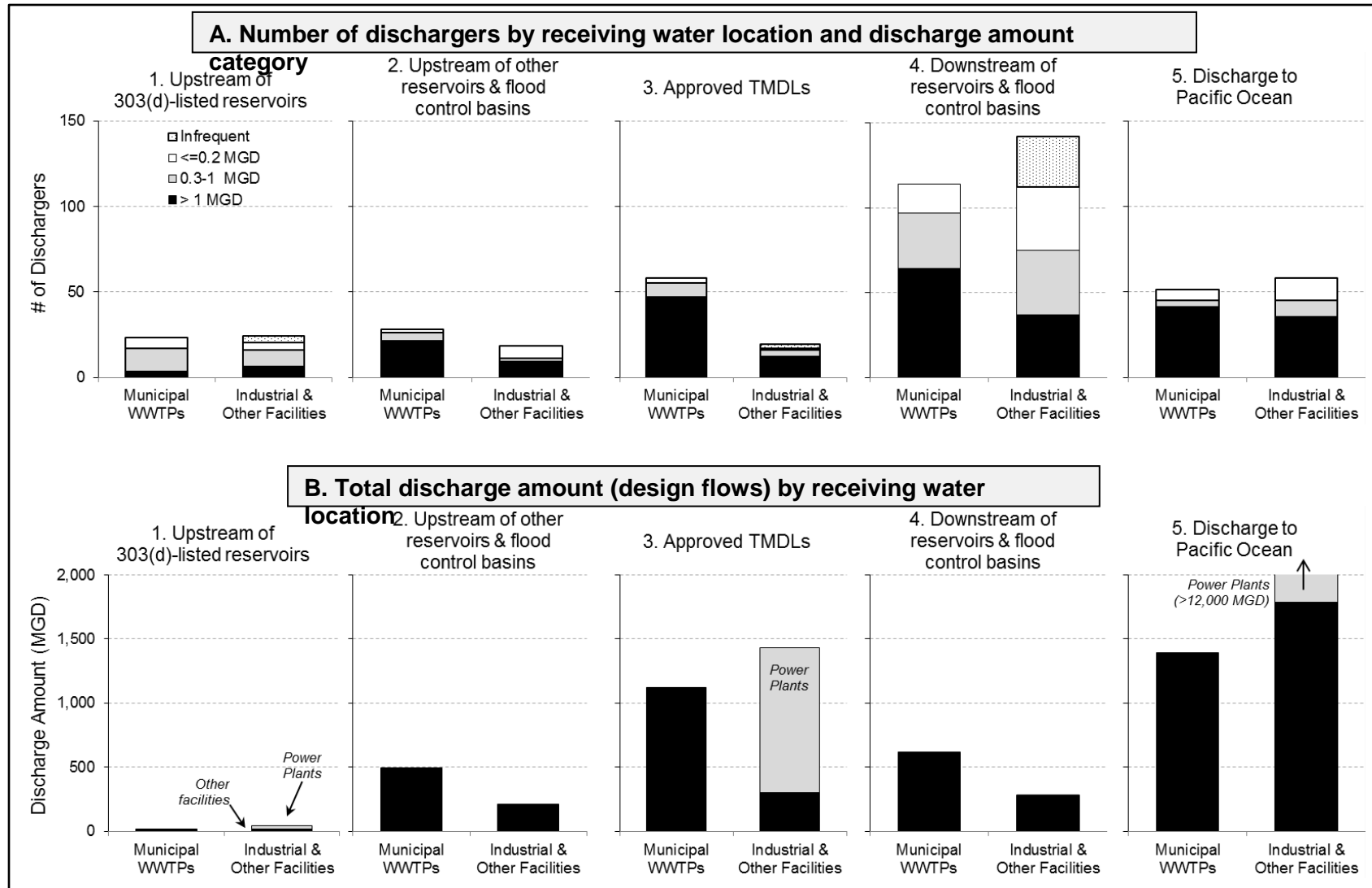


Figure 6.27: Bar chart of the number of NPDES-permitted facility dischargers and sum of permitted design flows grouped by receiving water location

The facilities are grouped by receiving water type. Facilities in group #3, “Approved TMDLs,” all discharge to water bodies downstream of any reservoir. This figure illustrates that there are much fewer facilities upstream of reservoirs than downstream, and that their total discharge volume is a small fraction of discharges downstream of reservoirs.

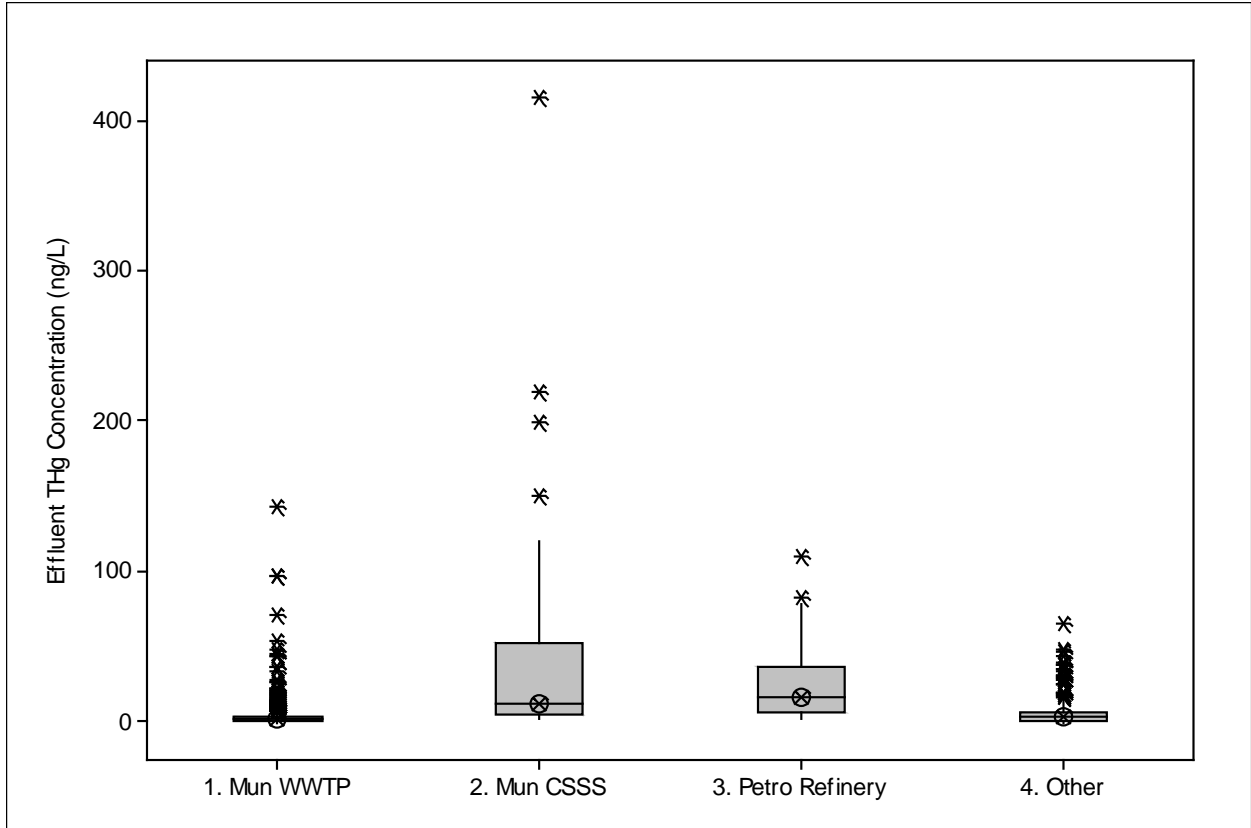


Figure 6.28: Box plot of effluent total mercury concentrations for four types of NPDES-permitted facility discharges

This figure summarizes effluent total mercury concentrations for four significantly different types of discharge (Kruskal-Wallis test,  $p < 0.001$ ): municipal wastewater treatment plants (Mun WWTPs), municipal combined stormwater sewer systems (Mun CSSS), petroleum refineries (Petro Refinery), and other types of facilities (Other). The boxes illustrate the interquartile ranges (25<sup>th</sup> and 75<sup>th</sup> percentiles). The middle horizontal lines indicate the medians. The asterisks illustrate outliers.

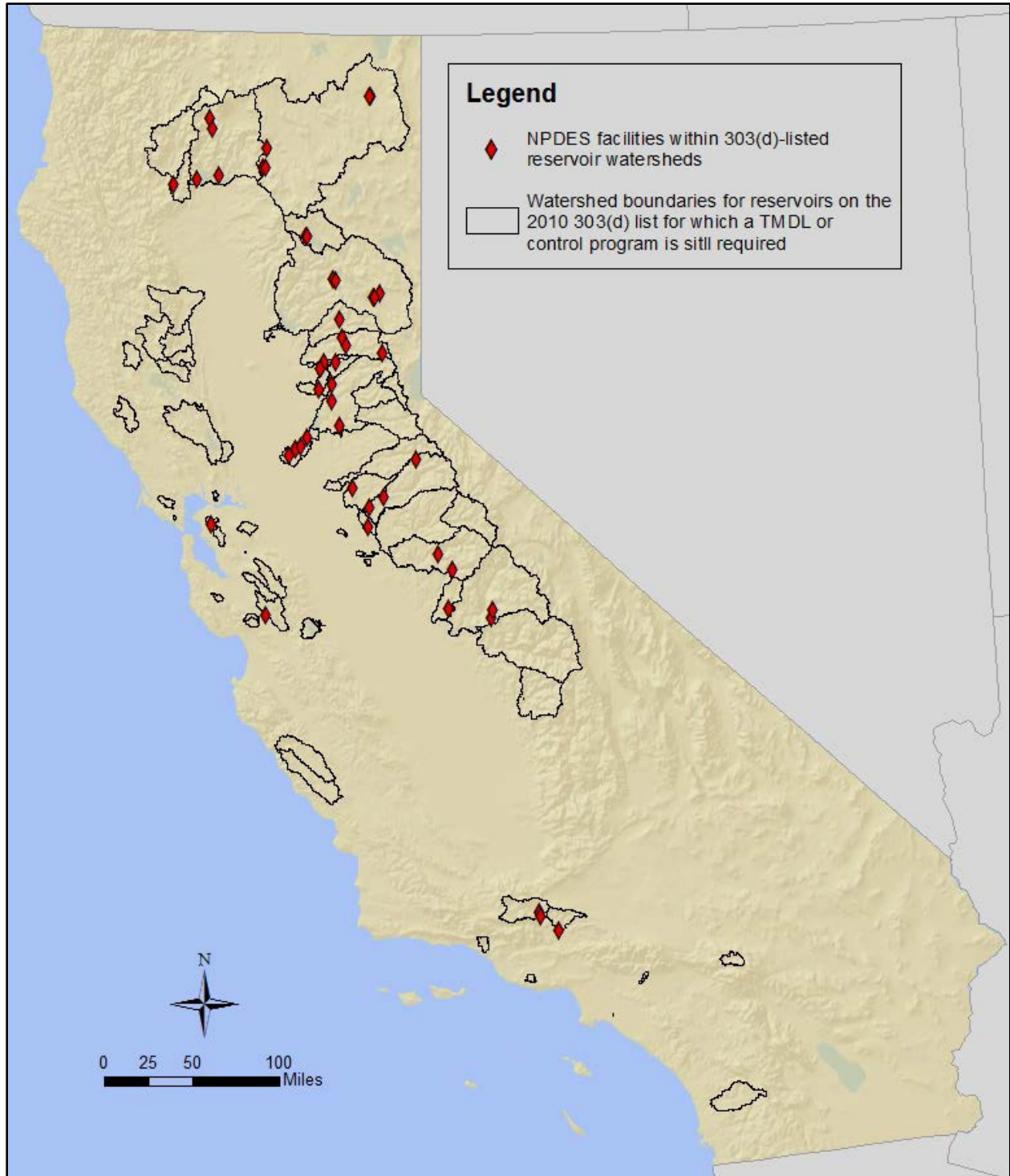


Figure 6.29: Statewide map of NPDES-permitted discharges from facilities with individual NPDES permits in 2010 303(d)-listed reservoir watersheds

This map shows only the facilities that discharge within the 303(d)-listed reservoirs' watersheds.

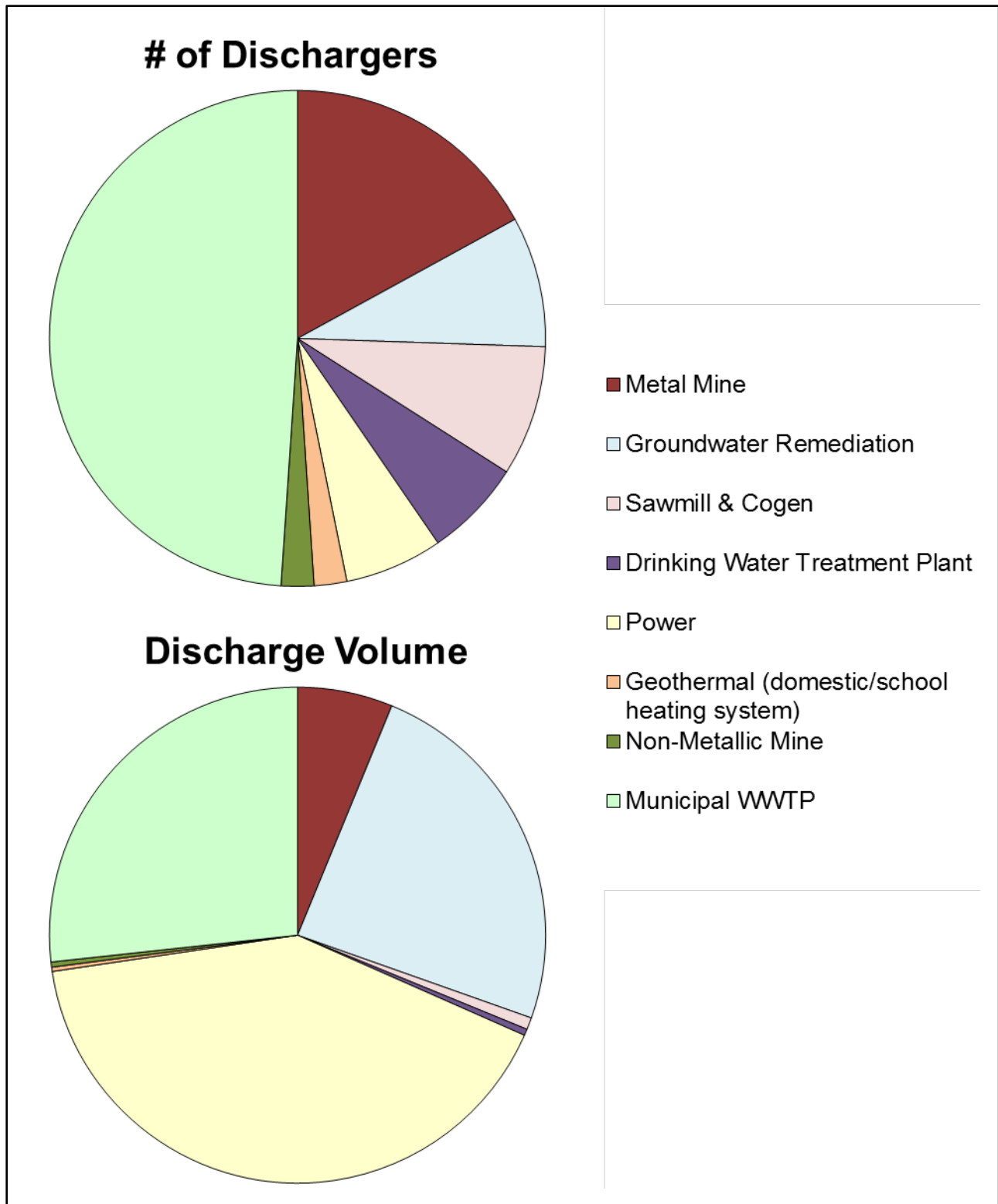


Figure 6.30: Pie charts illustrating the number of NPDES-permitted facility dischargers and sum of design flows by facility type in 2010 303(d)-listed reservoir watersheds

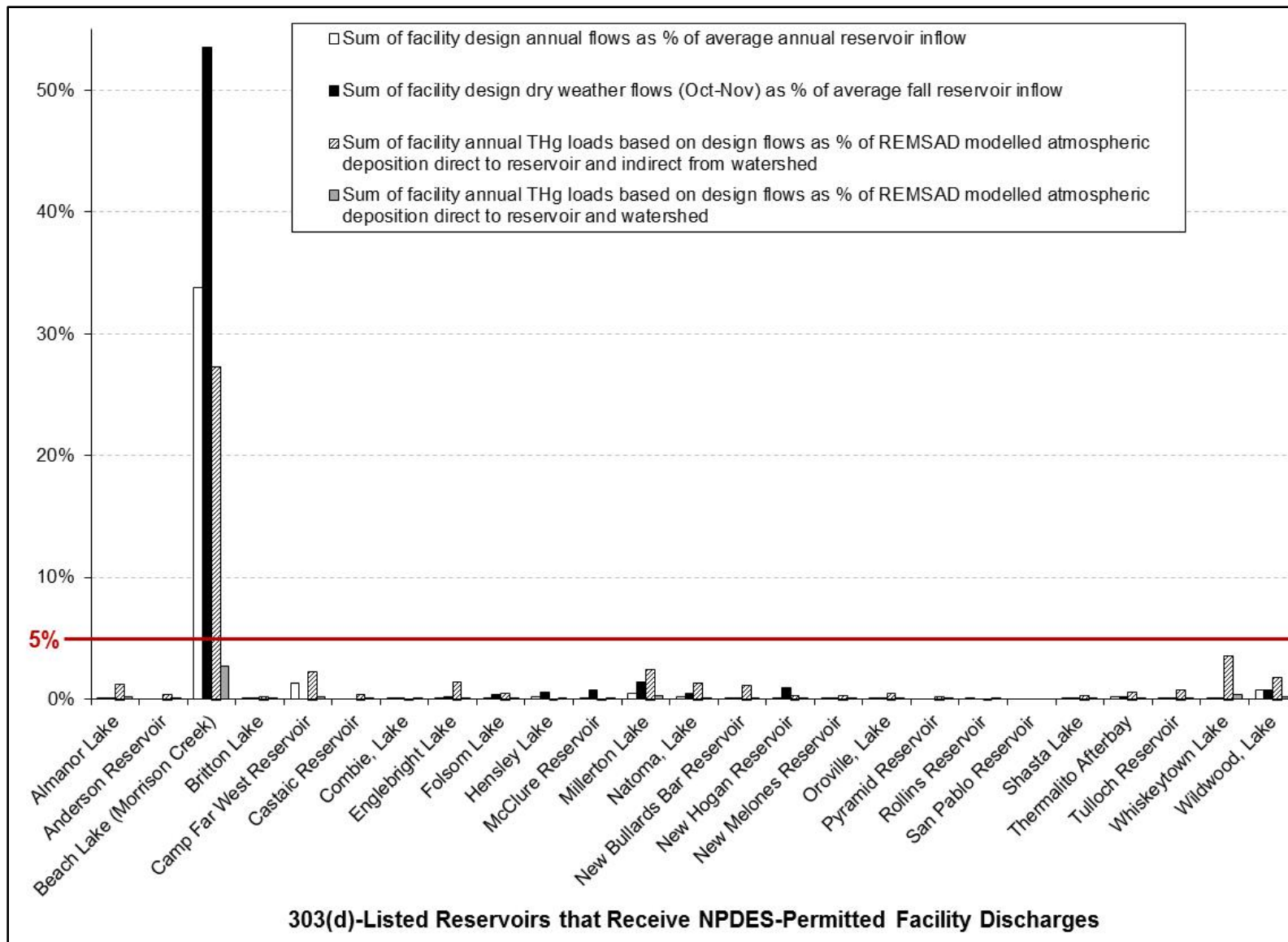


Figure 6.31: Bar chart comparing sum of NPDES-permitted facility design flows and total mercury loads to 2010 303(d)-listed reservoir inflows and REMSAD modelled atmospheric deposition



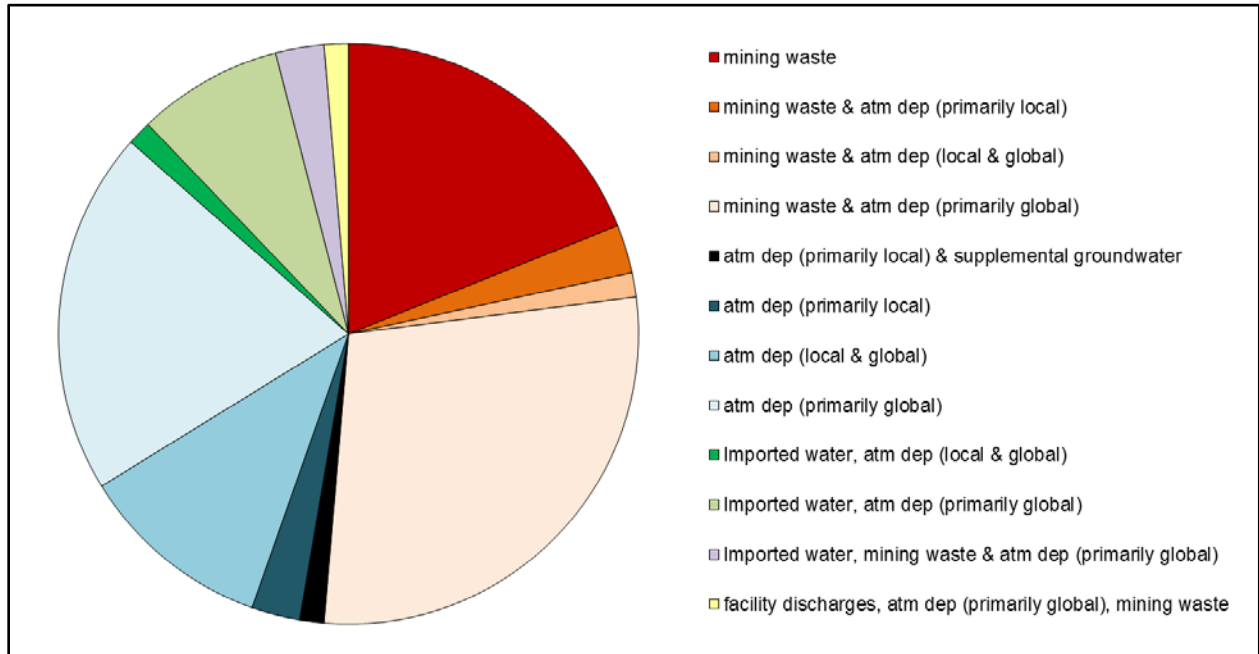


Figure 6.32: Pie chart illustrating the different combinations of sources that contribute to each of the 2010 303(d)-listed reservoirs

The pie chart represents 74 303(d)-listed reservoirs. Mining waste contributes to almost two thirds of the reservoirs. Atmospheric deposition is the primary anthropogenic mercury source to more than a third of the reservoirs, and global industrial emissions are the primary anthropogenic source to more than half of these.

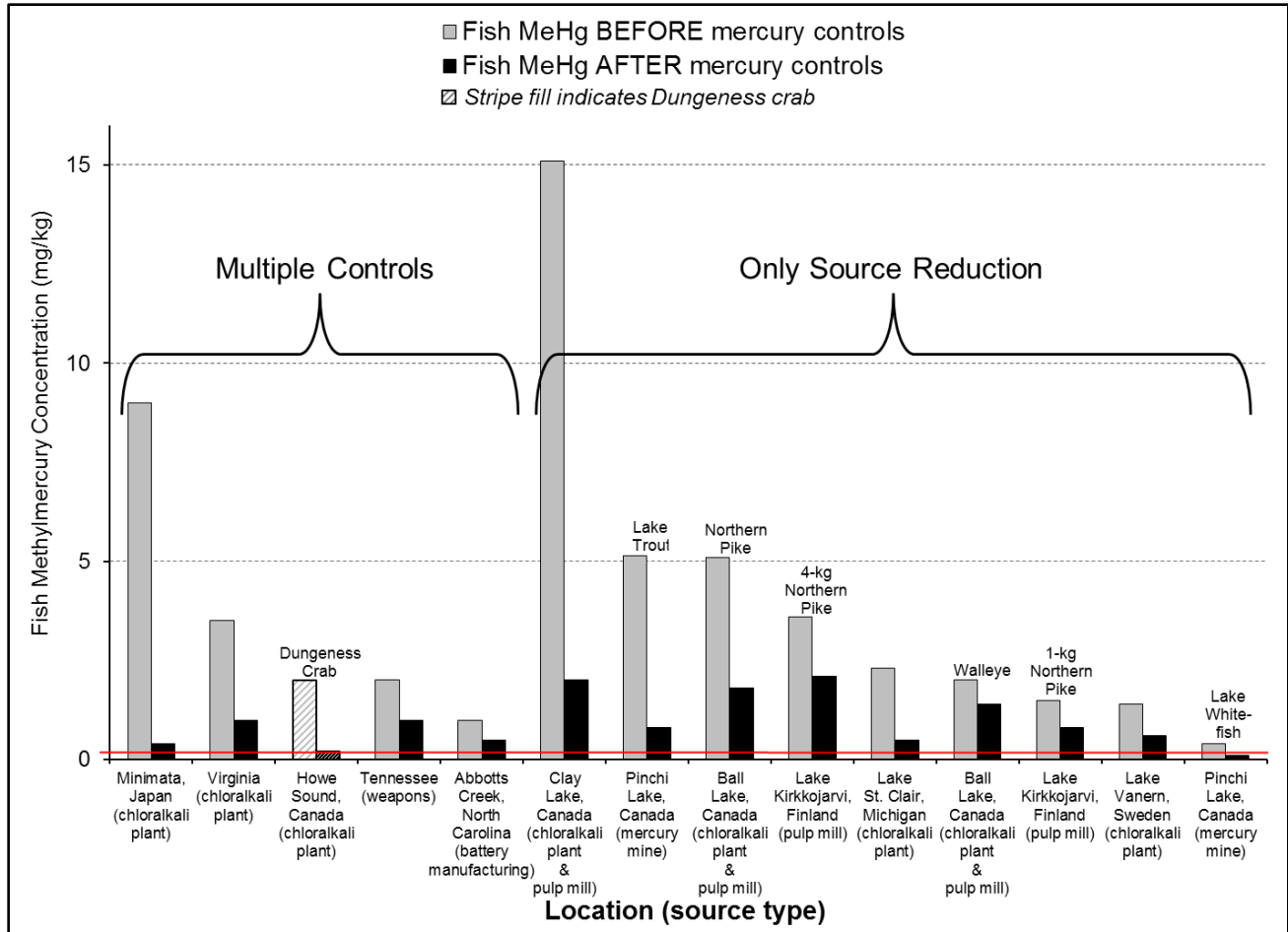


Figure 7.1: Chart illustrating mercury reductions in biota observed after mercury source controls at industrial sites

This chart illustrates 11 industrial sites from around the world that used source control to address mercury pollution. The left hand (grey) columns are before cleanup, the right hand (black) columns are after cleanup. “Multiple Controls” means source reduction and one or more other measures, such as dredging, excavation, or groundwater treatment, were used at these sites. On the right, “Only Source Control” was used at these sites. Fish methylmercury results are provided for two species or sizes at three of the sites, Pinchi Lake, Ball Lake and Lake Kirkkojarvi; Dungeness crab not fish results are provided for Howe Sound.

Substantial biota methylmercury reductions were achieved at all these sites. However, only one of these is a mine site. In addition, the proposed sport fish target of 0.2 mg/kg was achieved in fish tissue at only one of these sites, Pinchi Lake, in a lower trophic level species (lake whitefish) and not in lake trout; it also was achieved in Dungeness crab at Howe Sound.

[Sources: Armstrong and Scott 1979; Azimuth Consulting Group Inc. 2008; Lindstrom 2001; Lodenius 1991; Parks and Hamilton 1987; Southworth et al. 2000; Takizawa 2000; Turner and Southworth 1999]

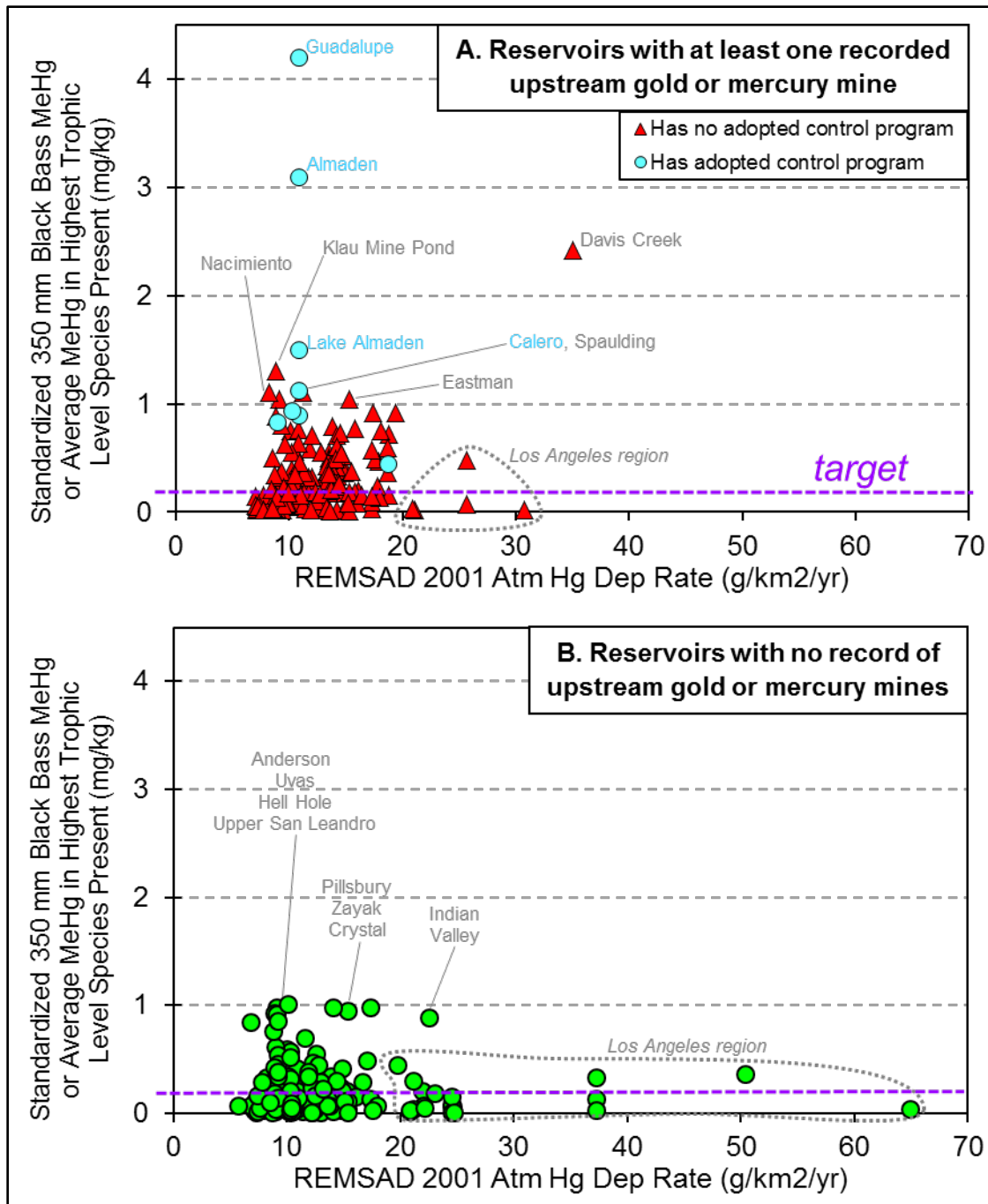


Figure 7.2: Graphs of atmospheric deposition and fish methylmercury concentrations in reservoirs with and without upstream mines

These graphs compare reservoir fish methylmercury concentrations to REMSAD modeled 2001 atmospheric Hg deposition rates and presence/absence of upstream historic mine sites. The reservoirs with the very highest fish methylmercury levels are associated with extensive mercury mining. However, numerous reservoirs have elevated fish methylmercury but do not have any record of any upstream mine sites. There are 60 reservoirs with high fish methylmercury but low atmospheric mercury deposition rates and no upstream mines. Conversely, there are many reservoirs with low fish methylmercury but very high atmospheric mercury deposition rates. These graphs illustrate how there is no one source or factor that explains all fish mercury impairments.

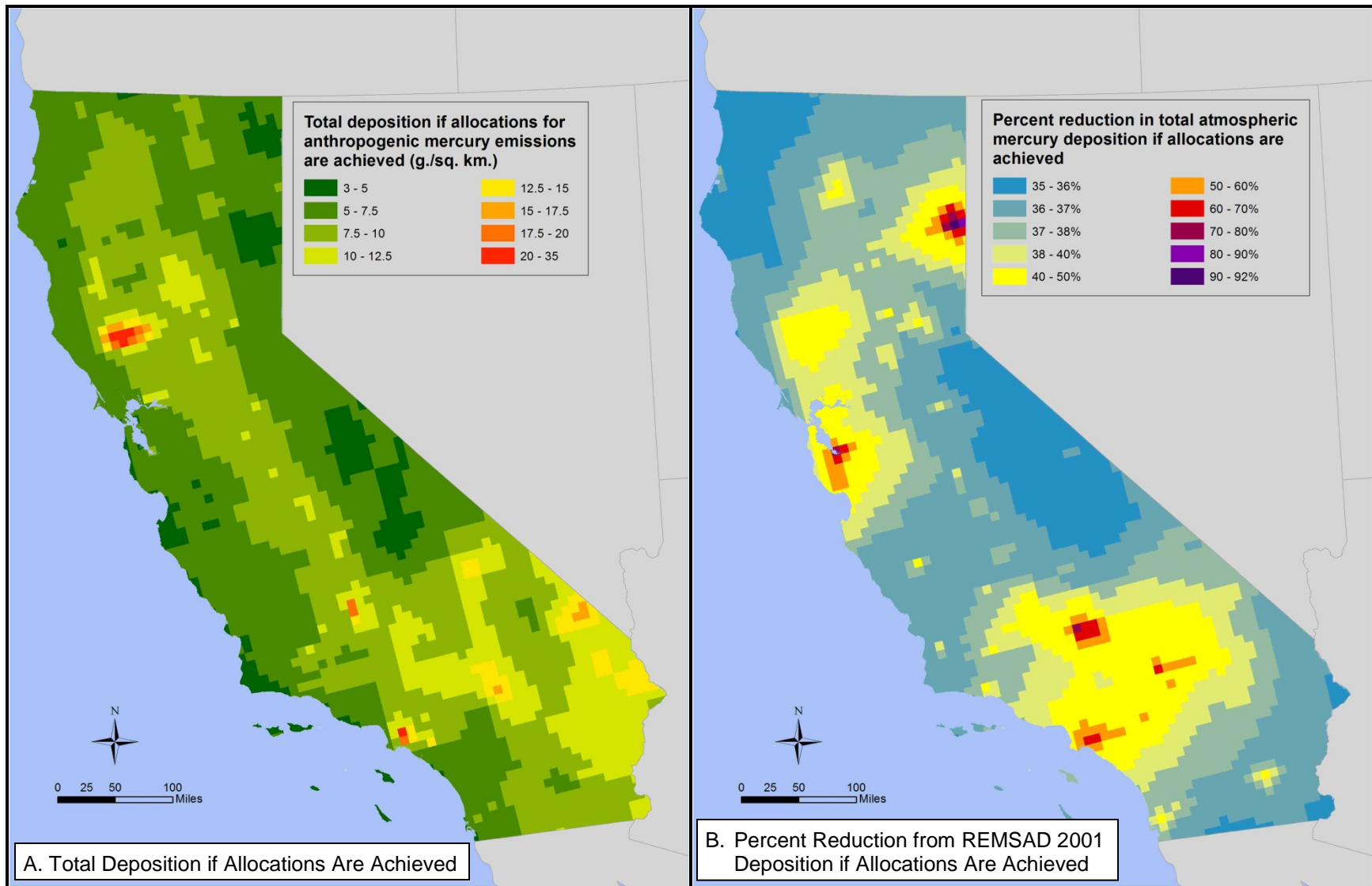


Figure 7.3: Statewide maps showing predicted atmospheric mercury deposition rates and percent reductions if anticipated California and global emission reductions and proposed allocations are achieved

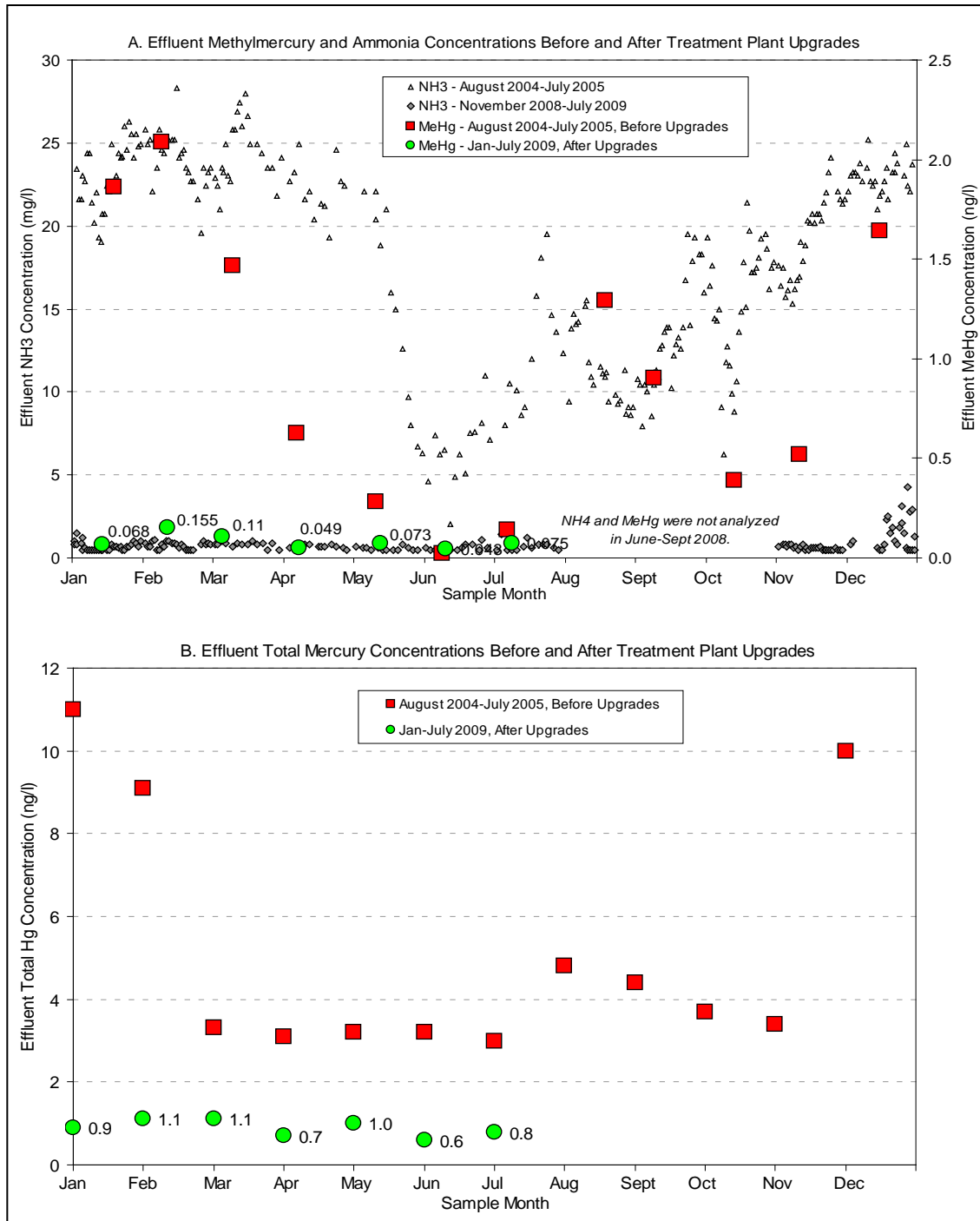


Figure 7.4: Graph illustrating City of Stockton municipal wastewater treatment plant (WWTP) effluent ammonia, methylmercury, and total mercury concentration data collected before and after WWTP upgrades

Average effluent methylmercury concentrations decreased by 91% subsequent to upgrading the treatment process at the City of Stockton’s WWTP. (Note, it is not known if the treatment plant upgrades are responsible for the methylmercury and mercury reductions, or if the reductions are a result of other operational or physical changes.)

[Source: Wood et al. 2010b, Figure 6.6]

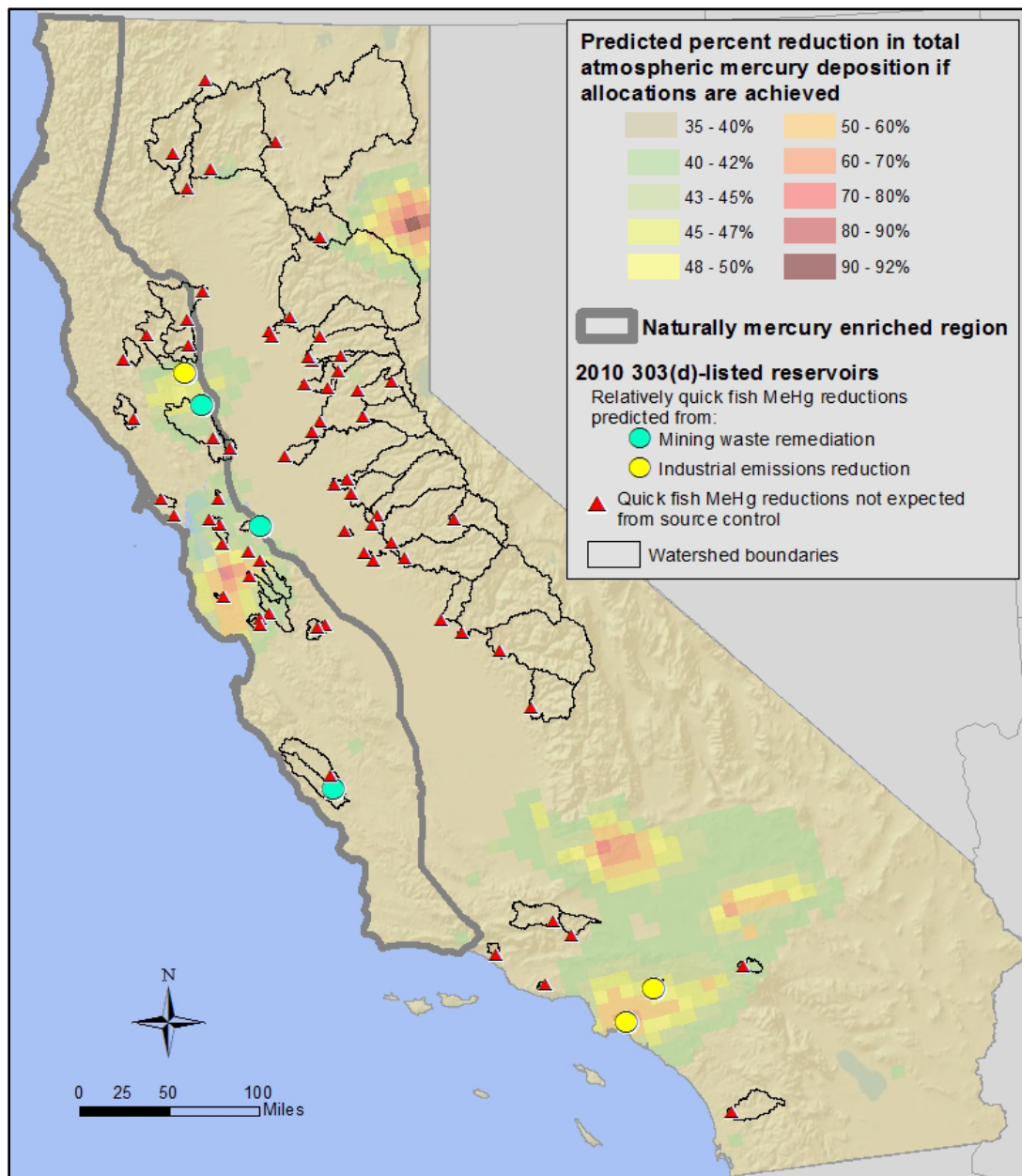


Figure 7.5: Statewide map highlighting the six 303(d)-listed reservoirs where relatively quick fish methylmercury reductions are predicted from source control

The three reservoirs predicted to have relatively quick benefits from mine remediation are, from north to south, Davis Creek, Marsh Creek, and Lake Nacimiento (Table 7.1). Similarly from north to south and west to east, the three reservoirs predicted to have relatively quick benefits from atmospheric deposition are Indian Valley, El Dorado Park, and Puddingstone. The rationale supporting these predictions is provided in section 7.2.7.

The red, orange, and yellow areas highlight where substantial reductions in atmospheric mercury deposition are expected if emission controls are achieved as anticipated (see Figure 7.3B). Atmospheric deposition from California industrial emissions is the primary anthropogenic source to Indian Valley, El Dorado Park, and Puddingstone Reservoirs, and they are located in regions expected to have substantial reductions in atmospheric deposition. Several other mercury-impaired reservoirs also are in such regions, but these reservoirs receive mercury from historic mine sites as well and therefore quick benefits from emission controls are not expected.

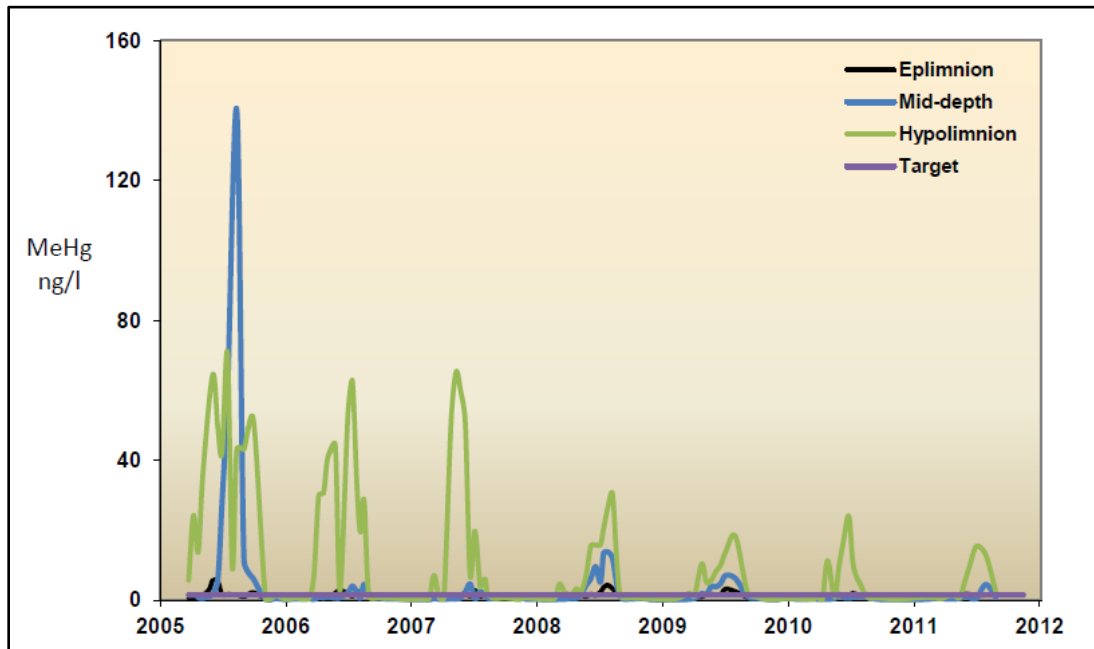


Figure 7.6: Graph illustrating seasonal maximum methylmercury concentrations in Lake Almaden, California, before and after installation of solar-powered circulators

The Santa Clara Valley Water District reported the following:

Annual maximum concentrations in the hypolimnion (green) varied over the study period, and were obviously affected by the circulator after it was set at the bottom in 2008 .... In 2005-2007 the maximum concentration in the hypolimnion was about 70 ng/L; in 2008 through 2011, the maximum concentration was 30, 18, 24 and 15 ng/L, respectively.

Mid-depth seasonal maximum concentrations were immediately affected by the circulator following installation in 2006, and remained below 10 ng/L during the reporting period.

[Source: Drury 2011, Figure 31]

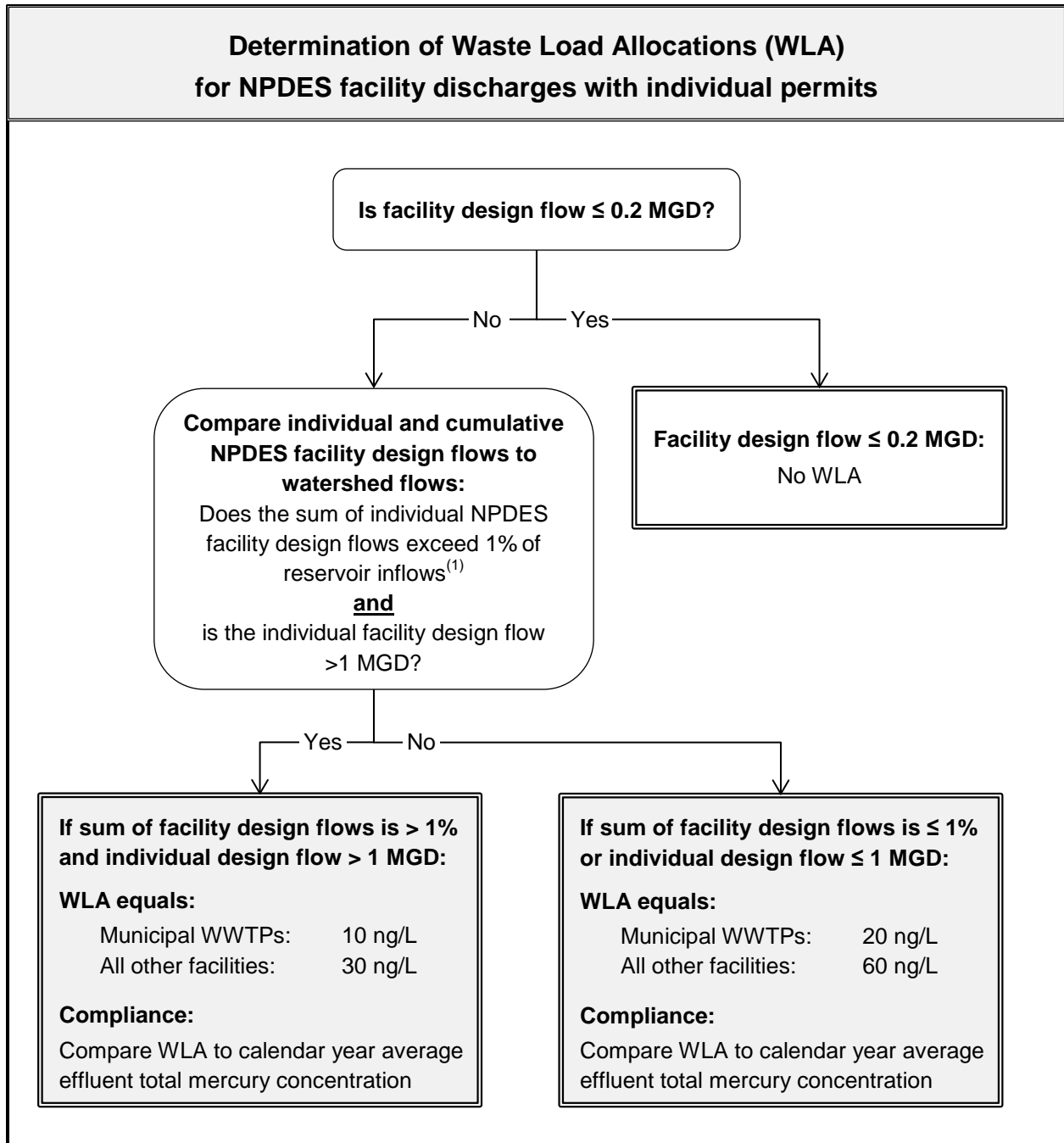


Figure 8.1: Flow chart for determining waste load allocations for facilities with individual NPDES permits upstream of mercury-impaired reservoirs

[Table 8.1 Notes provided on next page]



Figure 8.1 Notes:

- (1) The answer to the question, “Does the sum of individual NPDES facility design flows exceed 1% of reservoir inflows?” is yes if either the sum of annual design flows for NPDES-permitted facility discharges exceeds 1% of annual reservoir inflows, or the sum of dry weather design flows for NPDES-permitted facility discharges exceeds 1% of dry weather reservoir inflows.

Calculation methods:

Annual design flow for each facility is calculated by multiplying the facility daily design flow by 365, or by the potential maximum allowable number of days of discharge each year for facilities that do not discharge year round.

Dry weather design flow for each facility is calculated by multiplying the facility design flow by 61 (the number of days in October and November) or by the potential maximum allowable number of days of discharge during October and November for facilities that do not discharge year round.

Annual reservoir inflow for each reservoir is calculated by first summing the total inflow volume during each year of the entire period of gage record, and then dividing that sum by the number of years of the gage record.

Dry weather reservoir inflow for each reservoir is calculated by first summing the total inflow volume during October and November of each year of the entire period of gage record, and then dividing that sum by the number of years of the gage record.

If gaged inflow data are not available for a reservoir, gaged outflow data may be used instead. If no gaged reservoir inflow or outflow data are available, watershed precipitation runoff estimates may be used. Watershed precipitation runoff estimates should be based on at least five years of precipitation data.

For facilities such as hydro-power plants and fish hatcheries that make use of surface water intakes from the same water bodies as their discharge receiving waters, the annual and dry weather design flow calculations, WLAs, and effluent limitations apply to the discharges from internal waste streams, not to once-through cooling water discharges or other discharges of ambient surface water. The Water Boards will apply intake credits to once-through cooling water and other discharges as allowed by law.

If a facility has more than one outfall to a given reservoir's watershed, the WLA and effluent limitation are determined by the sum of all its outfalls in that reservoir watershed. The WLA and effluent limitation apply to all of the facility's outfalls in that watershed.

If future expansions or other new discharges from facilities with individual NPDES permits cause the watershed sum of annual or dry weather design flows to exceed 1% of reservoir inflows, then all the facilities in that reservoir watershed that discharge greater than 1 MGD shall be re-evaluated per the methodology described in Figure 1.